Identification of presynaptic proteins as neddylation targets

Doctoral thesis
to obtain a doctorate (PhD)
from the Faculty of Medicine
of the University of Bonn

Anna Victoria Denise Schuckel
from Bonn
2025

Written with authorisation of

the Faculty of Medicine of the University of Bonn

First reviewer: Prof. Dr. Valentin Stein

Second reviewer: Prof. Dr. Martin Müller

Day of oral examination: 4 April 2025

From the Institute of Physiology II

Für meine Eltern und meine Großeltern.

Table of Contents

List of abbreviations

AD	Alzheimer’s disease
Ala	Alanine
AMP	Adenosine monophosphate
AMPA	α-amino-3-hydroxy-5-methyl-4-isoxazolepropionic acid
AMPAR	AMPA receptor
APP	Amyloid precursor protein
APP-BP1	Amyloid precursor protein binding protein
Arg	Arginine
ATP	Adenosine triphosphate
AZ	Active zone
BSA	Bovine Serum Albumin
CAND1	Cullin-associated and neddylation-dissociated 1
CAZ	Cytomatrix at active zone
CFP	Cyan fluorescent protein
cGAS	Cyclic GMP-AMP synthase
Cof1	Cofilin1
Cul	Cullin
DMEM	Dulbecco´s Modified Eagle´s Medium
DMSO	Dimethyl sulfoxide
DNA	Deoxyribonucleic acid
ECV	Elongin B/C–Cul2–VHL complex

EGFR	Epidermal growth factor receptor
FCS	Fetal calf serum
GFP	Green fluorescent protein
HEK293T cell	Human Embryo Kidney 293T cell
KO	Knock-out
LB	Lysogeny broth
LE mutation	L165A, E166A mutation
LTP	Long-term potentiation
MEM	Minimum Essential Medium
mEPSC	Miniature excitatory synaptic current
MDM2	Mouse double minute 2 protein
MLN-4924	Pevonedistat
NAE1 (APP-BP1)	Nedd8-activating enzyme
Nedd8	Neuronal-precursor-cell-expressed developmentally downregulated 8
NEM	N-Ethylmaleimide
NMDA	N-methyl-D-aspartic acid
NMDAR	NMDA receptor
OD	Optical density
OPT10	1,10-Phenanthroline
PFA	Paraformaldehyde
Parkin	Parkin RBR E3 ubiquitin-protein ligase
PBS	Phosphate buffered saline
PCR	Polymerase chain reaction

PD	Parkinson´s disease
PINK1	PTEN-induced kinase 1
PPF	Paired-pulse facilitation
PRL11	Ribosomal protein L11
PSD-95	Postsynaptic density 95
PVDF	Polyvinylidene difluoride
Rbx	Ring Box Protein
RIM	Regulating synaptic membrane exocytosis protein
RING finger	Really Interesting Novel Gene finger
RIPA buffer	Radio-immunoprecipitation assay buffer
RT	Room temperature
SDS	Sodium dodecyl sulfate
SENP8 (NEDP1, DEN1)	Sentrin-specific protease 8
SNAP-25	Synaptosomal-associated protein 25
SNARE	Soluble N-ethylmaleimide-sensitive-factor attachment receptor
SOB medium	Super Optimal Broth medium
SOC medium	Super Optimal Broth medium with catabolic repressor
STING	Stimulator of interferon genes
Stx	Syntaxin
SUMO	Small ubiquitin-related modifier
SV	Synaptic vesicles
SV2A	Synaptic vesicle glycoprotein 2A
t-SNARE	Target SNARE protein

TBS	Tris-buffered saline
TBST	Tris-buffered saline with Tween® 20 Detergent
TEMED	Tetramethylethylendiamin
UBA1	E1 ubiquitin-activating enzyme
UBA3	Ubiquitin-activating enzyme 3
UBL	Ubiquitin-like protein
UCH-L3	Ubiquitin carboxyl terminal hydrolase isozym L3
v-SNARE	Vesicle SNARE protein
VAMP	Vesicle-associated membrane protein; Synaptobrevin
VHL	von Hippel–Lindau tumour suppressor protein
WT	Wild type
YFP	Yellow fluorescent protein

1 Introduction

The capacity of the brain to perform its functions depends on the efficacy of the neuronal communication. In order to achieve this, electrical activity is converted into a chemical signal in the form of neurotransmitters. The release of these neurotransmitters from presynaptic terminals is initiated by calcium influx and occurs via exocytosis of synaptic vesicles (SV). Due to the complexity and variety of the functions, it is important that the release can be adapted to specific conditions. The regulation and fine-tuning require a series of steps and the involvement of diverse proteins (Rizo and Xu, 2015). The modulation of each step can be achieved through modifications of the involved proteins, including the addition of phosphate, acetyl and methyl groups, the addition of lipids and sugars, or even the attachment of polypeptides. Ubiquitin and ubiquitin-like proteins (UBLs) represent a well-documented example of these modifications (Enchev et al., 2015, Ramazi and Zahiri, 2021, van der Veen and Ploegh, 2012).

1.1 Protein modification

A crucial post-translational modification is the covalent conjugation of ubiquitin and ubiquitin-like proteins (UBLs), including Nedd8, SUMO, Atg12, Atg8, FUB1, ISG15, and FAT10, to target proteins. The conjugation of these modifying agents occurs via an enzymatic cascade analogous to that of ubiquitin (Bawa-Khalfe and Yeh, 2010, Dye and Schulman, 2007, Haas et al., 1987, Ichimura et al., 2000, Kamitani et al., 1997, Kerscher et al., 2006, Liu et al., 1999, Loeb and Haas, 1992, Mizushima et al., 1998, Yeh et al., 2000). The attachment of different UBLs has been demonstrated to affect the function of their target protein. Ubiquitin, the most extensively studied modifier, is known to regulate homeostasis e.g. by labelling proteins to be degraded, but also has other, partly cell-specific functions (Enchev et al., 2015, Haas and Broadie, 2008, Ravid and Hochstrasser, 2008). In addition, the involvement of SUMO proteins in subcellular protein localisation, transcription, and the DNA repair process is well documented (Gareau and Lima, 2010). Members of the Atg8 family and Atg12 serve as regulators of autophagy (Schreiber and Peter, 2014), and other UBLs have been shown to play a role in oxidative stress, protein

translation, and in immune and inflammatory responses (van der Veen and Ploegh, 2012, Welchman et al., 2005).

The influence of ubiquitin and UBLs on neuronal processes, and in particular on synapses, is well documented. This influence is observed in a variety of processes, including neuronal development, neurogenesis, synaptogenesis, axon and dendrite outgrowth as well as pre- and postsynaptic function and activity-dependent plasticity (Haas and Broadie, 2008, Kawabe and Brose, 2011, Schwartz and Ciechanover, 2009, Yi and Ehlers, 2007). Ubiquitin, in particular, has been shown to interact with multiple targets within the presynapse (Haas and Broadie, 2008, Yi and Ehlers, 2007). Proteins such as synaptophysin, Stx1a, and RIM1α are subject to ubiquitination, yet the function of this modification remains unclear (Chin et al., 2002, Wheeler et al., 2002, Yao et al., 2007). Additionally, there is evidence that certain presynaptic proteins undergo SUMOylation. For instance, it has been demonstrated that neuronal activity enhances the SUMOylation of presynaptic proteins, resulting in a reduction in KCL-evoked glutamate release (Feligioni et al., 2009, Wilkinson et al., 2008). Moreover, SUMOylation of Syntaxin-1a (Stx1a) promotes its closed conformation and reduces binding to SNAP-25 (synaptosomal-associated protein 25) and VAMP2 (vesicle-associated membrane protein). In the same study, inhibition of SUMOylation resulted in decreased exocytosis levels and enhanced endocytosis. This suggests that SUMOylation of Stx1a delays endocytosis to allow for full exocytosis (Craig et al., 2015).

1.2 Neddylation

Another UBL of great importance is Neuronal-precursor-cell-expressed developmentally downregulated 8 (Nedd8) (Kumar et al., 1992). Nedd8 is an 81 amino acid polypeptide (Kamitani et al., 1997) of 9 kDa (Kumar et al., 1992) that is conserved across different animals and tissues (Rabut and Peter, 2008). In adult mice, Nedd8 expression was detected in several tissues, including heart, brain, lung, liver, muscle, kidney, spleen, and testicles (Kumar et al., 1993). In addition, Nedd8 exhibits homology in many different species, including humans, monkeys, rats, mice, dogs, bovine, rabbits, chicken, and even yeast (Kamitani et al., 1997, Kumar et al., 1992, Kumar et al., 1993). Comparative analysis with ubiquitin revealed that Nedd8 shares 60 % sequence identity and 80 % amino acid

homology with ubiquitin (Kamitani et al., 1997), reflected in the high degree of structural analogy (Whitby et al., 1998).

Similar to ubiquitin, Nedd8 is synthesised as precursor protein that must be cleaved at the C-terminal end prior to targeting a substrate (Kamitani et al., 1997, Shen et al., 2005, Wu et al., 2003). This process is facilitated by either sentrin-specific protease 8 (SENP8; also known as NEDP1 or DEN1) or ubiquitin carboxyl terminal hydrolase isozym L3 (UCH-L3) (Wada et al., 1998). While SENP8 has a high specificity for Nedd8 (Gan-Erdene et al., 2003, Shen et al., 2005, Wu et al., 2003), UCH-L3 is capable of acting on both ubiquitin and Nedd8 (Wada et al., 1998). Interestingly, the loss of one enzyme appears to be compensated for by the other, as the knockout of either SENP8 or UCH-L3 not result in neddylation defects (Chan et al., 2008, Kurihara et al., 2000).

Cleavage of the precursor exposes two conserved C-terminal glycines. Glycine 76 acts as a binding site by forming an isopeptide bond with a lysine residue of the target (Gong and Yeh, 1999, Kamitani et al., 1997, Rabut and Peter, 2008). The attachment of

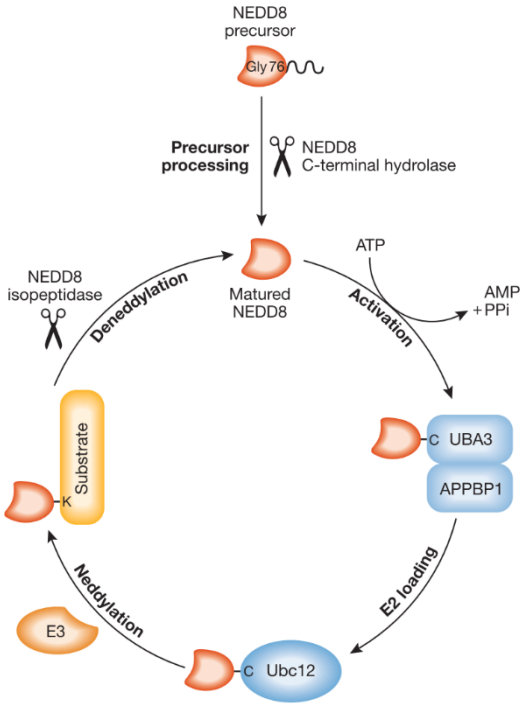

Figure 1: Schematic representation of the neddylation pathway

Nedd8 is synthesised as a precursor protein cleaved at the C-terminus. The E1 activating enzyme activates Nedd8 in an ATP-dependent manner. After activation, Nedd8 is transferred to an E2 conjugation enzyme, which then ensures the specific conjugation of NEDD8 to its substrates. Neddylation is reversible and catalyzed by isopeptidases. (Adapted from Rabut and Peter, 2008)

Nedd8 to the target protein requires a cascade of three enzymes: NEDD8 activating enzyme E1, NEDD8 conjugating enzyme E2, and NEDD8 ligase E3 (E1, E2, and E3; see Figure 1). Initially, Nedd8 is activated by the E1 activating enzyme. This enzyme consists of the regulatory subunit of Nedd8-activating enzyme (NAE1; also called APP-BP1) and the catalytic subunit ubiquitin-activating enzyme 3 (UBA3). The heterodimer chemically activates Nedd8 in an ATP-dependent manner by attaching AMP to the C-terminus of Nedd8 (Huang et al., 2004, Liakopoulos et al., 1998, Osaka et al., 1998, Walden et al., 2003). Interestingly, the E1 subunit UBA3 plays a role in preventing the activation of ubiquitin instead of Nedd8 because a conserved basic residue in UBA3 and Arg72 in ubiquitin are not compatible, in contrast to the analogous Ala72 in Nedd8 (Souphron et al., 2008; Walden et al., 2003). It is noteworthy that Arg72 plays a key role in the interaction between ubiquitin and the E1 ubiquitin-activating enzyme (UBA1) (Lee and Schindelin, 2008; Whitby et al., 1998). However, in the case of Nedd8 overexpression, Nedd8 can be activated by UBA1, transferred to most ubiquitin-specific E2 enzymes, and subsequently attached to ubiquitination substrates or incorporated into polyubiquitin chains (Hjerpe et al., 2012, Kim et al., 2011, Leidecker et al., 2012, Whitby et al., 1998).

After activation, Nedd8 is transferred to an E2 conjugating enzyme. The best studied E2 Ubc12 contains a distinct N-terminal prolongation that leads to a specialisation for Nedd8 (Gong and Yeh, 1999, Huang et al., 2008, Huang et al., 2007, Liakopoulos et al., 1998, Huang et al., 2004, Huang et al., 2007). However, a second E2, UbeF, was found that is particularly involved in neddylation of cullin 5 (Cul5) (Huang et al., 2009). E2 delivers the activated Nedd8 to the ligase E3, which then transfers Nedd8 to its target proteins, thereby forming an isopeptide bond. Only a few E3 ligases have been described to be involved in the Nedd8 pathway. These E3s are not exclusively involved in the process of neddylation but also play a role in ubiquitination. One example of E3 enzymes involved in neddylation is the Really Interesting Novel Gene (RING) finger domains, such as Ring Box Protein (Rbx)1 and Rbx2 (Huang et al., 2009, Kamura et al., 1999, Oved et al., 2006). Nedd8 targets can be mono-neddylated on a single or several lysine residues. In addition, Nedd8 can form chains on their targets by binding to the target and then to itself. For example, cullins are neddylated at several lysins, with some lysines being attached to Nedd8 chains (Enchev et al., 2015). Neddylation is a reversible process,

whereby SENP8, which is involved in the processing of Nedd8, also functions as a Nedd8 deconjugating enzyme (Wu et al., 2003, Yamoah et al., 2005).

1.2.1 Function of neddylation

Post-translational modifications can affect the function of their target in various ways. For neddylation, three different types of effects are known.

First of all, neddylating a protein can alter the three-dimensional structure and, through this, the biochemical properties (Rabut and Peter, 2008). A well-known example of this are the cullins. Cullins are involved in cell cycle control by regulating protein ubiquitination and consequently proteasomal degradation of proteins (Hori et al., 1999, Sarikas et al., 2011). Attachment of Nedd8 causes catalytic activation of the cullins by changing their C-terminal conformation (Duda et al., 2008, Rabut and Peter, 2008). This decreases the distance between ubiquitin and the substrate and increases its ubiquitination (Duda et al., 2008, Pan et al., 2004, Rabut and Peter, 2008, Saha and Deshaies, 2008). Moreover, neddylation of the epidermal growth factor receptor (EGFR) reveals additional lysines that can be used for further modifications (Oved et al., 2006, Rabut and Peter, 2008).

The second effect of neddylation is the prevention of protein interaction. Neddylation of cullins, for example, prevents the binding of CAND1 (Cullin-associated and neddylation-dissociated 1) (Goldenberg et al., 2004, Rabut and Peter, 2008). Furthermore, neddylation of the von Hippel–Lindau (VHL) tumour suppressor protein has been shown to inhibit the attachment of the scaffold component Cul2 and the formation of the ECV (Elongin B/C–CUL2–VHL) complex, thereby allowing the VHL interaction with fibronectin (Rabut and Peter, 2008, Russell and Ohh, 2008).

A third function of neddylation is the recruitment of new interaction partners. In a manner analogous to that of mono-ubiquitinated EGFR, neddylated EGFR is capable of assembling proteins of the endocytic machinery (Oved et al., 2006, Rabut and Peter, 2008). A further illustration of Nedd8-mediated protein interaction can be observed in the case of the cyclic GMP-AMP synthase (cGAS), where neddylation of cGAS can facilitate the dimerisation of this protein. Since cGAS has also been linked to poly-Nedd8 chains, it can be postulated that Nedd8 chains act as a nexus. The dimerisation of cGAS enhances

its ability to bind DNA, leading to a more pronounced activation of the cGAS-STING pathway (Li et al., 2021).

The second and third aspects are similarly reflected in the interactions of Nedd8 with ubiquitin and other UBLs. The binding and unbinding of ubiquitin and UBLs appears to occur in a dynamic manner. This principle applies to the interaction between ubiquitin and Nedd8, as well as to the interaction between Nedd8 and SUMO. Neddylation of EGFR also enhances its ubiquitination, which marks the receptor for degradation (Oved et al., 2006, Rabut and Peter, 2008). Consequently, neddylation can also reduce the stability of a protein. However, the Nedd8 protein can also enhance the stability of a given protein, as demonstrated by studies on the mouse double minute 2 (MDM2) protein (Watson et al., 2010).

1.2.2 Impact of neddylation in neurones

Of all UBLs, Nedd8 is the most highly expressed in neurones and therefore appears to play an important role at the neuronal level. In addition, the number of neddylated proteins increases with neuronal development, suggesting that neddylation is also essential for the correct development and maturation of neurones (Vogl et al., 2015). For example, neddylation has been demonstrated to be involved in the process of neurite outgrowth. This appears to be initiated by the neddylation of cofilin1 (Cof1), as evidenced by the regulation of actin dynamics by neddylated Cof1, whereas a non-neddylatable mutant is unable to form a dendritic tree (Einsfelder, 2022, Vogl et al., 2020). In addition, neddylation also affects spine formation and maintenance. Inhibition of neddylation reduced dendritic spine width and spine density (Scudder and Patrick, 2015, Vogl et al., 2015). The scaffold protein PSD-95, which plays a role in spine maturation, is a known Nedd8 target. A non-neddylatable PSD-95 mutant was unable to induce spine growth but led to filopodia-like precursors. This indicates that Nedd8 regulates spine formation and maintenance through PSD-95 (Vogl et al., 2015).

Electrophysiological recordings revealed that inhibition of neddylation decreased the frequency and amplitude of mEPSCs. Changes in amplitude are often attributed to changes at the post-synaptic level. To date, several studies have confirmed the influence of Nedd8 on postsynaptic processes. Inhibition of neddylation during induction has been

shown to reduce long-term potentiation (LTP) (Brockmann et al., 2019). This is consistent with the observation that neddylation is required for AMPA- and NMDA-mediated neurotransmission, as inhibition of neddylation reduces postsynaptic receptor density (Brockmann et al., 2019, Scudder and Patrick, 2015). The Nedd8 target PSD-95 serves to anchor AMPA receptors (AMPAR) at synapses, thereby influencing postsynaptic plasticity (Stein et al., 2003). Neddylation of PSD-95 may present a potential mechanism for regulating plasticity.

Furthermore, neddylation is critical for the stability of $Na_v1.1$. Inhibiting neddylation reduces sodium current density by decreasing the $Na_v1.1$ protein level (Chen et al., 2021).

As mentioned above, inhibition of neddylation does not only reduce mEPSC amplitude but also frequency. In contrast to amplitude changes, alterations in mEPSC frequency are associated with presynaptic processes (Brockmann et al., 2019). Indeed, Ubc12 and many neddylated proteins were found to be expressed in pre- and postsynaptic compartments (Vogl et al., 2015). Furthermore, neddylation was shown to influence the probability of vesicle release (Brockmann et al., 2019). This indicates that neddylation regulates synaptic transmission, at least in part. However, the mechanism behind this and the proteins involved remain unknown.

1.2.3 Neddylation in diseases

Nedd8 deregulation has been associated with neurodegenerative disorders (Dil Kuazi et al., 2003, Mori et al., 2005, Rabut and Peter, 2008). For example, dysregulated neddylation is a hallmark of Alzheimer´s disease (AD) (Zhang et al., 2024). Nedd8, which is normally located in the nucleus of hippocampal pyramidal cells and granule cells, has been detected in the cytoplasm of AD hippocampal neurones (Chen et al., 2012, Chen et al., 2003). The peptide amyloid beta (Aβ) that is involved in AD is produced from the amyloid precursor protein (APP) (Sehar et al., 2022). Neddylation of cullins activates the processing of APP (Chen et al., 2012, Walden et al., 2003, Zhang et al., 2024). Therefore, it is possible that neddylation plays a role in AD by influencing the regulation of Aβ levels. In addition, as previously described, amyloid precursor protein (APP)-binding protein (APP-BP1) forms the Nedd88 activating enzyme E1 together with UBA3 (Chen et al., 2012, Zhang et al., 2024). Another disease that is linked to neddylation is Parkinson´s

disease (PD). Brains of PD patients contained neddylated Parkin. Parkin is a RING-in-between-RING ubiquitin E3 ligase (Trempe et al., 2013) that is involved in mitophagy (Schreiber and Peter, 2014). Neddylation of Parkin leads to an increased ubiquitination (Choo et al., 2012, Um et al., 2012), which could promote the degradation of damaged mitochondria. Given that dysregulation of this process is associated with PD (Deas et al., 2011), neddylation of Parkin may contribute to this disease. Apart from Parkin, PINK is dysregulated in PD as well (Choo et al., 2012, Um et al., 2012, Zhang et al., 2024). It has been shown that gene mutations involving both Parkin and PINK are responsible for the pathogenesis of PD (Kitada et al., 1998, Zhang et al., 2024). Since previous studies suggest that PINK is another Nedd8 substitute, neddylation of PINK may play a role in PD as well (Xiong et al., 2009, Zhang et al., 2024).

In addition to neurodegenerative disorders, neddylation is also associated with several other diseases, including heart diseases (Li et al., 2020a, Zhang et al., 2024, Zou et al., 2019), immune-related diseases (Mao et al., 2023, Zhang et al., 2024, Zhang et al., 2016) and cancer (He et al., 2023, Zhang et al., 2024). This highlights the importance of neddylation as a post-translational modification and the need to further understand its mechanism and function.

1.2.4 Identifying neddylation targets

The current state of neddylation research implies its role in many yet uncharacterized processes, however one of the challenges of further research is the identification of additional neddylation targets. Rabut and Peter have established several criteria that must be met to successfully detect neddylation. One such aspect is the covalent binding of Nedd8 to the substrate (i). This binding must occur under endogenous conditions (ii) and by specific components of the neddylation machinery (iii). In addition to these minimum requirements, the following criteria can further characterise potential Nedd8 targets (Rabut and Peter, 2008):

(iv) Characterisation of the phenotype of a non-neddylatable mutant

(v) Identification of the specific Nedd8 ligase

(vi) Reconstitution of the neddylation reaction

(vii) Determination of the Nedd8 isopeptidase

In order to facilitate research on neddylation, methods that specifically inhibit individual steps of the neddylation process are relevant. One widely used method is the treatment with MLN-4924, which is an adenosine triphosphate analogue that blocks NAE1 (Brownell et al., 2010, Soucy et al., 2009). This inhibition is thought to reduce the levels of neddylated proteins, thus providing a way to ensure the attachment of Nedd8 by the specific machinery. This is necessary because in some cases Nedd8 can also be used for ubiquitination processes, as mentioned above. MLN-4924 can therefore be used to fulfil the third criterion.

The present study examines the neddylation of ten distinct proteins that modulate the presynapse through experimental means. The experimental results identified RIM1α and Stx1a as the most promising neddylation targets. The following introduction will therefore focus on these two proteins.

1.3 Synaptic transmission

Neuronal activity is based on the transmission of information from one neurone to another, which is facilitated by the release of neurotransmitters in response to an action potential. This release is mediated by the exocytosis of SVs at the active zone (AZ) of the presynapse. The AZ consists of the plasma membrane and a group of insoluble protein complexes attached to it, also referred to as the cytomatrix (CAZ) (Mochida, 2020, Südhof, 2012, Südhof, 2014, Wu et al., 2023). Significant representatives of CAZ proteins are RIMs, RIM-BP, ELKSs, Munc-13s, Liprin-αs, and Bassoon, which interact with numerous other presynaptic proteins. The CAZ is involved in SV release, with different proteins performing different functions. These functions include the recruitment of voltage-gated calcium channels, docking and priming of SVs, organisation of the release machinery, and fusion of SVs (Emperador-Melero and Kaeser, 2020, Gramlich and Klyachko, 2019, Mochida, 2020, Schoch and Gundelfinger, 2006, Südhof, 2012, Südhof, 2013b, Südhof and Rizo, 2011, Ziv and Garner, 2004). Once a protein complex consisting of RIM and other proteins has positioned the SVs at the AZ (Südhof, 2013b, Yang et al., 2023), the vesicles undergo a docking and priming process that makes the vesicles ready for release. During priming, the vesicle SNARE protein (v-SNARE) VAMP2 assembles with the target

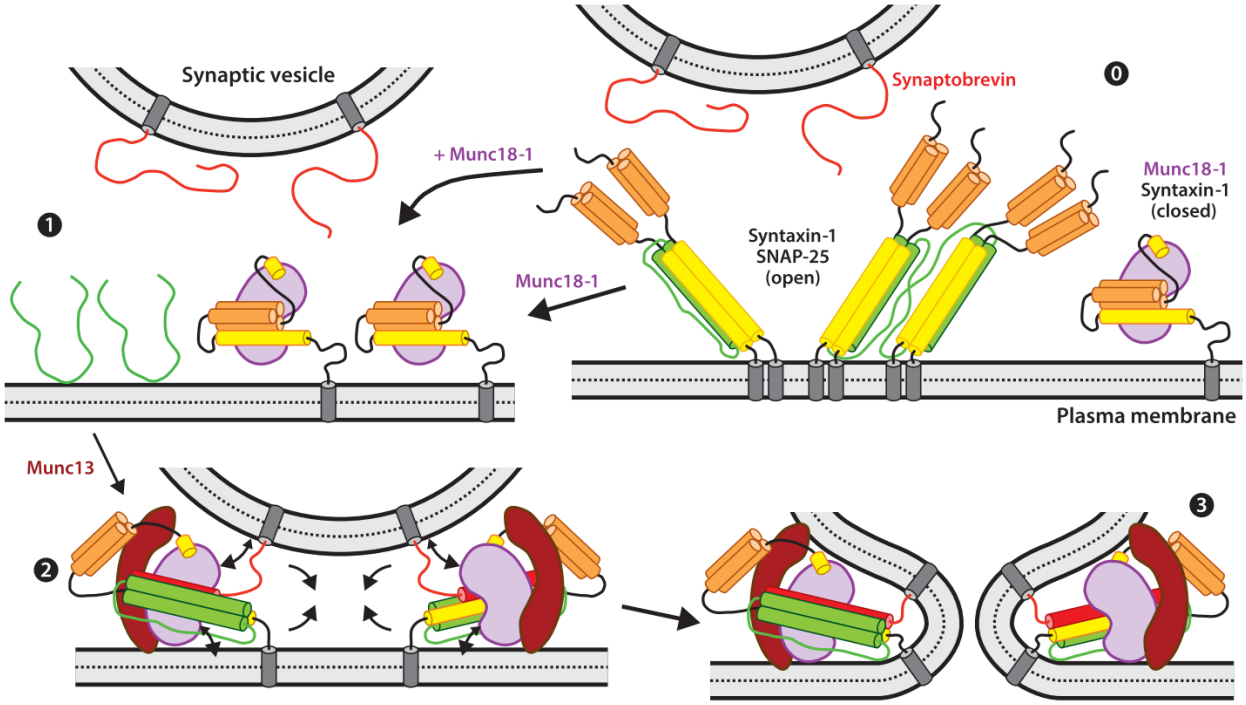

Figure 2: Model of synaptic vesicle fusion

Munc18-1 and closed Syntaxin-1 form a complex, directly or after disassembly of the Syntaxin-1–SNAP-25 complex (states 0 and 1). Munc13-1 opens Syntaxin-1 and, with Munc18-1, assembles the SNARE complex (state 2), leading to a primed state ready for membrane fusion (state 3). (Adapted from Rizo and Xu, 2015)

SNARE protein (t-SNARE) Stx1a and two motifs of the t-SNARE SNAP25 to form a tight SNARE complex. The formation of this four-helix bundle pulls the membranes into close proximity and mediates synaptic exocytosis (see Figure 2). Thus, SNARE proteins are critical for most types of intracellular membrane trafficking and vesicle fusion (Poirier et al., 1998, Rizo and Xu, 2015, Söllner et al., 1993, Sutton et al., 1998). Prior to calcium influx, synaptotagmin and complexin are also bound to the t-SNARE complex, clamping the fusion machinery, and preventing membrane fusion. Upon entering the presynapse, calcium binds to synaptotagmin, thereby activating the calcium sensor. This results in the replacement of complexin, and releases the SNARE complex from the fusion clamp, allowing exocytosis of neurotransmitters (Giraudo et al., 2006, Gramlich and Klyachko, 2019, Rizo and Xu, 2015, Schaub et al., 2006, Südhof, 2013b, Yang et al., 2023).

1.3.1 Syntaxin-1a

Syntaxins constitute a protein family that is involved in membrane fusion and exocytosis. In mammals, 15 different genes have been identified to code for Stx, whereby some of them exhibit different isoforms. Stx1, for instance, can be spliced into the significantly homologous isoforms Stx1a and 1b. The representatives of the syntaxin family exhibit differences in their cellular localisation and function (Bennett et al., 1993, Han et al., 2017, Teng et al., 2001, Yang et al., 2023). Stx1a is specific to the nervous system and is primarily located in the presynaptic plasma membrane, whereas Syntaxin-3 (Stx3) and Syntaxin-4 (Stx4) can be found in the plasma membrane of various cell types (Teng et al., 2001). Nevertheless, a more detailed examination of the distribution of Stx3 and Stx4 within neurones indicates that, while Stx3 is predominantly localised at the axonal plasma membrane, Stx4 is mainly observed at the somatodendritic plasma membrane (Soo Hoo et al., 2016).

Stx1a, as well as Stx3 and Stx4, consist of different domains. A short sequence of the N-terminal end called N-peptide has an essential role in exocytosis and vesicle priming (Misura et al., 2000, Zhou et al., 2013). The adjoining regulatory Habc domain comprises a three-helix bundle and is highly conserved in mammals (Fernandez et al., 1998). This domain is also involved in exocytosis and exerts an influence on spontaneous release and vesicle priming (Zhou et al., 2013). The Habc domain is adjacent to a linker, which is followed by the SNARE (H3) motif (Wang et al., 2017, Yang et al., 2023). The Habc and SNARE domains are capable of forming a closed, inactive conformation through binding with one another. The linker region that separates the two domains is essential for the conformational switch (Dulubova et al., 1999, Yang et al., 2023). As previously outlined, syntaxin constitutes a component of the SNARE complex. The SNARE motif represents the binding site, which, in conjunction with VAMP2 and SNAP-25, forms the four-helix bundle that characterises the SNARE complex (Ogawa et al., 1998, Yang et al., 2001). The binding of the SNARE domain with the Habc domain during the closed conformation effectively prevents this (Dulubova et al., 1999, Richmond et al., 2001). In contrast, the open conformation enables the interaction of Stx with other proteins, thereby also facilitating SNARE complex formation. Consequently, the transition from the closed to the open conformation represents a critical step in the process of membrane fusion

(Richmond et al., 2001). Subsequent to the SNARE domain, the C-terminus comprises the juxtamembrane and the transmembrane regions, which serve to anchor the protein in the membrane (Li et al., 2020b, van den Bogaart et al., 2011, Wang et al., 2017, Yang et al., 2023). However, Stx can switch between a mobile and an immobile state at the membrane. As part of the SNARE complex, Stx is bound to the cell membrane in the immobile phase. If SNARE complex formation is prevented, the mobility of Stx increases and the number of proteins clustered is reduced (Ribrault et al., 2011, Schneider et al., 2015, Yang et al., 2023).

As previously stated, the SNARE complex and the switch from the closed Stx1a to the open conformation is essential for SV fusion (see Figure 2). This is supported by the LE mutation (L165A, E166A) in the linker region of Stx1a, which maintains the open conformation. The prevention of the closed Stx1a conformation facilitates SNARE complex formation (Dulubova et al., 1999), thereby increasing the probability of release and the speed of release (Gerber et al., 2008). Munc18-1 and Munc13-1 play a major role in the regulation of the two conformations (Dulubova et al., 1999, Yang et al., 2015). Munc18-1 binds tightly to the N-peptide, Habc domain, and SNARE motif of the closed Stx1a (Misura et al., 2000). This plays a role in stabilising the inactive form of the protein, thereby preventing the formation of the SNARE complex and thus the transmission of neurotransmitters (Burkhardt et al., 2008, Chen et al., 2008, Deak et al., 2009, Ma et al., 2011). This form of Munc18-1-Stx1a binding (mode I) facilitates the transport of Stx1a to the membrane (Smyth, 2010), and prevents Stx1a from interacting with incorrect proteins or itself to avoid the formation of defective SNARE complexes (Misura et al., 2000, Rizo, 2018, Yang et al., 2023, Zhang and Hughson, 2021). Munc18-1 is also capable of binding to the SNARE complex (mode II). It has been demonstrated that Munc18-1 interacts with both the N-peptide and the SNARE domain of the open Stx. Consequently, the Habc domain is no longer considered essential (Dulubova et al., 2007, Rizo and Xu, 2015, Rizo et al., 2006). In order for Munc18-1 to bind to the SNARE complex, it must first be detached from the closed Stx1a. This process is regulated by tomosyn and Munc13-1 (Jahn and Fasshauer, 2012, Yang et al., 2023). Munc13-1 is also involved in the opening of Stx1a, which then facilitates the formation of the SNARE complex (Ma et al., 2011). The mode II of Munc18-1 and Stx1a binding is implicated in a number of processes, including

docking, priming, and membrane fusion (Dulubova et al., 2007, Rizo and Xu, 2015, Rizo et al., 2006, Smyth et al., 2010, Yang et al., 2023).

In addition to Stx1a, other members of the syntaxin family have also been observed to interact with Munc and other SNARE proteins. For instance, Stx4 is also known to participate in SNARE complex formation, which is supported by Munc18c (Rehman et al., 2017). Thereby, the fusion regulation is analogous to that observed with Munc18-1, although the inhibitory effect on closed Stx could not be proven (Yu et al., 2013). Nevertheless, as with Munc18-1, the interaction between Munc18c and Stx4 prevents the binding of Stx4 to SNAP-23. The open conformation of Stx4 precludes this influence of Munc18c and facilitates the binding of SNAP-23, thereby enabling the docking of Glut4 vesicles in adipocytes (D'Andrea-Merrins et al., 2007). In addition to its involvement in non-neuronal tissues, evidence indicates that Stx4 performs certain functions in neurones. While Stx1a plays a role in transmitter release as part of the SNARE complex, Stx4 is involved in the incorporation of NMDAR and AMPAR into the cell membrane, thereby also influencing synaptic plasticity (Bin et al., 2018, Kennedy et al., 2010, Mohanasundaram, 2010). Moreover, evidence from *Drosophila melanogaster* studies (hereafter Drosophila) indicates that postsynaptic Stx4 has a negative regulatory effect on the neurotransmitter release efficiency in Drosophila, as the absence of Stx4 resulted in an enhancement of neurotransmitter release, despite a reduction in the number of active zones. This could be attributed to an increase in presynaptic calcium channel CaC levels and a decrease in calcium cooperativity (Harris et al., 2018).

Apart from Stx4, Stx3 has also been demonstrated to regulate AMPAR exocytosis as well. However, this impact was confined to long-term potentiation (LTP) and did not extend to constitutive basal exocytosis (Jurado et al., 2013). Moreover, Stx3 is involved in the regulation of epithelial sodium channel expression and in axonal growth by facilitating the selective trafficking of membrane proteins to the axon (Rauh et al., 2020, Soo Hoo et al., 2016). These findings, along with others, illustrate that the syntaxin family and its involvement in membrane fusion serve multiple functions and can thus modify neurotransmission in various ways.

1.3.2 RIM1α

A crucial scaffold protein of the AZ is RIM1α. RIM1α interacts closely with other CAZ, thereby serving a variety of functions, including priming and anchoring of SVs, regulation of SV fusion and neurotransmitter release, and it is essential for both long- and short-term plasticity (Calakos et al., 2004, Castillo et al., 2002, Kaeser and Südhof, 2005, Kaeser et al., 2012, Kintscher et al., 2013, Mittelstaedt et al., 2010, Schoch et al., 2002, Südhof, 2012, Südhof, 2013a, b, Tan et al., 2022, Wu et al., 2023, Yang and Calakos, 2011). RIM1α is a multi-domain protein. From N- to C-terminus, RIM1α comprises an α-helically wrapped zinc finger domain, a PDZ domain, a C2A domain, a proline-rich conserved sequence (PRM1-3), and a C2B domain (Kaeser, 2011, Mittelstaedt et al., 2010, Wu et al., 2023). The second isoform of the RIM1 gene, RIM1β, is homologous to RIM1α but lacks the N-terminal α-helix (Kaeser et al., 2008). The different domains provide the basis for the interaction of RIM with a range of proteins.

For instance, the PDZ domain engages with RIM-BO and ELKS, whereas the C2B domain interacts with Liprinα (Wu et al., 2023, Zürner and Schoch, 2009). Another interaction partner of RIM is Rab3A, which plays a role in the transport of synaptic vesicles to the CAZ, participates in vesicle fusion and exocytosis, and thus regulates neurotransmitter release (Dulubova et al., 2005, Hutagalung and Novick, 2011, Schlüter et al., 2004). It is well established that Rab3A interacts with the α-helix and a SGAWFF motif at the end of the short α helix (Betz et al., 2001, Wang et al., 2001). This interaction facilitates exocytosis, whereas its absence may impair the probability of vesicle release (Schoch et al., 2002, Wang et al., 1997).

In addition, the zinc finger domain of RIM1α binds to the C2A domain present in Munc13-1 (Dulubova et al., 2005, Rizo and Xu, 2015), thereby stabilising Munc (Schoch et al., 2002). The assembly of the RIM1α-Munc13 heterodimer prevents the formation of homodimers by Munc13-1. The homodimerization has been demonstrated to inhibit vesicle fusion, thus the heterodimerization allows vesicle docking, priming, and, subsequently, vesicle fusion (Camacho et al., 2017, Deng et al., 2011, Dulubova et al., 2005, Liu et al., 2019, Rizo, 2018). RIM1α, Rab3A, and Munc13-1 can also form a ternary complex that is thought to be crucial for SV docking and the regulation of neurotransmitter release probability, given that the loss of this ternary complex results in a reduction in the

size of the readily releasable pool (Dulubova et al., 2005, Luo et al., 2017, Rizo, 2018, Sakane et al., 2006, Südhof, 2012).

Furthermoe, RIM1α facilitates the recruitment of voltage-gated calcium channels to the AZ, thereby playing a crucial role in the anchoring of the channels to the release site (Kaeser et al., 2012, Kaeser et al., 2011, Wu et al., 2019). RIM1α thus ensures that the spatial distance between the calcium channels and the vesicle, or more precisely the calcium sensor synaptotagmin, is minimal. This allows for the rapid binding of calcium to synaptotagmin, thus initiating an immediate reaction to the action potential (Kaeser, 2011, Südhof, 2012, Südhof, 2013b, Yang et al., 2023). The interaction of the C2B domain with the β-subunit of the calcium channels inhibits their inactivation, which subsequently enhances the release of neurotransmitters (Kiyonaka et al., 2007).

The listed interactions represent merely a fraction of the functions of RIM1α, yet they already demonstrate the extensive diversification and significance of RIM1α's tasks. It is thus reasonable to hypothesise that the various functions may be regulated by protein modification.

1.4 Aim of the study

Further research on neddylation in neurons is crucial, as previous studies have demonstrated that defective neddylation can contribute to the development of neurodegenerative disorders like Alzheimer´s disease or Parkinson´s disease. It has been demonstrated that neddylation plays a major role in synapses, for example, by influencing synapse maturation, LTP formation, and synaptic transmission (Brockmann et al., 2019, Vogl et al., 2015). Unfortunately, the knowledge about proteins involved, particularly within the presynapse, remains limited. Nevertheless, the identification of neddylation targets, and especially their non-neddylatable variants, is of significant interest, as it can facilitate research on the functions of neddylation. Given that inhibition of neddylation decreases the probability of transmitter release (Brockmann et al., 2019), it is likely that proteins involved in synaptic transmission are neddylated.

In this regard, it is my initial aim to analyse a number of presynaptic proteins for possible neddylation. The investigation will primarily focus on three key criteria: the covalent binding of Nedd8 to the target protein, the contribution of the neddylation-specific

machinery, and the identification of neddylated lysines. For this purpose, a pulldown assay based on avi-tagged Nedd8 will be performed to isolate Nedd8 and all covalently attached proteins. Initially, the following proteins will be analysed for possible neddylation: Stx1a, VAMP, SNAP-25b, Rab3A, SV2A, RIM1α, PINK, Parkin, E-Syt1, and E-Syt2.

2 Material und Methods

2.1 Material

2.1.1 Equipment

Table 1: Equipment used in this study

Equipment	Manufacturer
All-In-One Fluorescence Microscope BZ-X810	Keyence
Analytical Balance	ABS 220-4N, Kern
BioPhotometer	Eppendorf
Casting Module	Mini-PROTEAN® Tetra Cell Casting Module, Bio-Rad
Centrifuge	5702, Eppendorf
Centrifuge	5415 D, Eppendorf
Centrifuge	5810 R, Eppendorf
Centrifuge	5427R, Eppendorf
CO_2 Incubator	HERAcell 150, Heraeus
CO_2 Incubator	HERAcell™ VIOS 160i C, Heraeus
Electrophoresis Power Supply	Electrophoresis Power Supply, E835, Consort
Freezing container Mr. Frosty	Thermo Scientific™
Gene Pulser Electroporationssystem with Pulse Controler	Bio-Rad
Horizontal Shaker	Type 3005, Gesellschaft für Labortechnik GmbH
Imaging System	GelDoc Go Gel Imaging System, Bio-Rad
Imaging System	Odyssey® Fc Imaging System, LI-COR Biosciences
Incubator MIR-153	SANYO
Incubator Shaker HT Ecotron	Infors
Magnetic Stand	Invitrogen™ DynaMag™-2 Magnet, Fisher Scientific
Magnetic Stirrer	big squid ikamäleon, IKA
Magnetic Stirrer	IKAMAG RCT, IKA
Microscope	Axio Vert.A1, Carl Zeiss
Mini Trans-Blot Module	Mini Trans-Blot Module, Bio-Rad
Mini-Centrifuge	Color Sprout Plus Mini-Centrifuge, Biozym

Non-UV Transilluminator	Dark Reader® Non-UV Transilluminators DR-88M, Clare Chemical Research
PCR Thermal Cycler	Biometra T Professional Trio/Biometra Trio, Analytic Jena
pH Bench Meter	FiveEasy™ pH bench meter, FE20, Mettler-Toledo
Pipetboy	macroman, Gilson
Pipetts	Pipetman L, Gilson
Power Supply	Powerpac™ Basic Power Supply, Bio-Rad
Precision Scale	KB 2400-2N, Kern
Safety Cabinet	Herasafe™ 2030i, Fisher Scientific
Safety Laboratory Gas Burner	gasprofi 1 micro, WLD-Tec
Short Plates	Mini-PROTEAN® Short Plates, Bio-Rad
Spacer Plates with Integrated Spacers	Mini-PROTEAN® Spacer Plates with 1.0 mm/1.5 mm Integrated Spacers, Bio-Rad
Spectrophotometers	Nanodrop 2000c Spectrophotometers, Thermo Scientific
ThermoMixer	ThermoMixer™ C with Eppendorf SmartBlock 1.5 mL, Eppendorf
Tube Rotator	VWR Tube Rotator, Avantor
Ultrasonic Homogenizer	Sonopuls™ Ultrasonic homogenizer Mini20, Bandelin Electronic™
Vacuum Aspiration System	Vacusafe™, Integra
Vacuum Pump	ME 1 Vacuum Pump, Vacuubrand
Vertical Polyacrylamide Gel Electrophoresis System	Mini-PROTEAN® Tetra Cell, Bio-Rad
Vortexer	Vortex-Genie™ 2, Scientific Industries
Water bath	Schüttelwasserbad SW20, Julabo

2.1.2 Consumables

Table 2: Consumables used in this study

Consumables	Manufacturer
0.5 ml Reaction tube	Sarstedt
1.5 ml Reaction tube	Sarstedt
15 ml Reaction tube	Sarstedt
50 ml Reaction tube	Sarstedt
24 Well tissue culture plate	VWR
Cell culture dishes, Optilux, Ø 100 mm	Falcon
Cell scraper	Sarstedt
Easy-Grip tissue culture dishes Ø 6 cm	Falcon
Gene pulser electroporation cuvette	Bio-Rad
Immobilon-FL	Merck
Microscope cover glas 12 mm ø	Marienfeld superior
Microscope slides Super Frost Plus	Menzel-Glaser
Nunc™ Cryotube vials	Thermo Scientific
Serological pipettes	Sarstedt

2.1.3 Chemicals

Table 3: Chemicals used in this study

Chemical	Manufacturer
1,10-Phenanthroline, anhydrous	Alfa Aesar
10 % SDS	bioPLUS chemicals
20 % SDS	Serva
2-Mercaptoethanol	Sigma-Aldrich
2-Propanol	VWR
30 % Acrylamide/Bis solution 19:1	Bio-Rad
Agarose Standard	Carl Roth
Ammonium persulfate	Sigma
Aprotinin	Sigma-Aldrich
Bacto Tryptone	Becton, Dickinson and Company
Bacto Yeast extract	Becton, Dickinson and Company
Bovine fibronectin	Sigma-Aldrich
Bovine serum albumin, Fraction V	Biomol
Carbenicillin	Apollo Scientific
D-Biotin	PanReac AppliChem
Dimethyl sulfoxide	Sigma-Aldrich
Disodium phosphate	Merck KGaA
Dulbecco's Modified Eagle Medium	Gibco™
Ethanol	Sigma

Ethidium bromid	Sigma-Aldrich
Fetal calf serum	Sigma-Aldrich
Fluoroshield™ with DAPI	Sigma-Aldrich
Glucose	PanReac AppliChem
Glycerol	Sigma-Aldrich
Glycine	Carl Roth
Hydrochloric acid	VWR
Leupeptin	Panreac AppliChem
Kanamycin sulfate	USB Corp
Magnesium chloride	Merck KGaA
MLN-4947	Chemgood
Methanol	Carl Roth
Minimum Essential Medium	Gibco™
N-Ethylmaleimide	Merck KGaA
Nucleobond Xtra Midi	Macherey-Nagel
Nucleospin Gel and PCR clean-up	Macherey-Nagel
Nucleospin Plasmid	Macherey-Nagel
Paraformaldehyde	Merck
PBS tablets, pH.7,4	PanReac AppliChem
Penicillin/Streptomycin	Gibco™
Pepstatin A	Panreac AppliChem
Pierce Streptavidin magnetic beads	Thermo Scientific
Potassium chloride	Carl Roth
Sodium chloride	Merck KGaA
Sodium deoxycholate	Carl Roth
Sodium dodecyl sulfate	Merck KGaA
Sodium hydroxide	Avantor Performance Materials
TEMED	Carl Roth
Titriplex III	Merck KGaA
TransIT-293	Minus
Tris Base	Promega
Triton X-100	Sigma-Aldrich
Tween-20	Sigma
Urea	VWR Life Science

2.1.4 Organisms

Table 4: Organisms used in this study

Organism	**Strain**
Electrocompetent bacteria	*Escheria coli*
Eukaryotic cells	HEK293T

2.1.5 Antibodies

Table 5: Antibodies used in this study

Antibody	Incubation conditions	Manufacturer
IRDye® 680 RD Streptavidin	4 °C, overnight 1:5000	LI-COR Biosciences
Anti-GFP Antibody (N86/8)	4 °C, overnight 1:1000	NeuroMab
Anti-Flag Antibody (F7425)	4 °C, overnight 1:1000	Sigma-Aldrich
Anti-Nedd8 Antibody (ab81264)	4 °C, overnight 1:2000	abcam
IRDye® 800CW Goat anti-Mouse IgG Secondary Antibody	RT, 1 h 1:10000	LI-COR Biosciences
IRDye® 800CW Goat anti-Rabbit IgG Secondary Antibody	RT, 1 h 1:10000	LI-COR Biosciences

2.1.6 Plasmids

Table 6: Plasmids used in this study

Plasmid	Tag	Species	Reference
AAV CMV hum**BirA**		*E. coli*	Lab V. Gieselmann
pcDNA3.1 **Avi**:TEV:rig:**Nedd8**	Avi	*M. musculus*	Lab V. Stein
pcDNA3.1 **Nedd8 Flag**	Flag	*M. musculus*	Lab V. Stein
pEGFP-C1-**Stx1a**	EGFP	*M. musculus*	Lab S. Schoch
Stx3-pmCitrine	mCitrine	*R. norvegicus*	Addgene
Stx4-pmCitrine	mCitrine	*R. norvegicus*	Addgene
pLenti-Ef1a-GFP-**RIM1α**	GFP	*R. norvegicus*	Lab S. Schoch
pLenti-Ef1a-GFP-**PRM 1-3**	GFP	*R. norvegicus*	Lab S. Schoch
pLenti-Ef1a-GFP-**PRM 1-PA**	GFP	*R. norvegicus*	Lab S. Schoch
pLenti-Ef1a-GFP-**PRM 3-B**	GFP	*R. norvegicus*	Lab S. Schoch
pLenti-Ef1a-GFP-**Z-IUR**	GFP	*R. norvegicus*	Lab S. Schoch
pLenti-Ef1a-GFP-**Z-PRM 1-PA**	GFP	*R. norvegicus*	Lab S. Schoch
pEGFP-mCit-**Snap25b** D179K A199R	mCitrine	*R. norvegicus*	Addgene (53259)
pEGFP-**VAMP2**	EGFP	*M. musculus*	Addgene (42308)
pEGFP-**Rab3A**	EGFP	*H. sapiens*	Addgene (49542)
pAAV-**SV2**-GFP	GFP	*R. norvegicus*	Lab S. Schoch
pEGFP-**parkin WT**	EGFP	*H. Sapiens*	Addgene (45875)
pcDNA-DEST53 **PINK1** N-GFP	GFP	*H. sapiens*	Addgene (13315)
pEGFP-**E-Syt1**	EGFP	*H. sapiens*	Addgene (66830)
EGFP-**E-Syt2**	EGFP	*H. sapiens*	Addgene (66831)

2.1.7 Buffers and media

Table 7: Buffers and media used in this study

Buffer/medium	Components
Blocking solution	5 % BSA, 10 mM Tris Base, 150 mM NaCl, pH 7.6
HEK293T freezing medium	MEM (Gibco), 10 % FBS/FCS, 10 % DMSO
HEK293T medium	500 ml DMEM (Gibco), 50 ml FCS (Gibco), 5 ml Penicillin/Streptomycin (Gibco)
LB medium	10 g/l Tryptone, 5 g/l Yeast extract, 10 g/l NaCl, pH 7
PBS	130 mM NaCl, 10 mM Na_2HPO_4, pH 7.4
RIPA	50 mM Na_2HPO_4, 130 mM NaCl, 0,1 % (w/v) SDS, 1 % (v/v), Triton X-100, 0.5 % (w/v) Sodium deoxycholate, pH 7.0
Running buffer	25 mM Tris Base, 192 mM Glycine, 0.1 % (w/v) SDS, pH 8-9
Sample buffer	8.31 % (v/v) Glycerol, 2.77 mM Tris HCl pH 6.8, 4.22 % (w/v) SDS, 3.3 % (v/v) 2-Mercaptoethanol, 40 µM Biotin
SOB medium	20 g/l Tryptone, 5 g/l Yeast extract, 0.5 g/l NaCl, 2.5 mM KCl, 10 mM $MgCl_2$, pH 7
SOC medium	20 g/l Tryptone, 5 g/l Yeast extract, 0.5 g/l NaCl, 2.5 mM KCl, 10 mM $MgCl_2$, 20 mM Glucose, pH 7
TBS	10 mM Tris Base, 150 mM NaCl, pH 7.6
TBST	10 mM Tris Base, 150 mM NaCl, 0.01 % Tween-20, pH 7.6
TE buffer	1 M Tris-HC, 0,5 M EDTA, pH 8
Transfer buffer	25 mM Tris Base, 192 mM Glycine, 20 % (v/v) Methanol, pH 8-9
Trypsin	45 ml PBS, 5 ml 0.25 % Trypsin-EDTA (Gibco)
Washing buffer 2	8 M Urea, 10 mM Tris HCl pH 8, 100 mM Na_2HPO_4 pH 8, 10 mM 2-Mercaptoethanol, 0.1 % (v/v) Triton X-100
Washing buffer 3	8 M Urea, 2.5 mM Tris HCl pH 6.8, 100 mM Na_2HPO_4 pH 6.2, 10 mM 2-Mercaptoethanol, 0.1 % (v/v) Triton X-100

2.1.8 Software

Table 8: Software used in this study

Software	Reference
BZ-X800 Analyser	Keyence
BZ-X800 Viewer	Keyence
Geneious	Dotmatics
ImageStudio	Licor Odyssey
Prism 8	GraphPad
PyMOL	Schrödinger

2.2 Methods

2.2.1 Cell culture

To prevent contamination, all cell culture procedures were conducted under sterile conditions in a cell culture hood equipped with vertical laminar airflow (Herasafe™ 2030i, Fisher Scientific). The used material was decontaminated with 70 % (v/v) ethanol. Unless stated otherwise, all experiments were performed using HEK293T cells. HEK293T cells are immortalised human embryonic kidney cells that have been transformed with adenovirus 5, which enables the cells to produce a high level of recombinant protein, particularly in vectors with a CMV promoter. Additionally, HEK293T cells possess an SV40 T antigen, which allows them to produce further proteins in vectors with a SV40 promoter (Yuan et al., 2018). Despite their renal origin, HEK cells express markers for a range of other cell types, including neurones, thereby exhibiting characteristics associated with early-stage neuronal differentiation (Hu et al., 2018, Stepanenko and Dmitrenko, 2015). The existing literature on neuronal studies in HEK cells, the robustness and rapid growth of the cell line, coupled with the fact that the cell line is already well-established in our laboratory, led to the decision to perform all experiments using the HEK293T cell line.

2.2.1.1 Cultivation of HEK293T cells

HEK293T cells were cultured in coated 10 cm dishes (Greiner, Bio-One) containing 10 ml Dulbecco´s Modified Eagle´s Medium (DMEM, Gibco) with 10 % fetal calf serum (FCS, Gibco) and 1 % penicillin/streptomycin (Gibco). To mimic a cell´s natural environment, the cells were grown in an incubator maintaining a 5 % (v/v) carbon dioxide (CO_2)/air atmosphere and a temperature of 37 °C. Cells were monitored daily for density and passaged two to three times per week when they reached 80-90 % confluency. After draining the culture medium, the cells were rinsed with 10 ml phosphate buffered saline (PBS), and 1 ml trypsin was used to detach and separate the cells. To stop trypsinization, 9 ml DMEM with supplements was added to the dish. Cells were resuspended and replated according to experimental requirements. In general, the splitting ratio was 1:10.

For transfection, the cells were seeded at a 70 % density onto coated 6 cm dishes. All cells were utilised between passages 14 and 24.

2.2.1.2 Cryopreservation and Revitalisation of HEK293T cells

For long-term storage, HEK293T cells were kept at -150 °C. Once the cells scheduled for freezing reached a confluency of 80-90 %, they were washed with 10 ml PBS, trypsinised, and resuspended in accordance with the previously described protocol. After counting the cells, they were centrifuged at 150 *x g* for five minutes. The cell pellet was resuspended in an appropriate volume of freezing medium to achieve a final cell concentration of 2-4 x 10^6 cells/ml. Cryotubes were filled with 1 ml of the cell solution and frozen in an isopropanol-buffered freezing stand at a cooling rate of -1 per minute in a -80 °C freezer. Upon reaching -80 °C, the cells were transferred to a -150 °C freezer for long-term storage.

To revitalise the cells, they were thawed rapidly. This was facilitated by placing the cryotube in a water bath with a temperature of 37 °C. As soon as possible, the cells were added to 10 ml DMEM and centrifuged at 150 *x g* for five minutes. Following the drainage of the old medium, the cells were resuspended in fresh DMEM and plated on a coated 10 cm dish. After 24 hours the cells were passaged to ensure cell growth and to remove any dead cells, debris, and any residual traces of DMSO.

2.2.1.3 Transfection and cell treatment

Three hours after seeding, cells were transfected with different plasmids. In summary, 500 µl DMEM was combined with up to 7 µg DNA and 20 µl TransIT and then incubated for 20 minutes at room temperature (RT). If required, biotin was added to the cells at a final concentration of 40 µM. After the incubation, the transfection mixture was applied to the cells. 24 hours after transfection, cells were treated with DMSO or MLN-4924 at a final concentration of 1 µM according to the experimental design.

2.2.2 Biochemical methods

2.2.2.1 Protein isolation and purification

Two days after transfection, the cells were harvested for subsequent protein isolation and purification. Initially, the cells were rinsed with warm PBS. Using a cell scraper, the cells were harvested in 1 ml cold RIPA buffer, which had been supplemented with protease inhibitors Aprotinin, Pesptatin A, Leupeptin, OPT10 and NEM. The cells were lysed at 37 °C and disrupted by sonication. A volume of 50 µl from the sample was transferred to another reaction tube and hereafter referred to as 'lysate'. Subsequently, 25-30 µl of streptavidin magnetic beads were added to the remaining sample. The mixture was rotated overnight at 4 °C. After incubation, the beads were washed with 1 ml cold RIPA buffer supplemented with protease inhibitors for five minutes. This was followed by a single wash step with Wash Buffer 2 and two wash steps with Wash Buffer 3 for 10 minutes each. Following a third wash step with Wash Buffer 3 lasting five minutes, the samples were transferred to a new reaction tube. The wash buffer was removed, and the beads were resuspended in 1x sample buffer. The sample obtained in this way is referred to as a 'pulldown'. Twofold loading buffer was added to the lysate sample in a 1:1 ratio. Proteins were eluted at 98 °C for 10 minutes.

2.2.2.2 SDS polyacrylamide gel electrophoresis (SDS Page)

Sodium dodecyl sulphate (SDS) polyacrylamide gel electrophoresis was used to separate the proteins according to their respective molecular weights (Laemmli, 1970). For this purpose, a polyacrylamide gel was prepared, the percentage of which depends on the size of the protein of interest (for the exact recipe, please refer to Table 9, Table 10). Following preparation as described in 2.2.2.1, the samples were centrifuged at 11,000 x g for two minutes. In the following step, a prestained protein marker and 25 µl of every sample were applied to the gel. Prior to this, the magnetic beads were isolated with the magnetic stand in order to prevent their application onto the gel. The voltage was adjusted to 70 V until all protein samples were aligned at the end of the stacking gel. The proteins were then separated at 100 V for approximately 90 minutes.

Table 9: Resolving Gels for Tris-glycine SDS-Polyacrylamide Gel Electrophoresis

	Solution components	**Component volumes (ml) per gel mold volume**			
		10 ml	**15 ml**	**20 ml**	**30 ml**
6 %	**H_2O**	5.3	7.9	10.6	15.9
	30 % acrylamide mix	2.0	3.0	4.0	6.0
	1.5 M Tris (pH 8.8)	2.5	3.8	5.0	7.5
	10 % SDS	0.1	0.15	0.2	0.3
	10 % ammonium persulfate	0.1	0.15	0.2	0.3
	TEMED	0.008	0.012	0.016	0.024
8 %	**H_2O**	4.6	6.9	9.3	13.9
	30 % acrylamide mix	2.7	4.0	5.3	8.0
	1.5 M Tris (pH 8.8)	2.5	3.8	5.0	7.5
	10 % SDS	0.1	0.15	0.2	0.3
	10 % ammonium persulfate	0.1	0.15	0.2	0.3
	TEMED	0.006	0.009	0.012	0.018
10 %	**H_2O**	4.0	5.9	7.9	11.9
	30 % acrylamide mix	3.3	5.0	6.7	10.0
	1.5 M Tris (pH 8.8)	2.5	3.8	5.0	7.5
	10 % SDS	0.1	0.15	0.2	0.3
	10 % ammonium persulfate	0.1	0.15	0.2	0.3
	TEMED	0.004	0.006	0.008	0.012

12 %	**H_2O**	3.3	4.9	6.6	9.9
	30 % acrylamide mix	4.0	6.0	8.0	12.0
	1.5 M Tris (pH 8.8)	2.5	3.8	5.0	7.5
	10 % SDS	0.1	0.15	0.2	0.3
	10 % ammonium persulfate	0.1	0.15	0.2	0.3
	TEMED	0.004	0.006	0.008	0.012

Table 10: 5 % Stacking Gels for Tris-glycine SDS-Polyacrylamide Gel Electrophoresis

Solution components	**Component volumes (ml) per gel mold volume**		
	6 ml	**8 ml**	**10 ml**
H_2O	4.1	5.5	6.8
30 % acrylamide mix	1.0	1.3	1.7
1.0 M Tris (pH 6.8)	0.75	1.0	1.25
10 % SDS	0.06	0.08	0.1
10 % ammonium persulfate	0.06	0.08	0.1
TEMED	0.006	0.008	0.01

2.2.2.3 Western Blot

After electrophoresis, the proteins were transferred to a polyvinylidene difluoride (PVDF) membrane. The protein transfer was conducted using a wet-tank blotting system at 4 °C, typically overnight at a low voltage of 30 V. In some instances, the voltage was elevated to 100 V in order to complete the transfer in 90 minutes. Subsequent to electroblotting, the membranes were permitted to dry for one hour at RT. After activation, the PVDF membranes were blocked in TBS containing 5 % BSA for two hours with gentle agitation. This was done to minimise non-specific binding. The membrane was then incubated with the primary antibody overnight at a temperature of 4 °C. The antibody concentration was

depended on the recommended dose and personal experience (for details, refer to Table 5). The incubation times varied between 24 and 72 hours. Following the primary antibody incubation, the membrane was washed in TBST three times for 10 minutes each. This step served the elimination of unbound antibody residues. Subsequently, the membrane was incubated with the secondary antibody for one hour at RT. To remove unbound secondary antibodies, the membrane was again washed three times with TBST for 10 minutes each. Finally, the fluorescence signal was detected using the Odyssey® Fc Imaging System (LI-COR Biosciences).

2.2.3 Analysis

Each experiment was repeated multiple times and analysed using Image Studio. Statistics were compiled in Prism. Unless stated otherwise, significance was tested using Student's t-test. Differences were considered significant if their p-value was less than 0.05. The data is presented as mean ± S.E.M. Comparisons between different proteins were made mainly within a membrane to minimise the effect of confounding factors.

2.2.4 Imaging

For the imaging approaches, the cells were seeded at a density of 70 % onto glass coverslips, which had been coated with 1% bovine fibronectin in PBS at 37 °C for 30 minutes. Three hours post-seeding, the cells were transfected with various plasmids. The transfection mixture, consisting of 50 µL DMEM, 0.5 µg DNA, and 2 µL TransIT, was incubated for 20 minutes at RT, and then applied to the cells. The next day, the cells were fixed with 4 % PFA in PBS for 15 minutes at RT. Thereafter, the PFA was removed, and the cells were washed with 1 ml PBS thrice. Subsequently, the coverslips were mounted on microscope slides using Fluoroshield™ with DAPI. After drying, the cells were analysed under the fluorescence microscope BZ-X810.

2.2.5 Molecular methods

2.2.5.1 Production of electrocompetent bacteria

In this study, *Escherichia coli* (*E. coli*) was used for all applications involving bacteria. To produce more electrocompetent bacteria, *E. coli* from a frozen stock were plated on an antibiotic-free LB plate and incubated at 37 °C overnight. After 16 to 20 hours, a single colony was selected and transferred to 50 ml of Super Optimal Broth (SOB) medium. The inoculated medium was agitated gently at 37 °C for approximately 12 hours. On the subsequent day, the fresh SOB medium was re-inoculated with the bacteria at a ratio of 1:100. The culture was incubated at 37 °C under mild shaking until the optical density (OD600) reached 0.6. Bacteria were then cooled on ice and centrifuged at 4 °C, 2000 xg for 15 minutes. After discarding the supernatant, the bacteria were resuspended in 10 % glycerol and subjected to another centrifugation process. The washing procedure was repeated twice, decreasing the volume of 10 % glycerol every time. In the third centrifugation step, the relative centrifugal force was reduced to 1750 x g. The supernatant was discarded. The bacteria were resuspended in 2 ml of 10 % glycerol and the optical density (OD600) was again measured. The bacterial sample was diluted with 10 % glycerol to achieve an OD600 of precisely 1. The bacteria were then aliquoted and directly transferred into liquid nitrogen. To confirm the quality of the electrocompetent bacteria, a transformation with puc19 was conducted and spreaded on a LB plate containing ampicillin. The efficiency of the bacteria was catalysed depending on the number of clones. It was anticipated that approximately 109 colonies per microgram of DNA would be observed. The bacteria were subsequently transferred to a -80 °C freezer for long-term storage.

2.2.5.2 Transformation of electrocompetent bacteria

For plasmid reproduction, a quantity of up to 100 ng of DNA was introduced into 50 µl of a suspension containing bacteria. The resulting mixture of bacteria and DNA was transferred to a cold electroporation cuvette and subjected to electroporation at 25 µF, 400 Ω and 2.5 kV. The time constant should be set at 8. After electroporation, 1 ml of SOC

medium was added to the bacterial suspension. Subsequently, the bacteria were transferred to a reaction tube and incubated at 37 °C for 30 minutes. If the DNA had been generated through ligation, the incubation time was extended to 60 minutes. After the incubation period, 100 µl of the bacterial suspension was plated onto LB agar plates containing the relevant antibiotics. Following the transformation of the ligated DNA, the bacterial suspension was centrifuged at 1750 x g for 10 minutes. The majority of the supernatant was discarded, and the entire suspension was plated onto LB agar plates. All plates were incubated at 37 °C overnight.

2.2.5.3 Isolation and purification of DNA

After the transformation of electrocompetent bacteria, a single colony was selected and used to inoculate 100 ml of LB medium containing the appropriate antibiotics. The bacteria were gently agitated at 37 °C overnight. The DNA isolation and purification was conducted in accordance with the instructions provided with the used Kit (Nucleospin Plasmid, Nucleobond Xtra Midi, Macherey-Nagel). The bacterial suspension was centrifuged at 5000 x g and 4 °C for approximately 10 minutes. The supernatant was subsequently discarded. The bacteria were resuspended in Resuspension buffer containing RNase A and *E. coli* were lysed by incubating them in a lysis buffer at RT for five minutes. After this, lysis was stopped by the addition of neutralisation buffer, and the mixture was transferred onto the column contained in the kit. While a filter captured cell debris and other unwanted particles, the DNA was bound by the column. The DNA was subjected to multiple wash steps and then eluted. For larger quantities, an isopropanol precipitation and an additional ethanol washing step were employed. The DNA was then dissolved again in Tris/EDTA buffer. The DNA concentration was quantified using a nanodrop. For long-term storage, the DNA samples were transferred to a -80 °C freezer, while commonly used plasmids were stored at 4 °C.

2.2.5.4 Restriction digestion

In order to assess the functionality of the plasmids and for cloning purposes, plasmids were specifically cut with restriction enzymes. The enzymes selected for use were

optimally adapted to these respective uses. The precise composition of a restriction digest was as followes:

- 0.5-2 µg DNA
- 1 µl restriction enzyme
- 2 µl ThermoFisher FastDigest Green Buffer 10x
- water was added up to 20 µl

The restriction digest was incubated at a temperature of 37 °C for one hour. Although the incubation time and the amount of restriction enzyme used could vary depending on the enzyme used. If the restriction digestion was part of a cloning procedure including a PCR, the quantity of the restriction digest components was adjusted so that the entire PCR preparation was digested.

2.2.5.5 Polymerase chain reaction

Polymerase chain reaction (PCR) was used to amplify DNA fragments and to introduce mutations into the sequence of a plasmid. For instance, specific primers were utilised to generate restriction sites in order to transfer particular sequences into another plasmid or to incorporate point mutations. A typical PCR approach comprised the following components:

- 1 pg-10 ng DNA
- 1 µL 10 mM dNTPs
- 1 µl forward primer
- 1 µl reverse primer
- 0.5 µL Phusion DNA Polymerase
- 10 µl 5X Phusion HF Buffer
- water was added up to 50 µl

A standard PCR approach typically involved a series of essential steps. This included temperature and length-based adjustments dependent on the utilised DNA fragment and

primers employed. Firstly, the DNA was denatured at 96 °C for 30 seconds. In the subsequent step, the primers annealed to the DNA. The temperature of this step was therefore dependent on the melting temperature of the used primers. The annealing process was limited to a maximum of 15 seconds. During the elongation phase, the polymerase incorporated nucleoside triphosphates into the DNA fragment. The temperature was adjusted to the optimum working temperature of the polymerase, which is 72 °C. The time required for this step was contingent upon the length of the amplified fragment and the polymerase's working speed, respectively. After elongation, the DNA was denatured once again, this time at 96 °C for a limited duration of 15 seconds. The previously mentioned steps were then repeated several times in a looped manner until a specified number of loops was reached, which typically ranged from 24 to 40 repetitions. Finally, the DNA fragments were stored at 4 °C until further processing.

2.2.5.6 Agarose gel electrophoresis

Agarose gel electrophoresis was performed for the analysis of DNA fragments according to their respective molecular size. The gel was prepared by dissolving 1 % agarose in TAE buffer and adding 0.005 % (v/v) ethidium bromide. The samples were combined with DNA-loading buffer and applied to the gel. Following digestion in FastDigest Green Buffer, the samples were loaded onto the gel without the addition of further loading buffer. An appropriate marker was employed to identify the sizes of DNA fragments. All agarose gels were run at 90-100 V for 30-60 min, and the results were visualised using a GelDoc Go Imaging System.

2.2.5.7 DNA purification after gel electrophoresis

The DNA sample was purified using the NucleoSpin Gel and PCR Clean-up Kit. For this, the DNA fragments of the desired size were excised from the agarose gel and incubated in 200 µl NTI buffer per 100 mg gel at 50 °C for 10 minutes until the gel was dissolved. Subsequently, the samples were transferred to NucleoSpin Gel and PCR Clean-up columns and centrifuged at 11,000 x g for 30 seconds, thereby facilitating the binding of

the DNA to the silica membrane. The column was washed twice with ethanolic NT3 buffer and centrifuged at 11,000 x g for 30 seconds. In order to dry the silica membrane, the columns were centrifuged another time at 11,000 x g for one minute. Following this, the DNA was eluted by incubating the membrane in 15-30 µl NE buffer for one minute and subsequent centrifugation at 11,000 x g for one minute.

2.2.5.8 Ligation

In the process of cloning, DNA digestion and purification were typically followed by ligation of the DNA fragment, which includes the gene of interest and a vector. The ligation reaction mixture was prepared as shown below:

- 20-100 ng vector DNA
- 1-5:1 insert
- 2 µl 10x ligase buffer
- 1 µl T4 ligase
- water was added up to 20 µl

For each ligation sample, one control was prepared containing only vector DNA. The volume used for the insert was replaced with water. All ligation samples and controls were incubated overnight at 4 °C. After transformation as previously described (see 2.2.5.2), the control and sample plates were compared. In the case of successful ligation, only the sample plate contained colonies; no colonies were anticipated on the control plates. The DNA was isolated and purified as explained in 2.2.5.3. To verify successful ligation, a restriction digestion (see 2.2.5.4) was performed, and the sample was sequenced using a Mix2Seq Sanger Kit.

2.2.5.9 Inserting point mutations

To introduce a point mutation, three PCRs were performed using four different primers. In addition to the forward (1) and reverse primers (2), which bind to the N- and C-termini of the gene of interest, a forward (3) and reverse primer (4) were designed that bind directly

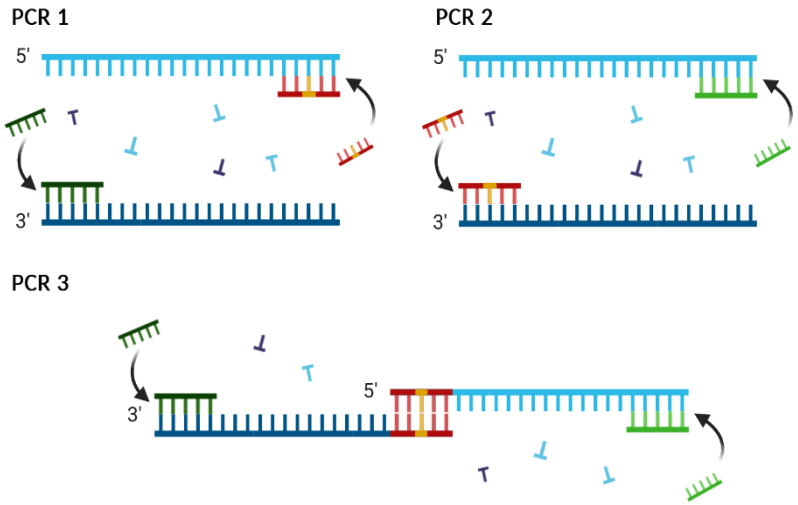

Figure 3: Schematic overview of the three PCRs for inserting a point mutation.

The first PCR uses a forward primer at the N-terminus and a reverse primer over the codon of the amino acid to be modified.The second PCR uses a reverse primer at the C-terminus and a forward primer with the desired mutation. Primers 3 and 4 are modified to encode the desired amino acid. A third PCR is performed using the first two PCR products and primers 1 and 2. Created with BioRender.com

over the codon of the amino acid to be altered. The sequence of the primers was modified to encode the desired amino acid rather than the original one. It is important to note that the modified base should be positioned centrally within the primers (see Figure 3). The first PCR was conducted with the forward primer binding to the N-terminus of the gene of interest (1) and the reverse primer incorporating the desired mutation (4), and the second PCR was run with the reverse primer binding to the C-terminus of the gene of interest (2) and the forward primer including the mutation (3). Information on how to perform the PCR can be found in section 2.2.5.5. After purification of the DNA (see 2.2.5.7), a third PCR was performed with the products of the first two PCRs and the primers 1 and 2. The resulting DNA fragments, which should now be the length of the gene of interest and contain the mutation, were then digested (see 2.2.5.4) and ligated (2.2.5.8) back into a vector.

3 Results

Neddylation plays a role in the post-translational modification of synaptic proteins. Immunoblotting of synaptosomes have demonstrated that both pre- and postsynaptic proteins undergo neddylation (Vogl et al., 2015). In addition, electrophysiological recordings and biochemical experiments support this hypothesis. It seems probable that proteins involved in synaptic transmission are neddylated, given that inhibiting neddylation has been shown to decrease the probability of transmitter release (Brockmann et al., 2019). However, specific proteins have not been identified yet. The aim of this study was therefore, the detection of further presynaptic proteins that are modified through neddylation. To achieve this, I performed a biotin-streptavidin-pulldown with an Avi-tagged Nedd8.

3.1 Neddylation of presynaptic proteins

Avi-tagged Nedd8 and the mCitrine-tagged candidate protein were co-expressed in HEK293T cells. The presynaptic proteins that were investigated for potential neddylation are listed in Table 11. After transfection, the Avi-tag was biotinylated by co-expressed biotin ligase BirA. Following the harvesting of the cells, I isolated the neddylated proteins through magnetic streptavidin beads that bind to the biotinylated Avi-tag of Nedd8. Finally, the neddylated proteins were detected by Western blotting against the GFP-tag. Isolation of the neddylation candidates indicates that Nedd8 is bound to all of the tested proteins. Nedd8 is a protein with structural and functional similarities to ubiquitin. Given this similarity, it is plausible that overexpressed Nedd8 is attached to a protein through the mechanism of ubiquitination rather than neddylation (Hjerpe et al., 2012, Kim et al., 2011, Leidecker et al., 2012, Whitby et al., 1998; for further details please refer to chapter 1.2). To eliminate the possibility of an attachment through atypical neddylation, a second dish of transfected HEK293T cells was treated with MLN-4924, a neddylation-specific NAE1 inhibitor. Upon closer examination of the results, it became evident that MLN-4924 treatment did not result in a decreased signal intensity across all samples.

Table 11: Neddylation target candidates

Parkin
PINK1
Rab3A
RIM1α
SNAP-25b
SV2A
Stx1a
E-Syt1
E-Syt2
VAMP2

3.2 Neddylation of syntaxin

Due to the established impact of neddylation on synaptic transmission, the first protein of interest was Stx1a. Stx1a is a component of the SNARE complex, which is of high importance for vesicle fusion during synaptic transmission (Rizo and Xu, 2015). Although Stx1a plays a role in exocytosis and vesicular transport mechanisms in other cell types as well, Nothern blot analysis revealed that Stx1a transcripts were exclusively expressed in brain tissue and not in the kidney (Bennett et al., 1993, Lam et al., 2005, Yang et al., 2023). It was therefore assumed that the expression of Stx1a in HEK293T cells that derive from kidney cells may not be optimal, despite some studies confirming the efficacy of HEK293T cells for neuronal studies. Given the additional advantages of HEK293T cells and the fact that they have already been established in our laboratory, the decision to use HEK293T cells was maintained (see 2.2.1). In addition to Stx1a, the syntaxin protein family includes other proteins that are highly similar in structure and function. In the kidney,

for instance, Stx4 is known to be involved in vesicle transport (Mandon et al., 1996, Mistry et al., 2009). Given that Stx1a and Stx4 are homologous, it was decided that the expression of Stx4 in HEK293T cells would be an appropriate starting point for the first experiments.

3.2.1 Neddylation of Stx4

As previously described, HEK239T cells were transfected with Stx4-mCitrine, Avi-Nedd8 and the biotin ligase BirA. Avi-Nedd8 and any associated proteins were isolated using

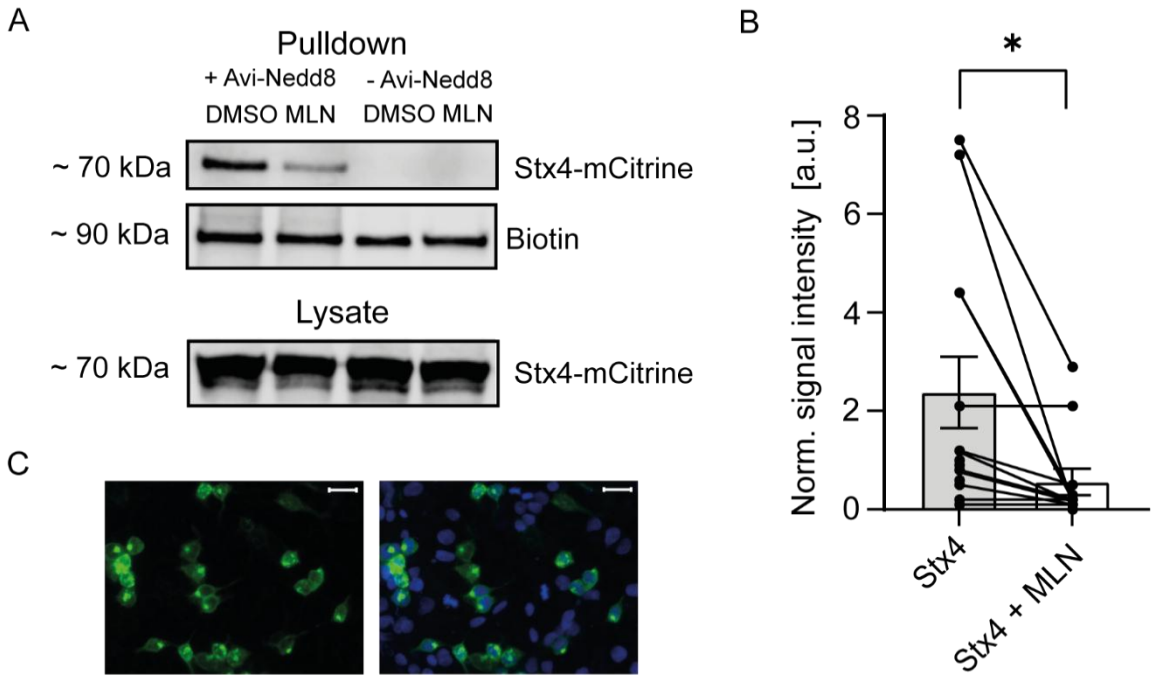

Figure 4: Neddylation of Stx4

(A) The representative western blot demonstrates that Stx4-mCitrine could be isolated with magnetic streptavidin beads in the presence of Avi-Nedd8, but not without. A primary GFP antibody was used for the Stx4-mCitrine detection and fluorescently labelled streptavidin for biotinylated carboxylases. The samples on the left side of the blot were co-transfected with Avi-Nedd8, while the samples on the right side were not. In both cases, one sample was treated with vehicle (DMSO) and the other with 1 µM MLN-4924. The expected size of Stx4-mCitrine is approximately 62 kDa; binding of Avi-Nedd8 increases the size to 76 kDa. Experiments were conducted using HEK293T cells. (B) The GFP signal was normalised with the carboxylase bands. Treatment with MLN-4924 resulted in a significant reduction in Stx4-mCitrine neddylation. The data is presented as mean ± SEM (76 % decrease, paired t-test: p-value=0.0171, N=12). (C) The microscopic image shows HEK293T cells transfected with Stx4-mCitrine and stained with DAPI (right). The signal was predominantly localised to the cell membrane. Scale bar, 20 µm.

magnetic streptavidin beads and separated by western blot. The blots illustrate the results of the pulldown procedure as well as the lysate, which comprises all the proteins present in the cell prior to the pulldown process.

Light microscopic examination of the transfected cells revealed an increased GFP signal in the cell, indicating that Stx4-mCitrine expression was succesful (see Figure 4C). The signal was predominently located in the plasma membrane suggesting that Stx4-mCitrine was present in the membrane and therefore correctly folded in the HEK293T cells. To identify the neddylation candidate proteins, an anti-GFP antibody was used that specifically targets the tag associated with these proteins. The anti-GFP antibody (clone N86/8) from Neuromab (see Table 5) has been shown to recognise the jellyfish green fluorescent protein (GFP), as well as the cyan and yellow fluorescent proteins (CFP and YFP). Therefore, it is not exclusively specific for GFP. The mCitrine tag used in this study is identical to YFP except for two amino acids and differs from GFP by only seven amino acids. Due to this strong similarity, the anti-GFP antibody can also be used to detect mCitrine. The blot of the lysate demonstrated two bands detected by the anti-GFP antibody, at the levels of the mCitrine-tagged Stx4 (62 kDa) and another at 76 kDa. The higher band exhibited greater intensity and corresponded to the size of the mCitrine-tagged Stx4 and bound Avi-Nedd8. A band at 76 kDa was also clearly visible on the blot showing the eluted proteins from the pulldown assay (see Figure 4A). When the neddylation pathway was blocked by the addition of MLN-4924, a statistically significant reduction in the intensity of the band was observed (see Figure 4B). The pronounced impact of MLN-4924 was not discernible in the case of bands at 90 kDa that were detected by flourescently labelled streptavidin. These bands were suggested to be endogenously biotinylated carboxylases and demonstrated the eficiancy of the pulldown procedure. In a control experiment, Stx4-mCitrine was expressed with BirA but without Avi-Nedd8. In the absence of Avi-Nedd8, no band could be seen in blots probing the eluate of the pulldown assay (see Figure 4A). These results confirmed that the mCitrine-tagged Stx4 was indeed isolated by Avi-Nedd8 and not by endogenous biotinylation, thereby suggesting that Stx4 is a promising Nedd8 target candidate.

A further step in identifying neddylation targets is the discovery of the neddylated lysine residues. As Stx4 contains a large number of lysines, the cloning of truncated proteins represented a valuable approach to accelerate the search. Like all syntaxins,

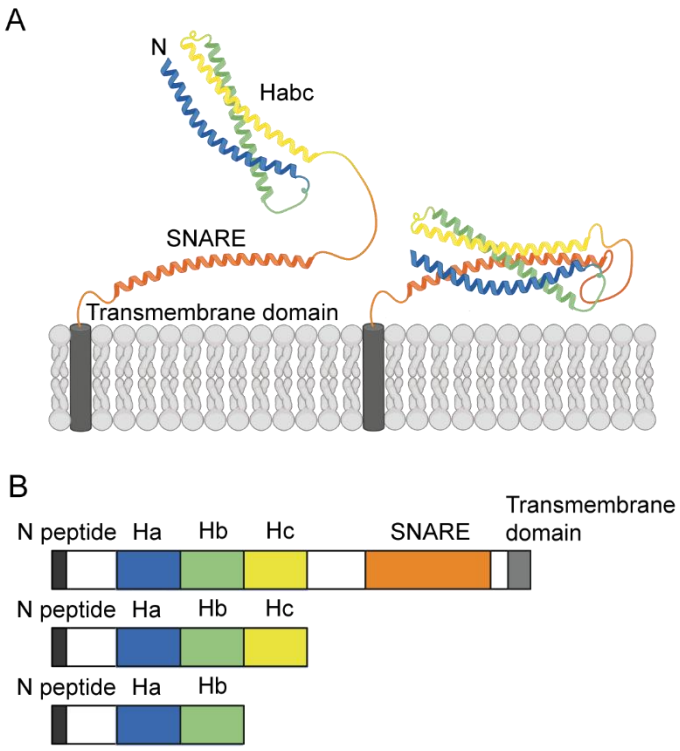

Figure 5: Domains of syntaxin and truncated forms

Stx comprises distinct domains, including the N-petide, the Habc domain, a linker, the SNARE motif, a juxtamembrane region and a transmembrane region. (A) The binding of the Habc and the SNARE domain results in an inactive closed conformation. (B) To facilitate the identification of neddylated lysine residues, truncated proteins were created that lack the SNARE domain or both the SNARE and Hc domain. Created with BioRender.com

Stx4 is comprised of distinct domains. The N-terminal end of the protein contains a short sequence, the N-peptide, which is followed by the Habc and the SNARE domain. The Habc and SNARE domains are separated by a linker that facilitates their interaction and the formation of an inactive conformation. The C-terminus, comprising the juxtamembrane and transmembrane regions, serves to anchor the protein within the membrane (see Figure 5A; please refer to 1.3.1). In order to reduce the number of potential neddylated lysine residues, C-terminal clones were truncated. Stx4-Habc, which lacks the SNARE and the transmembrane domain, was cloned with the intention of eliminating the importance of lysines located in these C-terminal domains. To create Stx4-Hab, the Habc domain was additionally truncated (see Figure 5B). After removing the transmembrane domains of both truncated Stx4 proteins, the protein was no longer membrane-anchored

but rather cytosolic. This was also reflected in the light microscopic images of the transfected cells (see Figure 6C). Western blot analysis using anti-GFP antibodies revealed the presence of prominent bands at 50 kDa and 41 kDa in the lysate eluates of both the DMSO and MLN-4924 treated samples. The molecular weight of these bands was consistent with that of Stx4-Habc and Stx4-Hab. This confirmed the successful transfection and expression of the truncated proteins. The blot probing the eluted proteins from the pulldown assay exhibited only a narrow, faint band corresponding to Stx4-Habc. No band was observed in the Stx4-Hab lane of the same blot. The biotinylated carboxylase bands acted as a control demonstrating that the absence of the Stx4-Hab band was not caused by insufficient pulldown procedure but presumably because Stx4-Hab was not bound to Avi-Nedd8, thus preventing isolation of this protein by magnetic streptavidin beads (see Figure 6A). The experiment was repeated multiple times for both truncated proteins. In the case of Stx4-Hab, no GFP band was visible in any of the blots probed with pulldown eluates. In three out of five blots, a GFP band similar to the one shown in the example blot was detected in the Habc samples from the pulldown assay (see Figure 6A). A comparison of the signal intensity of the GFP bands corresponding to Stx4-Habc with those of WT Stx4 samples in blots probing pulldown eluates showed that the intensity of the WT bands was higher than that of the Stx4-Habc samples, even in samples treated with MLN-4924 (see Figure 6B). These results suggest that the SNARE and Hc domain participate in neddylation of Stx4. The complete elimination of the Stx4 band in blots showing eluates of the pulldown assay, after removing the Hc and SNARE domains, while a slight band was partially visible after removal of the SNARE domain, indicated that the lysine residues located in the Hc domain should be analysed first. The Hc domain of Stx4 contains five lysine residues: K123, K124, K140, K151 and K161. To prevent any potential interaction with Avi-Nedd8, all five lysines were replaced by an arginine. Arginine is a polar, positively charged amino acid that consists of a long side chain similar to that of lysine. A notable difference between the two amino acids is the presence of a guanidium group in arginine, which results in the amino acid being slightly larger. Due to the similar characteristics, especially with regard to polarity and positive charge, it is assumed that the mutation does not impair the tertiary structure of the protein (Sokalingam et al., 2012). The expression of the mutant forms of Stx4 in HEK293T cells indicated that the protein was folded correctly. In contrast to the truncated proteins, which

were distributed throughout the cytosol, the GFP signal of all five mutants was concentrated at the cell membrane (see Figure 7C, Figure 8C). This indicated that the expression of Stx4 K123R, K124R and K123-124R was successful. The first lysines examined were K123 and K124. As both lysins are in close proximity to each other, a double mutant was included in the investigation. The western blot of the lysate samples revealed the presence of two bands, detected by an anti-GFP antibody, with a similar similar molecular weight. The higher band was observed to have a molecular weight of approximately 76 kDa, which corresponds to the Stx4-Avi-Nedd8-complex. The lower band exhibited a molecular weight of 62 kDa, which is comparable to that of Stx4-mCitrine.

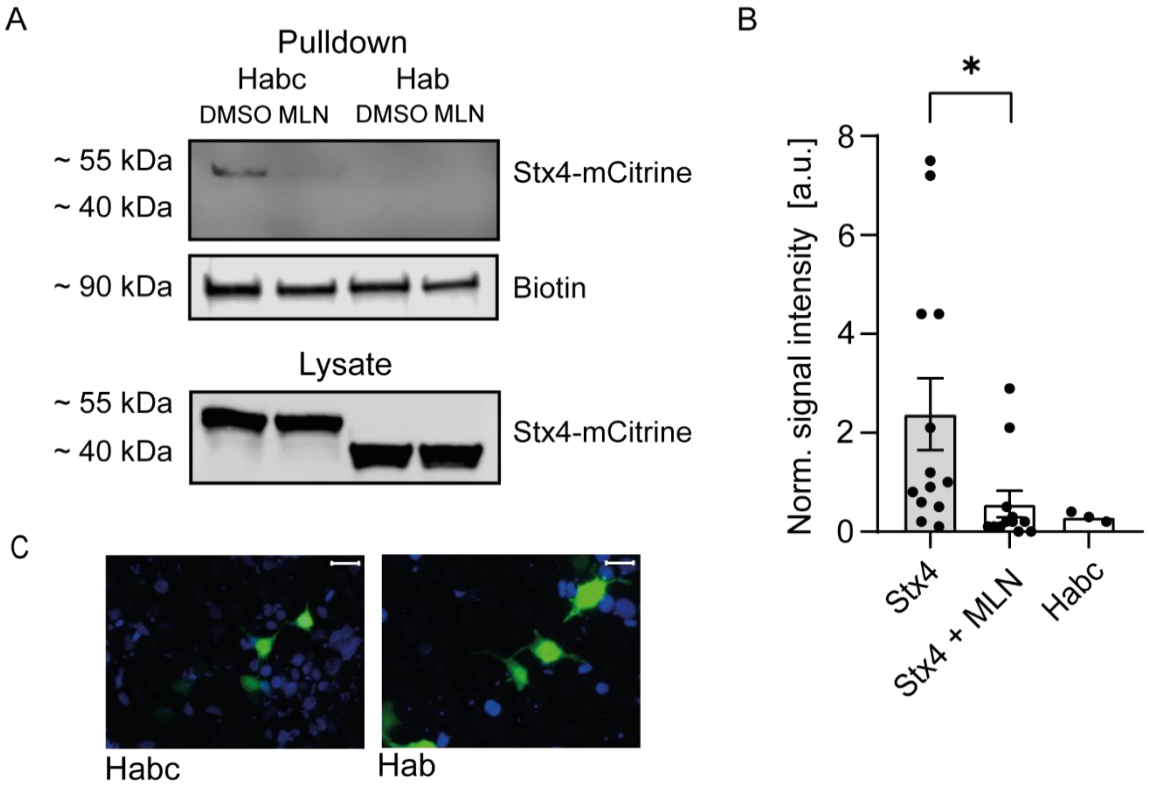

Figure 6: Neddylation of truncated Stx4

(A) The representative western blot demonstrates that Stx4-Habc could be isolated with magnetic streptavidin beads; no isolation was possible for Stx4-Hab (N=4). A primary anti-GFP antibody was used for the Stx4-mCitrine detection and fluorescently labelled streptavidin for biotinylated carboxylases. The samples were treated either with vehicle (DMSO) or with 1 µM MLN-4924. The expected size of Stx4-Habc is 49 kDa; the band corresponding to Stx4-Hab is at a size of 41 kDa. Avi-Nedd8 attachment increases the size by 14 kDa. Experiments were conducted using HEK293T cells. (B) The GFP signal was normalised with the carboxylase bands. Removing the SNARE domain decreased neddylation by 88 %. (N=3). The data is presented as mean ± SEM. (C) The microscopic image shows HEK293T cells transfected with truncated Stx4-mCitrine and stained with DAPI. Scale bar, 20 µm.

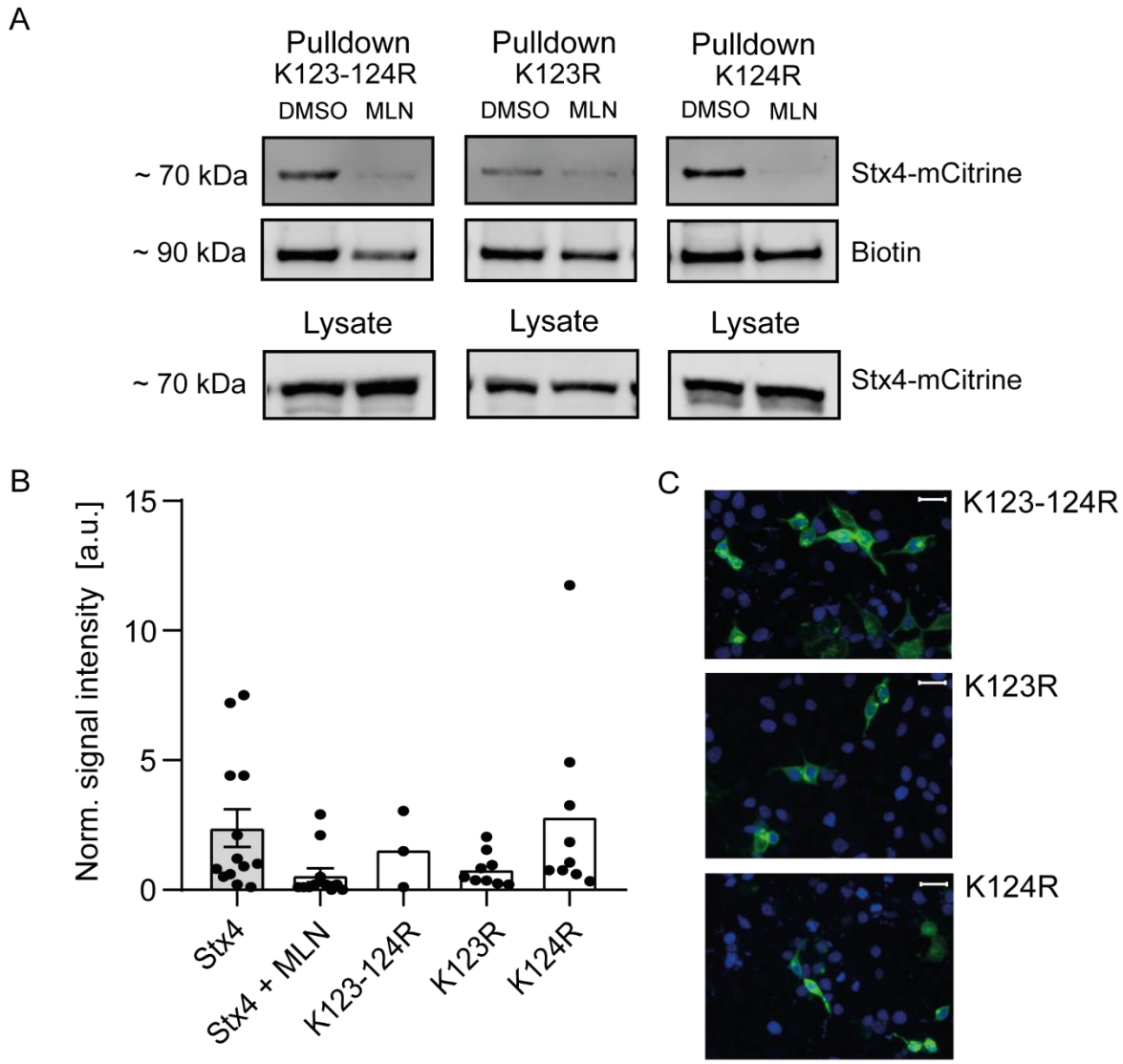

Figure 7: Neddylation of Stx4 K123-124R, K123R and K124R

(A) The representative western blot demonstrates that all Stx4 mutants could be isolated with magnetic streptavidin beads. A primary anti-GFP antibody was used for the Stx4-mCitrine detection and fluorescently labelled streptavidin for biotinylated carboxylases. The samples were treated either with vehicle (DMSO) or with 1 µM MLN-4924. The expected size of Stx4-mCitrine is 62 kDa; binding of Avi-Nedd8 increases the size to 76 kDa. Experiments were conducted using HEK293T cells. (B) The GFP signal was normalised with the carboxylase bands. The substitution of the lysine residues with arginine at positions 123 and 124 resulted in a modification of the neddylation level of Stx4. The data is presented as mean ± SEM (K123-124R: 36 % decrease, paired t-test: p-value=0.8689, N=3; K123R: 67 % decrease, unpaired t-test: p-value=0.0902, N=9; K124R: 16 % increase, unpaired t-test: p-value=0.7525, N=9). (C) The microscopic image shows HEK293T cells transfected with mutated Stx4-mCitrine and stained with DAPI. The signal was predominantly localised to the cell membrane. Scale bar, 20 µm.

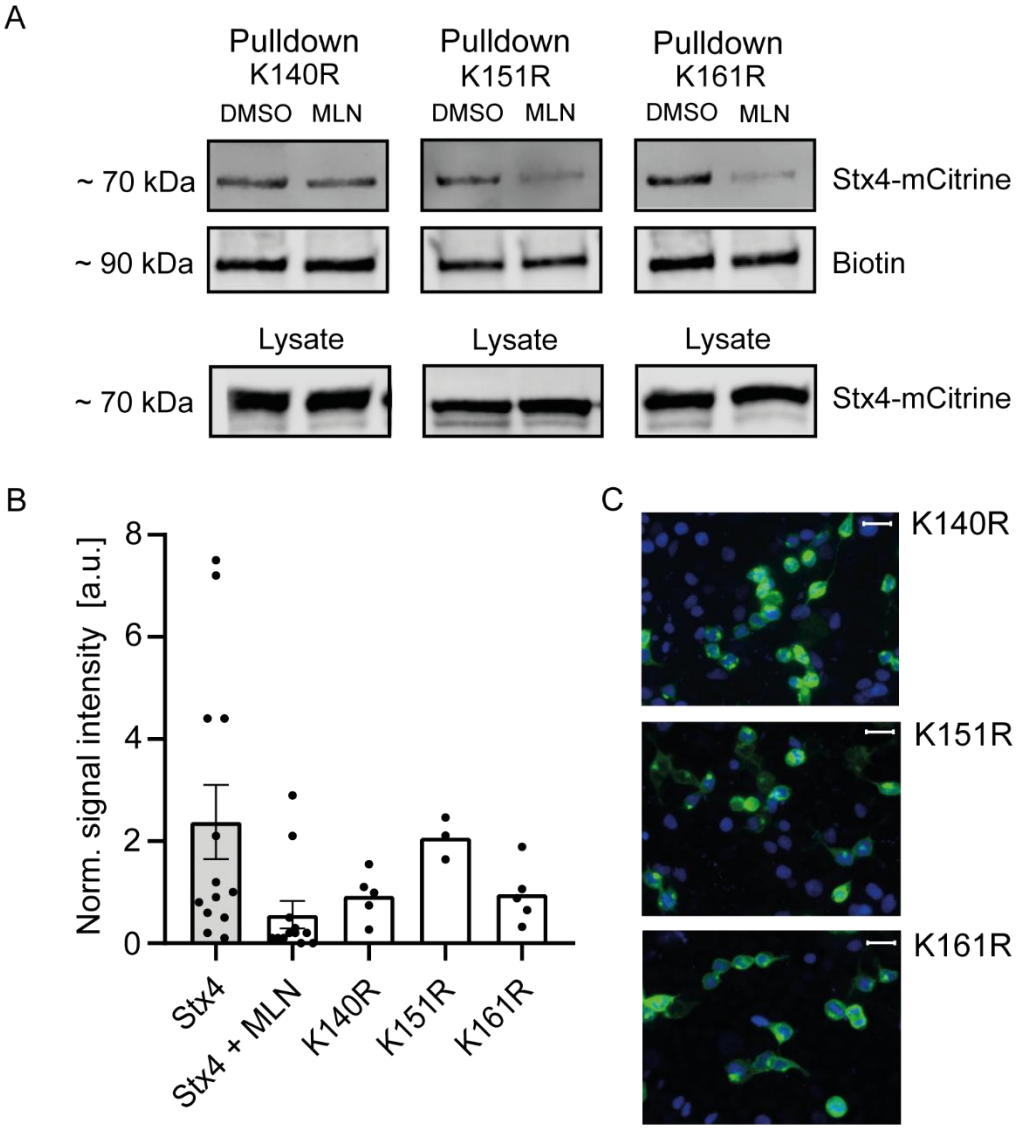

Figure 8: Neddylation of Stx4 K140R, K151R and K161R

(A) The representative western blot demonstrates that all Stx4 mutants could be isolated with magnetic streptavidin beads. A primary anti-GFP antibody was used for the Stx4-mCitrine detection and fluorescently labelled streptavidin for biotinylated carboxylases. The samples were treated either with vehicle (DMSO) or with 1 µM MLN-4924. The expected size of Stx4-mCitrine is 62 kDa; binding of Avi-Nedd8 increases the size to 76 kDa. Experiments were conducted using HEK293T cells. (B) The GFP signal was normalised with the carboxylase bands. The substitution of the lysine residues with arginine at positions 140, 151 and 161 resulted in a modification of the neddylation level of Stx4. The data is presented as mean ± SEM (K140R: 63 % decrease, unpaired t-test: p-value=0.2455, N=5; K151R: 13 % decrease, unpaired t-test: p-value=0.8465, N=3; K161R: 59 % decrease, unpaired t-test: p-value=0.2563, N=5). (C) The microscopic image shows HEK293T cells transfected with mutated Stx4-mCitrine and stained with DAPI. The signal was predominantly localised to the cell membrane. Scale bar, 20 µm.

Despite the mutations, GFP bands were also observed in blots of pulldown assay eluates, thereby demonstrating that isolation of the mutated Stx4 was still possible (see Figure 7A). Furthermore, all three Stx4 mutants exhibited sensitivity to MLN-4924. However, the Stx4 mutants could not be isolated in every pulldown assay that was conducted. The double mutants K123,124R and K123R were only detected in 50 % of the pulldown eluates, while GFP bands were observed in 70 % of the blots probing K124R. In addition, the degree of signal intensity exhibited by the GFP bands in the pulldown eluates differed for all mutants, while the intensity of the carboxylase bands, which served as a positive control, remained similar across all samples. The band intensity of K124R was particularly prominent, whereas that of K123R appeared to be less pronounced. In comparison to the values observed for WT Stx4, K123-124R and K124R showed no meaningful difference. In contrast, the band intensity of K123R only reached 33 % of WT intensity (see Figure 7B). Given that MLN-4924 has been shown to result in an intensity decrease of 25 %, this reduction can be considered a significant impact.

Subsequently, lysines 140, 151 and 161 were analysed for neddylation. The presence of GFP bands in the blot of lysate proteins as well as the carboxylase bands observed in the western blot of eluated pulldown samples indicated that both the expression and the pulldown procedure were successful. All three variants of mutated Stx4 were isolated through magnetic streptavidin beads as well, yet the intensity of the different samples once more exhibited variation (see Figure 8A). This difference was particularly apparent in the provided graph. The band intensity of the K151R samples reached values that were comparable to those of the WT. However, the mean intensity of the mutants K140R and K161R was found to be reduced compared to the values observed for WT samples. This reduction represented only 37 % of the WT value for K140R and 41 % for K161R (see Figure 8B). Together with the preceding findings, it can be surmised that K124 and K151 do not significantly contribute to the process of neddylation. Conversely, mutation of K140 and K161 led to a reduction in band intensity, which indicates a potential participation in neddylation. Lysine 123 is of particular interest, exhibiting a reduction of 33 %, making it a promising Nedd8 target residue.

A series of prior studies on Cofilin1 conducted in our laboratory led to the hypothesis that the binding site for Ubc12 is constituted by three triangular lysines of the

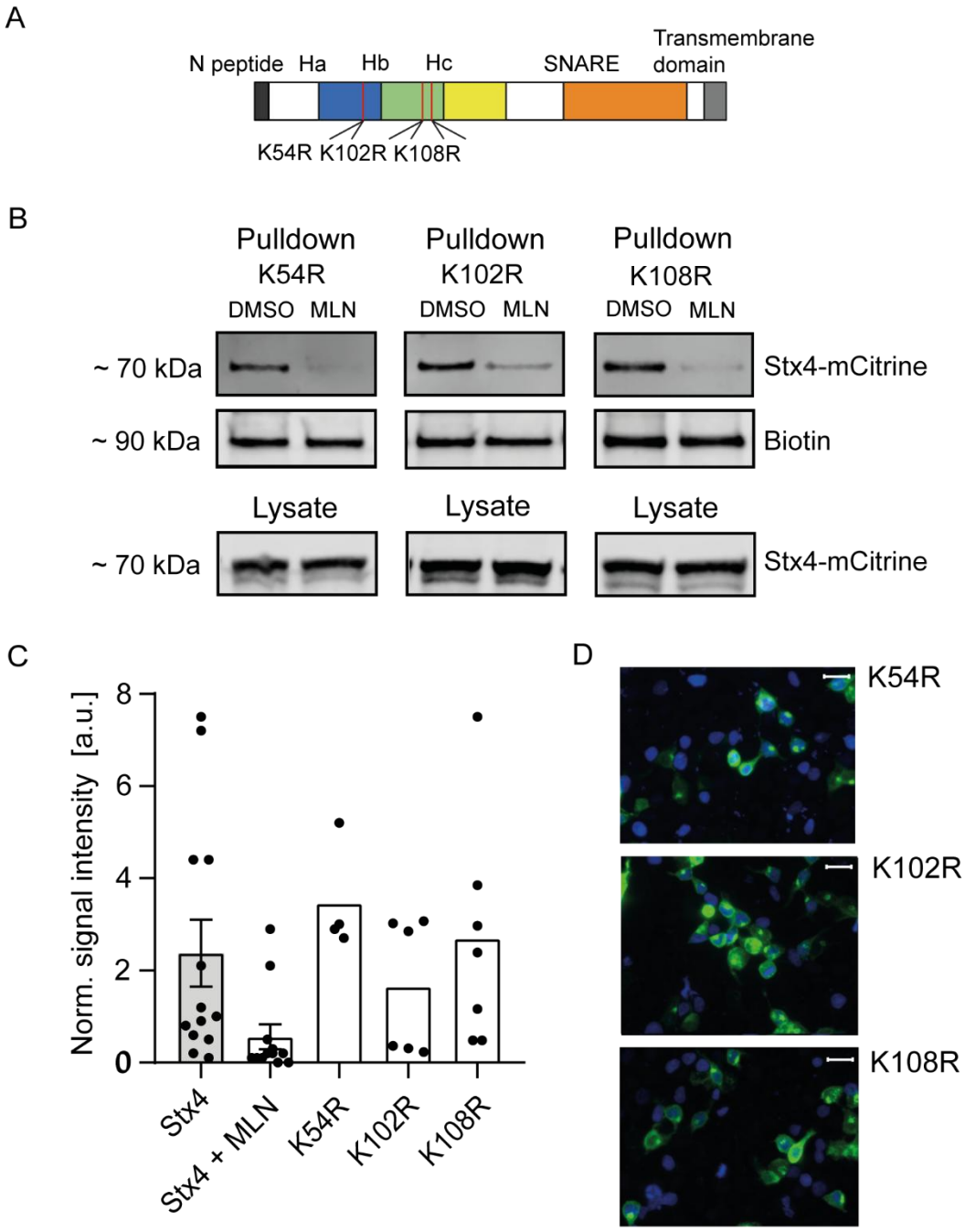

Figure 9: Neddylation of Stx4 K54R, K102R and K108R

(A) The mutated lysine residues are located in the Ha and Hb domain. Created with BioRender.com (B) The representative western blot demonstrates that all Stx4 mutants could be isolated with magnetic streptavidin beads. A primary anti-GFP antibody was used for the Stx4-mCitrine detection and fluorescently labelled streptavidin for biotinylated carboxylases. The samples were treated either with vehicle (DMSO) or with 1 µM MLN-4924. The expected size of Stx4-mCitrine is 62 kDa; binding of Avi-Nedd8 increases the size to 76 kDa. Experiments were conducted using HEK293T cells. (C) The GFP signal was normalised with the carboxylase bands. The substitution of the lysine residues with arginine at positions 54, 102 and 108 resulted in a modification of the neddylation level of

Stx4. The data is presented as mean ± SEM (K54R: 45 % increase, unpaired t-test: p-value=0.4465, N=4; K102R: 34 % decrease, unpaired t-test: p-value=0.532, N=6; K108R: 13 % increase, unpaired t-test: p-value=0.7981, N=7). (D) The microscopic image shows HEK293T cells transfected with mutated Stx4-mCitrine and stained with DAPI (right). The signal was predominantly localised to the cell membrane. Scale bar, 20 µm.

target protein. This hypothesis is based on the observation that glutamate 78, aspartate 117 and glutamate 143 of Ubc12 also form a triangle that is negatively charged. The attraction of the three amino acids and the positively charged lysines may be of great importance with regard to the binding of Ubc12 to the target protein (Einsfelder, 2022). On the basis of the assumption that lysines 123, 140 and 161 play a role in neddylation of Stx4, the protein was examined for the presence of analogous triangles. Three triangles were of particular interest: K54, K140 and K151; K54, K140 and K161; and K102, K108 and K123/124. In order to investigate whether these triangles serve as binding sites, lysines 54, 102 and 108, which are located in the Ha or Hb domain, were also mutated to arginine (see Figure 9A). The three mutated Stx4 variants also exhibited a pronounced GFP signal in the cell membrane of transfected HEK293T cells (see Figure 9D). It was therefore assumed that the proteins were correctly folded. The bands of the lysate samples corresponding to Stx4-mCitrine and the carboxylase bands, which serve as a positive control for the pulldown procedure, displayed strong intensities. In addition, bands corresponding to the mutated Stx4-mCitrine could also be observed in the blots showing the eluted proteins of the pulldown assay (see Figure 9B). The band intensity of samples treated with MLN-4924 was found to be lower than that of samples treated with DMSO. Nevertheless, in comparison to the WT bands, none of the mutations resulted in a clearly reduced band intensity. The mean intensity of K108R samples was similar to that of the WT. Conversely, mutation of lysine 54 even resulted in an increase in band intensity (see Figure 9C). Overall, these results suggest that lysines 54, 102 and 108 are unlikely to represent a binding site for Nedd8. Similarly, the hypothesis that the amino acid lysine plays a significant role in the binding of Ubc12 to the target protein could not be proven either.

3.2.2 Neddylation of Stx1a

Following the identification of Stx4 as a promising candidate for neddylation, it was of great interest to investigate Stx1a as well. As previously observed for Stx4, light microscopy revealed that the GFP signal was not uniformly distributed in HEK293T cells but showed a predominant localisation to the cell membrane (see Figure 10C). This suggested that Stx1a-GFP was also correctly folded despite its low natural abundance in the kidney. Western blots confirmed the successful expression of Stx1a-GFP. Anti-GFP antibodies detected two bands in the blots probing the lysate as well as the pulldown

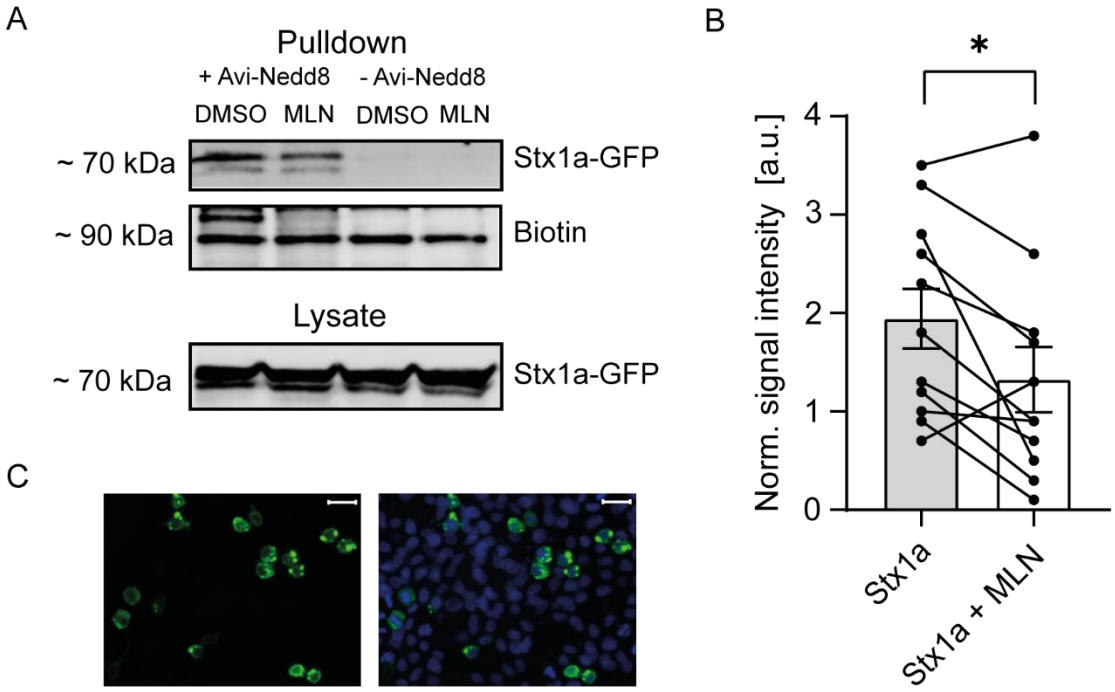

Figure 10: Neddylation of Stx1a

(A) The representative western blot demonstrates that Stx1a-GFP could be isolated with magnetic streptavidin beads in the presence of Avi-Nedd8, but not without. A primary anti-GFP antibody was used for the Stx1a-GFP detection and fluorescently labelled streptavidin for biotinylated carboxylases. The samples on the left side of the blot were co-transfected with Avi-Nedd8, while the samples on the right side were not. In both cases, one sample was treated with vehicle (DMSO) and the other with 1 µM MLN-4924. The expected size of Stx1a-GFP is approximately 61 kDa; binding of Avi-Nedd8 increases the size to 75 kDa. Experiments were conducted using HEK293T cells. (B) The GFP signal was normalised with the carboxylase bands. Treatment with MLN-4924 resulted in a significant reduction in Stx1a-GFP neddylation. The data is presented as mean ± SEM (32 % decrease, paired t-test: p-value=0.0219, N=11). (C) The microscopic image shows HEK293T cells transfected with Stx1a-GFP and stained with DAPI (right). The signal qs predominantly localised to the cell membrane. Scale bar, 20 µm.

samples. In contras to Stx4, the size difference of these bands was not 13 kDa, which would be expected for Avi-Nedd8 attachment. It is therefore unlikely that the two bands represent Stx1a without and with bound Avi-Nedd8. Apart from Nedd8, other post-translational modifications are known to alter the band size of proteins in western blots. Stx1a is modulated through various modifications like phosphorylation and palmitoylation (Vardar et al., 2022). The latter was shown to influence the size of Stx1a in western blots. The different band sizes are therefore probably the result of other post-translational modifications.

To ensure that the isolation of Stx1a-GFP during the pulldown process was not due to endogenous biotinylation but due to the binding of Avi-Nedd8, a second approach was performed without Avi-Nedd8. After the pulldown assay, the western blot revealed a clear band detected by an anti-GFP antibody in the sample transfected with Avi-Nedd8, which was absent in the lane without Avi-Nedd8. In contrast, the blots probed with lysate proteins showed GFP bands with similar intensities for all four samples. Furthermore, in blots probing pulldown eluates, the bands corresponding to the carboxylases, which serve as a positive control for the pulldown procedure, were visible in the lanes of both the samples with Avi-Nedd8 co-expressing and Avi-Nedd8 deficient samples (see Figure 10A). This suggested that the missing GFP band in the blots of pulldown eluates was a consequence of a lack of neddylation rather than an impaired expression or pulldown procedure. Western blot analysis using fluorescence-labelled streptavidin revealed the presence of an additional band at 105 kDa in the pulldown eluates from samples co-expressing Avi-Nedd8, which was removed by MLN-4924 treatment. The molecular weight of this band is consistent with that of Cul1 bound to Avi-Nedd8, indicating that the band corresponded to Cul1-Avi-Nedd8 complexes. The absence of this band in Avi-Nedd8-deficient samples further supported the hypothesis that Stx1a cannot be isolated without Avi-Nedd8 due to the lack of neddylation. Although the differences between DMSO treated and MLN-4924 treated samples did not appear to be pronounced, the diagram still demonstrated that MLN-4924 significantly decreased the band intensity (see Figure 10B). Given that MLN-4924 does not induce deneddylation but only prevents new neddylation, the weaker effect of MLN-4924 does not negate the possibility that Stx1a is a promising Nedd8 target.

In order to narrow down the choice of neddylated lysines, truncated variants of Stx1a were examined (see Figure 5). First, the SNARE domain was removed to generate

GFP-tagged Stx1a-Habc, and the Hc domain was eliminated in addition, creating Stx1a-Hab. A further variant, also lacking the Hb domain, was examined. In the absence of the transmembrane anchor, all three truncated proteins were evenly distributed in the cytosol instead of being more abundant in the membrane (see Figure 11B). In contrast to Stx4, the blot showing the eluted proteins from the pulldown assay did not show a GFP band for any of the three truncated Stx1a proteins. Nevertheless, the robust GFP bands in the blots of the lysate samples and the carboxylase bands used as a positive control for the pulldown assay demonstrated that both the protein expression and the pulldown had been successfully achieved. The efficacy of the neddylation with Avi-Nedd8 was evidenced by the presence of a cullin band above the carboxylase band in the DMSO samples (see

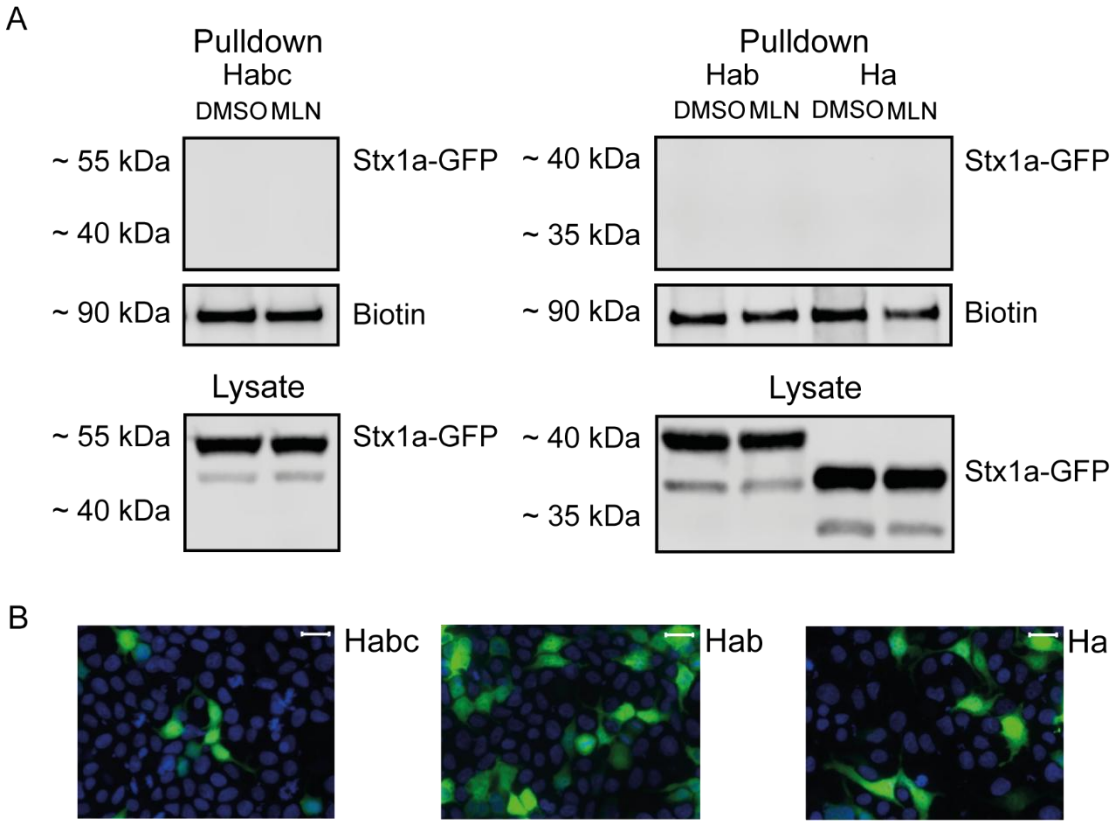

Figure 11: Neddylation of truncated Stx1a

(A) The representative western blot demonstrates that no isolation was possible for Stx1a-Habc (N=13), Stx1a-Hab (N=10) and Stx1a-Ha (N=7). A primary anti-GFP antibody was used for the Stx1a-GFP detection and fluorescently labelled streptavidin for biotinylated carboxylases. The samples were treated either with vehicle (DMSO) or with 1 µM MLN-4924. The expected size of Stx1a-Habc is 50 kDa; the band corresponding to Stx1a-Hab is at a size of 40 kDa; the size of Stx1a-Ha is expected to be 35 kDa. Experiments were conducted using HEK293T cells. (B) The microscopic image shows HEK293T cells transfected with truncated Stx1a-GFP and stained with DAPI. Scale bar, 20 µm.

Figure 12: Homology between the different syntaxins

Lysine 123, the most promising neddylation residue in Stx4, is absent in Stx1. The lysines closest to position 123 are 117 and 126. A double mutant, K117,126R, was cloned for simultaneous investigation. Created with BioRender.com

Figure 11A). Therefore, the inability of the truncated variants to undergo neddylation may be the reason why the anti-GFP antibody was unable to detect the truncated Stx1a-GFP in the blots examining the pulldown eluates. The results suggested that the SNARE domain has an influence on neddylation. However, the data presented did not show the irrelevance of the other domains. For this reason, it was not possible to exclude particular lysins. Consequently, the homology of Stx1a and Stx4, together with the results of previous experiments, were considered in order to select a mutation.

In Stx4, lysine 123 was identified as the most promising neddylation residue. Lysine 123 is not present in Stx1a. However, lysine residues in close proximity to position 123 include lysine 117 and lysine 126 (see Figure 12). To initially test both lysines simultaneously, a double mutant (K117,126R) was cloned (see Figure 13A). Despite the mutation, the western blot probing the pulldown eluates displayed a band detected by an anti-GFP antibody (see Figure 13B). The molecular weight of 75 kDa was consitent with the Stx1a-Avi-Nedd8-complex. However, the intensity of the band corresponding to Stx1a K117,126R was found to be less pronounced than that of the WT samples on the same blot. While the bands of all four lysate samples were of similar intensity, the carboxylase band of the DMSO treated WT samples was more prominent than the others. These results showed that even though the protein expression was successful in all samples, the pulldown in the example blot appeared to exhibit different efficiencies (see Figure 13B). Given that the efficiency of the pulldown becomes irrelevant due to the normalisation process, it is not a factor to considere when analysing the diagram. The demonstrates that the mean signal intensity of mutant samples was only 35 % of that observed in WT samples. (see Figure 13C). Normalizing the band intensities of DMSO treated K117-126R

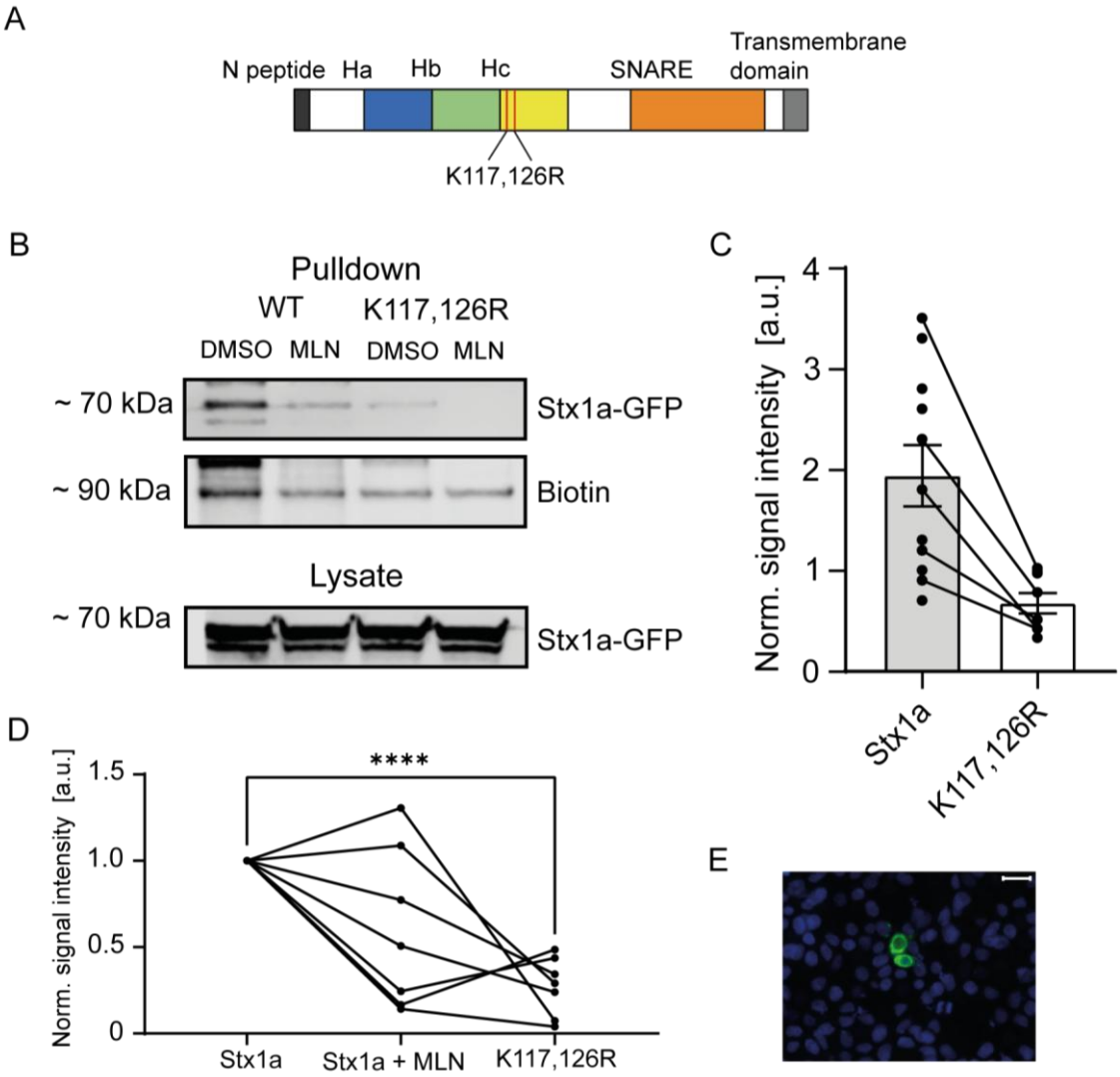

Figure 13: Neddylation of Stx1a K117,126R

(A) The mutated lysine residues are located in the Hc domain. Created with BioRender.com (B) The representative western blot demonstrates that Stx1a K117,126R could be isolated with magnetic streptavidin beads. A primary anti-GFP antibody was used for the Stx1a-GFP detection and fluorescently labelled streptavidin for biotinylated carboxylases. The samples were treated either with vehicle (DMSO) or with 1 µM MLN-4924. The expected size of Stx1a-GFP is 61 kDa; binding of Avi-Nedd8 increases the size to 75 kDa. Experiments were conducted using HEK293T cells. (C) The GFP signal was normalised with the carboxylase bands. The substitution of the lysine residues at positions 117 and 126 with arginine resulted in a significant reduction in Stx1a-GFP neddylation. The data is presented as mean ± SEM (K117,126R: 65 % decrease, paired t-test: p-value=0.0673, N=7). (D) The signal intensity of the band corresponding to the MLN-4924 treated sample and the sample of K117,126R was normalised with the Stx1a WT bands. Both MLN-4924 treatment and mutation resulted in a significant reduction in Stx1a-GFP neddylation. The data is presented as mean ± SEM (84 % decrease, paired t-test: p-value=0.0001, N=7). (E) The microscopic image shows HEK293T cells transfected with mutated Stx1a-GFP and stained with DAPI. Scale bar, 20 µm.

samples and MLN-4924 treated WT samples to DMSO treated WT samples accentuated this reduction even further. The decrease caused by the mutation was more prominent than that caused by MLN-4924 treatment (see Figure 13D). Therefore, a reduction of signal intensity through mutation was more reliable than through MLN-4924 treatment.
In conclusion, Stx1a is a promising Nedd8 candidate as well whereby the lysines at positions 117 and 126 may participate in the neddylation process of Stx1a.

3.2.3 Neddylation of Stx3

Another homologue of Stx1a and Stx4 is Stx3. Although the natural abundance of Stx3 in the brain is low, it is still involved in certain neuronal processes (Bennett et al., 1993, Jurado et al., 2013, Soo Hoo et al., 2016). Following the results of previous experiments indicating the potential of Stx1a and Stx4 as neddylation targets, Stx3 also appeared to be an interesting candidate. Light microscopy images demonstrated that Stx3-mCitrine was successfully expressed and attached to the plasma membrane thereby suggesting that the protein was folded in accordance with the requirement (see Figure 14C). Western blot analysis using anti-GFP antibodies revealed that Stx3 could be isolated with magnetic streptavidin beads. Following the pulldown procedure, a faint but robust band at 61 kDa was observed for the DMSO treated sample, while no band was visible in the lane of the sample treated with MLN-4924 (see Figure 14A). The diagram provides a more detailed illustration of the band intensity decrease by MLN-4924 treatment (see Figure 14B). The robust GFP bands in both DMSO and MLN-4924 treated lysate samples and the carboxylase bands in blots probing eluates of the pulldown assay suggested the successful protein expression and pulldown procedure. Therefore, the results indicated that Stx3 was bound to Avi-Nedd8 through neddylation-specific machinery suggesting that Stx3 is another promising Nedd8 target protein. Stx1a and Stx3 share a very similar amino acid sequence; both proteins have lysine at the positions 117 and 126 (see Figure 12). Based on previous results the question arises if lysine residues 117 and 126 of Stx3 contribute to neddylation as well.

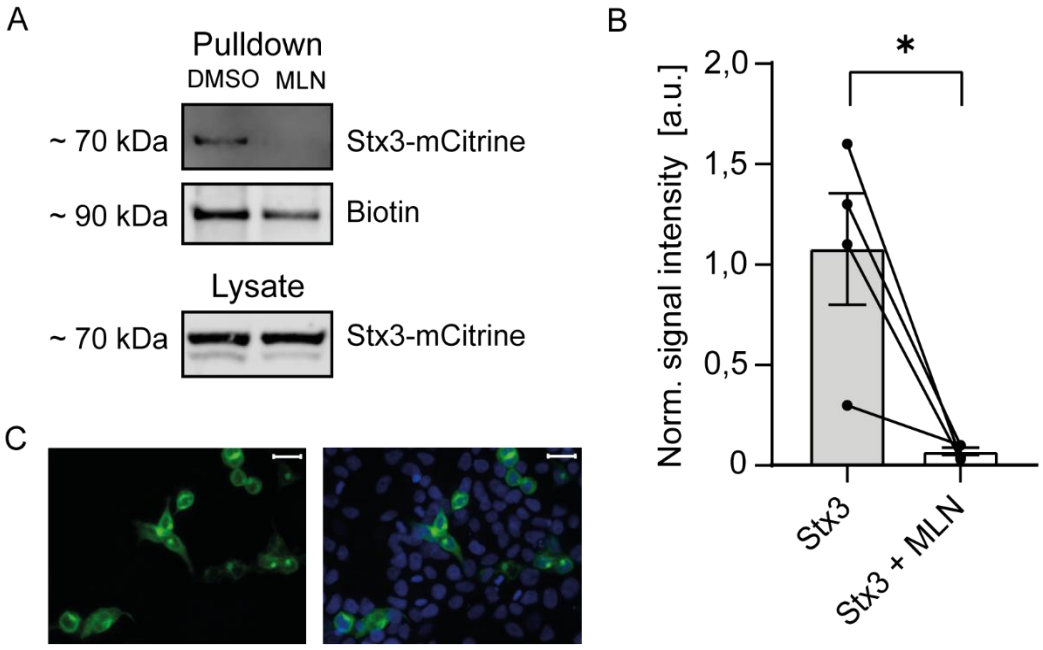

Figure 14: Neddylation of Stx3

(A) The representative western blot demonstrates that Stx3-mCitrine could be isolated with magnetic streptavidin beads in the presence of Avi-Nedd8. A primary anti-GFP antibody was used for the Stx3-mCitrine detection and fluorescently labelled streptavidin for biotinylated carboxylases. The samples on the left side of the blot were treated with vehicle (DMSO) and the samples on the right with 1 µM MLN-4924. The expected size of Stx3-mCitrine is approximately 62 kDa; binding of Avi-Nedd8 increases the size to 76 kDa. Experiments were conducted using HEK293T cells. (B) The GFP signal was normalised with the carboxylase bands. Treatment with MLN-4924 resulted in a significant reduction in Stx3-mCitrine neddylation. The data is presented as mean ± SEM (90 % decrease, paired t-test: p-value=0.0397, N=4). (C) The microscopic image shows HEK293T cells transfected with Stx3-mCitrine and stained with DAPI (right). The signal was predominantly localised to the cell membrane. Scale bar, 20 µm.

The experiments demonstrated that different proteins from the syntaxin family are promising Nedd8 targets. In particular, lysines present in the Hc domain appear to be involved in the neddylation of the syntaxins.

3.3 Neddylation of RIM1α

Experimental evidence suggests that the impact of neddylation extends beyond its influence on synaptic transmission, and is also affecting LTPs. For example, the inhibition of neddylation has been demonstrated to have a negative influence on the formation of

LTPs (Brockmann et al., 2019). The previous work investigated proteins that play a significant role in synaptic transmission to assess the possibility of their neddylation. Subsequent investigation will focus on identifying additional proteins that may contribute to the inhibition of LTP formation. One protein that has been demonstrated to influence LTPs is RIM1α (Calakos et al., 2004, Castillo et al., 2002, Kaeser and Südhof, 2005, Kintscher et al., 2013, Yang and Calakos, 2011).

The GFP-tagged RIM1α was succesfully expressed in HEK293T cells (see Figure 15C) and subsequently detected by western blotting. The bands of the lysate samples are weak but still clearly visible.Iin the western blot probing the eluates of the pulldown assay, the anti-GFP antibody detected bands at 164 kDa that likely correspond to RIM1α-GFP

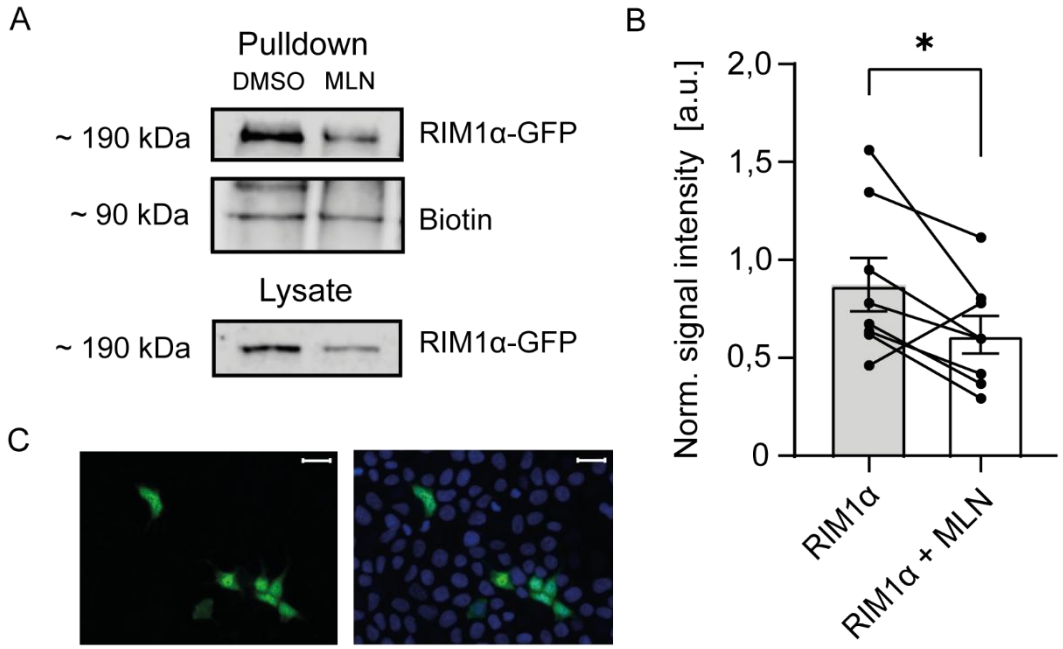

Figure 15: Neddylation of RIM1α

(A) The representative western blot demonstrates that RIM1α-GFP could be isolated with magnetic streptavidin beads in the presence of Avi-Nedd8. A primary anti-GFP antibody was used for the RIM1α-GFP detection and fluorescently labelled streptavidin for biotinylated carboxylases. The samples on the left side of the blot were treated with vehicle (DMSO) and the samples on the right with 1 µM MLN-4924. The expected size of RIM1α-GFP is approximately 192 kDa; binding of Avi-Nedd8 increases the size to 206 kDa. Experiments were conducted using HEK293T cells. (B) The GFP signal was normalised with the carboxylase bands. Treatment with MLN-4924 resulted in a significant reduction in RIM1α-GFP neddylation. The data is presented as mean ± SEM (34 % decrease, paired t-test: p-value=0.0432, N=8). (C) The microscopic image shows HEK293T cells transfected with RIM1α-GFP and stained with DAPI (right). Scale bar, 20 µm.

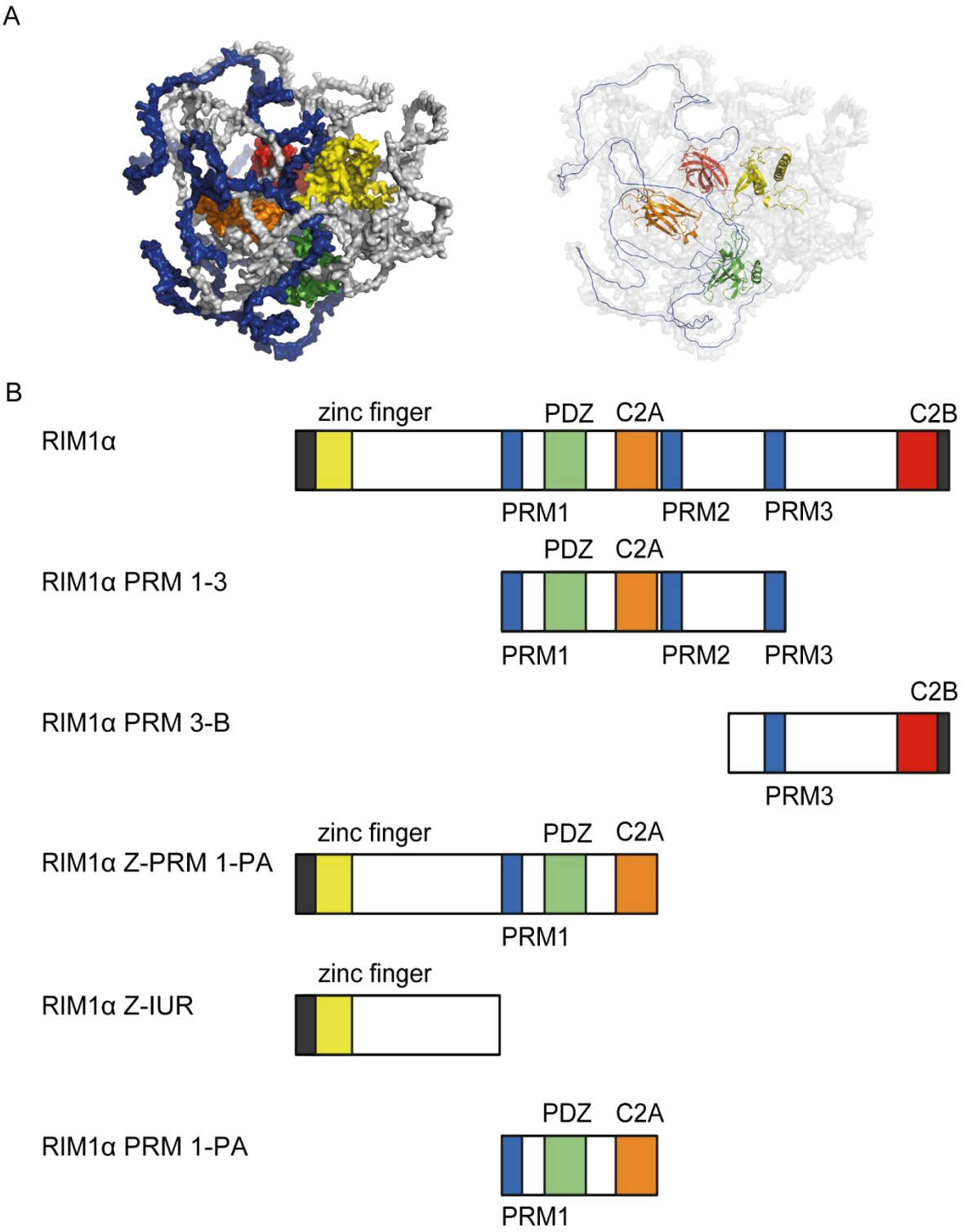

Figure 16: Domains of RIM1α and truncated forms

(A) RIM1α comprises distinct domains, including an α-helically wrapped zinc finger domain (yellow), a PDZ domain (green), a C2A domain (orange), a proline-rich conserved sequence (PRM1-3; blue) and C2B domain(red). The used structure (AF-Q86UR5-F1-model_v4) was predicted by Alphafold (Jumper et al., 2021, Varadi et al., 2024), colour coding was done with PyMOL. (B) To facilitate the identification of neddylated lysine residues, truncated proteins were created that lack different domains. Created with BioRender.com

(see Figure 15A) demonstrating that it is possible to isolate RIM1α through the use of magnetic streptavidin beads. The band intensity of samples treated with MLN-4924 was observed to be decreased in comparison to the bands of DMSO treated samples. Although the intensity after MLN-4924 treatment still reached 65 % of the intensity observed for DMSO bands, the reduction was constant and significant (see Figure 15B). In contrast, the signal intensity of bands corresponding to the carboxylases was not reduced by MLN-4924 treatment. As MLN-4924 only prevents new neddylation and does not remove already bound Nedd8, the presented results indicated that RIM1α is a promising Nedd8 target.

RIM1α is a large protein, with a molecular weight of 100 kDa. This results in a large number of lysines being considered as Nedd8 target residues. To facilitate the search, truncated proteins were used once more. These proteins were provided by the laboratory of Susanne Schoch. A selection of truncated proteins tagged with GFP was made ensuring that each domain was absent in at least one truncated protein (see Figure 16). The expression of all truncated proteins was successful, as confirmed by the detection of bands using an anti-GFP antibody in the blots of lysate samples. While the carboxylase bands appeared to be weak in a small number of samples, the bands corresponding to truncated RIM1α-GFP were distinct and robust in the blot probing pulldown eluates, but the intensity of the different mutations exhibited variation (see Figure 17A). To more clearly elucidate the contrasts, the intensities of the truncated protein samples were normalised in relation to the band intensity of WT samples. The signal intensities exhibited by GFP-tagged RIM1α Z-IUR and PRM 1-PA were comparable to those observed for the WT samples (see Figure 17B). Therefore, removing the C-terminal region starting at the PRM1 domain does not affect the efficacy of the pulldown procedure and the removal of the N-terminal region up to the PRM1 region and the C-terminal region starting from the PRM2 region has no effect either. However, removing the C-terminal region commencing at the PRM2 domain resulted in an increase in signal intensity. The only truncated proteins that exhibit decreased band intensities were PRM 1-3 and PRM 3-B, which lack sections of the N-terminus (see Figure 17B). PRM 1-3 is missing the N-terminal region extending up to the PRM1 domain, whereas PRM 3-B is lacking the N-terminal region including the PRM2 domain. Knowing that both truncated proteins that miss parts of the N-terminal region result in significantly decreased band intensities, the neddylated lysine is

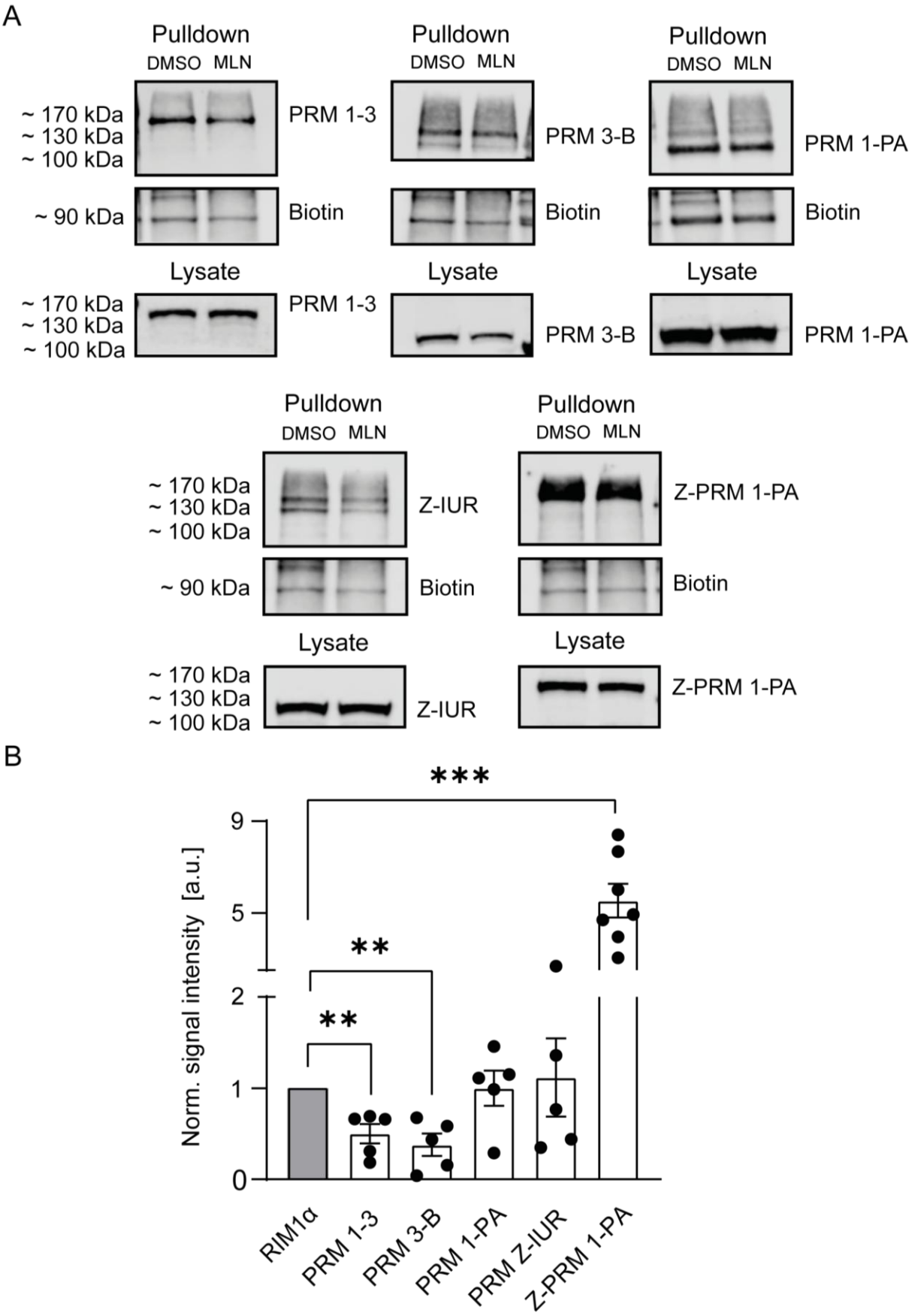
A
Pulldown
DMSO MLN
~ 170 kDa
~ 130 kDa
~ 100 kDa
PRM 1-3
~ 90 kDa
Biotin
Lysate
PRM 1-3
PRM 3-B
PRM 1-PA
Z-IUR
Z-PRM 1-PA
B
Norm. signal intensity [a.u.]
***
**
**
RIM1α
PRM 1-3
PRM 3-B
PRM 1-PA
PRM Z-IUR
Z-PRM 1-PA

Figure 17: Neddylation of RIM1α PRM 1-3, PRM 3-B, PRM 1-PA, Z-IUR, Z-PRM 1-PA

(A) The representative western blot demonstrates that all RIM1α mutants could be isolated with magnetic streptavidin beads. A primary anti-GFP antibody was used for the RIM1α-GFP detection and fluorescently labelled streptavidin for biotinylated carboxylases. The samples were treated either with vehicle (DMSO) or with 1 µM MLN-4924. Experiments were conducted using HEK293T cells. The binding of Avi-Nedd8 increases the size by 14 kDa. (PRM 1-3-GFP: 99 kDa; PRM 3-B-GFP: 87 kDa; PRM 1-PA-GFP: 70 kDa; Z-IUR-GFP: 85 kDa; Z-PRM 1-PA-GFP: 127 kDa) (B) The GFP signal was normalised with the carboxylase bands. The truncation resulted in a modification of the neddylation level of RIM1α. The data is presented as mean ± SEM (PRM 1-3: 50 % decrease, paired t-test: p-value=0.0093, N=5; PRM 3-B: 62 % decrease, paired t-test: p-value=0.0071, N=5; PRM 1-PA: paired t-test: p-value=0.9976, N=5; Z-IUR: 11 % increase, paired t-test: p-value=0.795, N=5; Z-PRM 1-PA: 500 % increase, paired t-test: p-value=0.0009, N=7).

presumably located in the n-terminal region up to PRM1.

Overall, the presented results suggest that RIM1α is a Nedd8 target protein, with the targeted lysine residues potentially located within the N-terminal region.

3.4 Investigating other synaptic proteins

3.4.1 Neddylation of SNAP-25b and VAMP2

Following the discovery that Stx1a is a potential Nedd8 candidate, there was a significant interest in investigating other proteins within the SNARE complex. For this reason, either VAMP2-GFP or SNAP-25b-mCitrine was expressed in HEK293T cells and subsequently tested for neddylation, by the use of a pulldown assay.

SNAP-25b is known to be peripherally attached to the plasma membrane (Chen and Scheller, 2001), as evidenced by the light microscopic images, which showed an enhanced mCitrine signal in the membrane (see Figure 18C). The blot of the lysate sample displayed strong bands at 50 kDa that were detected by an anti-GFP antibody. In contrast, no bands were observed in the blot probing eluted proteins from the pulldown assay. The presence of carboxylase bands on the same blot, however, provides evidence that the pulldown procedure itself was successful (see Figure 18A). Of the seven blots conducted, only three displayed faint GFP bands (see Figure 18B), whereby the MLN-4924 treated samples exihibited an eight-fold greater mean band intensity than the control samples. Therefore, MLN-4924 sensitivity could not be shown.

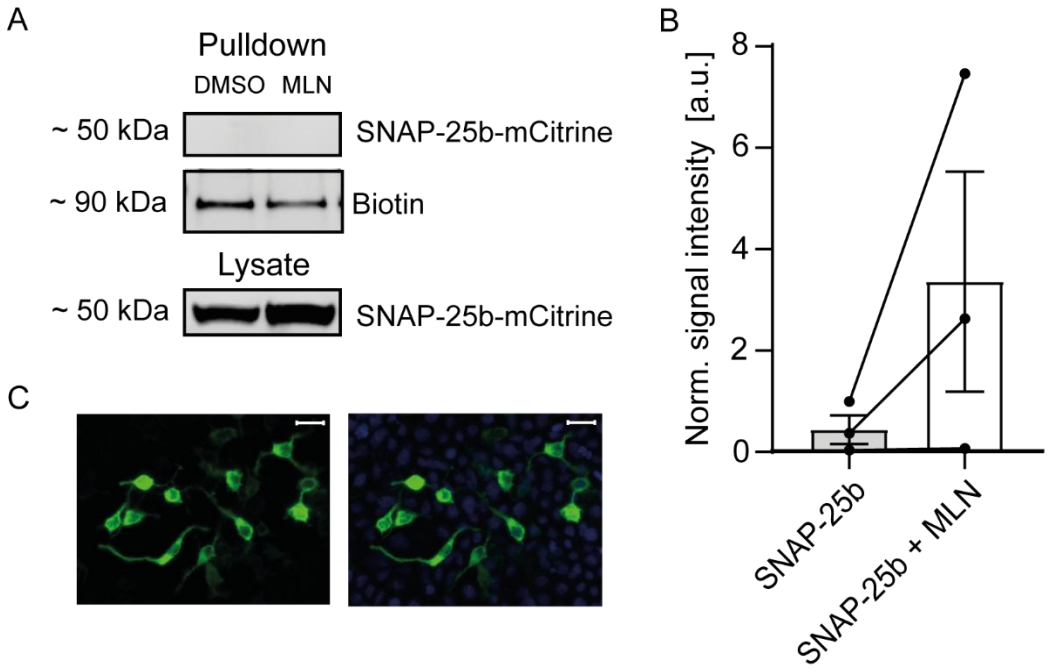

Figure 18: Neddylation of SNAP-25b

(A) The representative western blot demonstrates that SNAP-25b-mCitrine could not be isolated with magnetic streptavidin beads in the presence of Avi-Nedd8. A primary anti-GFP antibody was used for the SNAP-25b-mCitrine detection and fluorescently labelled streptavidin for biotinylated carboxylases. The samples on the left side of the blot were treated with vehicle (DMSO) and the samples on the right with 1 µM MLN-4924. The expected size of SNAP-25b-mCitrine is approximately 50 kDa; binding of Avi-Nedd8 increases the size to 64 kDa. Experiments were conducted using HEK293T cells. (B) The GFP signal was normalised with the carboxylase bands. Treatment with MLN-4924 resulted in an increase in SNAP-25b-mCitrine neddylation. The data is presented as mean ± SEM (700 % increase, paired t-test: p-value=0.2618, N=3). (C) The microscopic image shows HEK293T cells transfected with SNAP-25b-mCitrine and stained with DAPI (right). The signal was predominantly localised to the cell membrane. Scale bar, 20 µm

The transfection of HEK293T cells with GFP-tagged VAMP2 resulted in the accumulation of a GFP signal distributed throughout the cell (see Figure 19C). VAMP2 is localised to the membranes of vesicles (Chen and Scheller, 2001). The punctual distribution may therefore be indicative of a scuccessful expression and correct protein folding. The robust bands observed in the blot of the lysate samples as well as the carboxylase bands in the pulldown blot served as a control, demonstrating that the expression of VAMP2-GFP and the pulldown procedure were successful. The blot showing the samples of the pulldown assay displayed GFP bands indicating that the isolation of VAMP2 through Avi-Nedd8 and magnetic streptavidin beads was effective

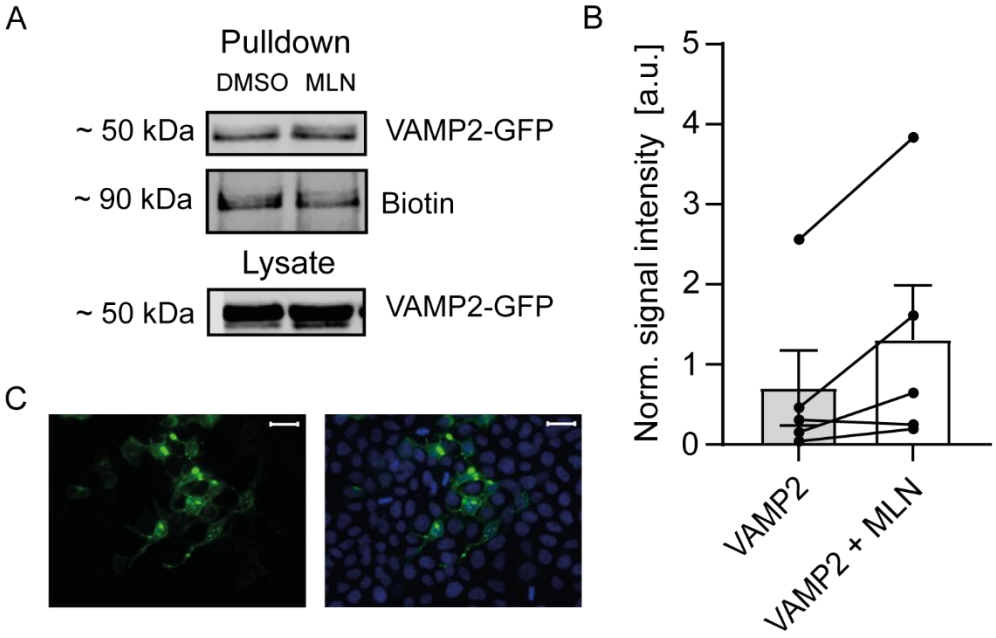

Figure 19: Neddylation of VAMP2

(A) The representative western blot demonstrates that VAMP2-GFP could be isolated with magnetic streptavidin beads in the presence of Avi-Nedd8. A primary anti-GFP antibody was used for the VAMP2-GFP detection and fluorescently labelled streptavidin for biotinylated carboxylases. The samples on the left side of the blot were treated with vehicle (DMSO) and the samples on the right with 1 µM MLN-4924. The expected size of VAMP2-GFP is approximately 40 kDa; binding of Avi-Nedd8 increases the size to 54 kDa. Experiments were conducted using HEK293T cells. (B) The GFP signal was normalised with the carboxylase bands. Treatment with MLN-4924 resulted in an increase in VAMP2-GFP neddylation. The data is presented as mean ± SEM (86 % increase, paired t-test: p-value=0.0853, N=5). (C) The microscopic image shows HEK293T cells transfected with VAMP2-GFP and stained with DAPI (right). Scale bar, 20 µm

(see Figure 19A). A comparison of the DMSO and MLN-4924 treated samples revealed that the MLN-4924 treatment had no decreasing but even an increasing effect on the band intensity in all five blots (see Figure 19B). Thus, it was not possible to ascertain whether the neddylation occurred via the Nedd8 machinery. Despite successful isolation, a conclusion regarding the neddylation of SNAP-25b and VAMP2 cannot be drawn.

3.4.2 Neddylation of Rab3A and SV2A

One protein that has been linked with RIM1α is Rab3A. The interaction between the two proteins is of great importance for the anchoring of SVs to the active zone and for

processes such SV release (Schoch et al., 2002, Wang et al., 1997). After RIM1α was shown to be a potential Nedd8 target, GFP-tagged Rab3A was also tested for neddylation. The light microscopic pictures revealed an evenly distributed GFP signal throughout the cell (see Figure 20C). This finding was consistent with the known distribution of the inactive form of Rab3A in the cytosol. Western blots probing eluted proteins from the pulldown assay exhibited faint GFP bands (see Figure 20A). The bands observed in the blot of the lysate samples as well as the carboxylase bands in the pulldown blot served as a control for the successful expression of Rab3A-GFP and the pulldown procedure. It was therefore proposed that the reason for the low intensity of bands detected by an anti-GFP antibody in blots probing the pulldown eluates was a consequence of the neddylation rate of Rab3A. In comparison to the bands of DMSO treated samples, MLN-4924

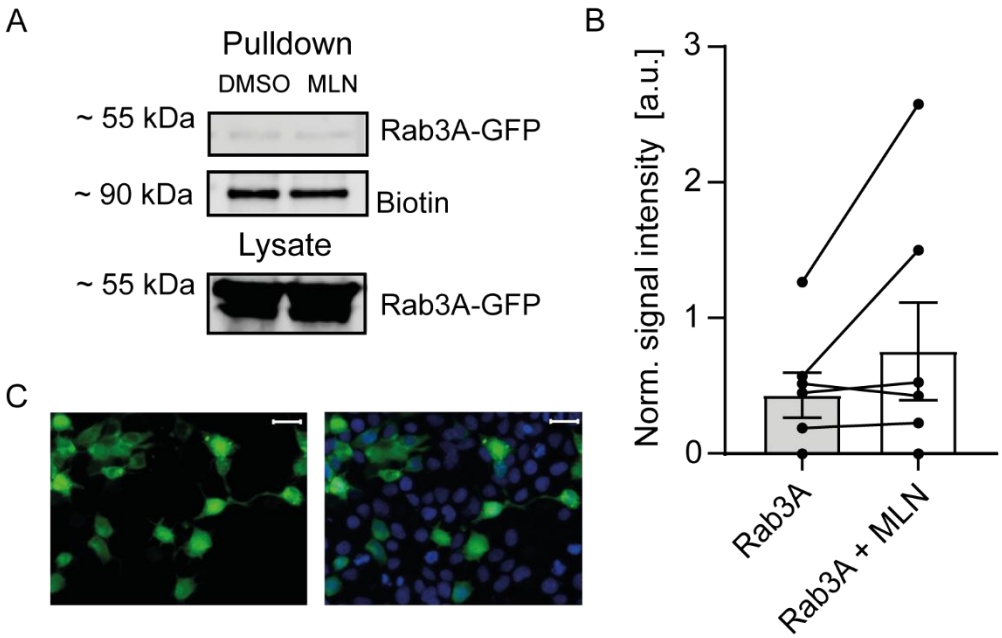

Figure 20: Neddylation of Rab3A

(A) The representative western blot demonstrates that Rab3A-GFP could be isolated with magnetic streptavidin beads in the presence of Avi-Nedd8. A primary anti-GFP antibody was used for the Rab3A-GFP detection and fluorescently labelled streptavidin for biotinylated carboxylases. The samples on the left side of the blot were treated with vehicle (DMSO) and the samples on the right with 1 µM MLN-4924. The expected size of Rab3A-GFP is approximately 53 kDa; binding of Avi-Nedd8 increases the size to 67 kDa. Experiments were conducted using HEK293T cells. (B) The GFP signal was normalised with the carboxylase bands. Treatment with MLN-4924 resulted in an increase in Rab3A -GFP neddylation. The data is presented as mean ± SEM (75 % increase, paired t-test: p-value=0.1747, N=7). (C) The microscopic image shows HEK293T cells transfected with Rab3A-GFP and stained with DAPI (right). Scale bar, 20 µm

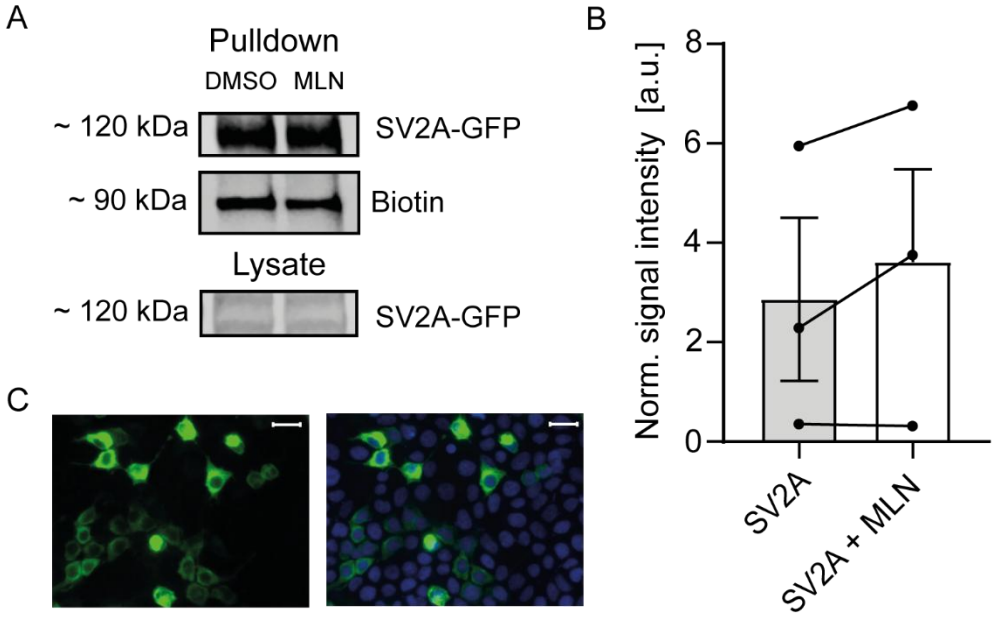

Figure 21: Neddylation of SV2A

(A) The representative western blot demonstrates that SV2A-GFP could be isolated with magnetic streptavidin beads in the presence of Avi-Nedd8. A primary anti-GFP antibody was used for the SV2A-GFP detection and fluorescently labelled streptavidin for biotinylated carboxylases. The samples on the left side of the blot were treated with vehicle (DMSO) and the samples on the right with 1 µM MLN-4924. The expected size of SV2A-GFP is approximately 100 kDa; binding of Avi-Nedd8 increases the size to 114 kDa. Experiments were conducted using HEK293T cells. (B) The GFP signal was normalised with the carboxylase bands. Treatment with MLN-4924 resulted in an increase in SV2A-GFP neddylation. The data is presented as mean ± SEM (26 % increase, paired t-test: p-value=0.2270. N=3). (C) The microscopic image shows HEK293T cells transfected with SV2A-GFP and stained with DAPI (right). Scale bar, 20 µm

treatment resulted in an increased intensity (see Figure 20B). Therefor, no MLN-4924 sensitivity could be demonstrated.

Another protein that is involved in vesicle priming is SV2A (Rossi et al., 2022). SV2A is also a membrane-bound protein as evidenced by the light microscopic images (see Figure 21C). The presence of GFP bands in the DMSO and MLN-4924 treated lysate samples, along with the detection of carboxylase bands in the blots analysing the eluates of the pulldown assay, provided evidence that the expression of GFP-tagged SV2A and pulldown procedure were both successful. The blot probing the eluates from the pulldown assay exhibited robust bands that were detected by an anti-GFP antibody (see Figure 21A). Nevertheless, MLN-4924 treatment resulted in increased band intensities rather

than a decrease (see Figure 21B). In consequence of the above, the necessity for a MLN-4924 sensitivity is absent in this case as well, which precludes the ability to draw any definitive conclusions about the neddylation.

3.4.3 Neddylation of PINK1 and Parkin

In addition to proteins that are directly involved in synaptic transmission, other proteins are known to influence neuronal signalling. This is achieved, for example, by maintaining calcium homeostasis. Two key proteins in this process are PINK1 and Parkin (Barazzuol et al., 2020). Interestingly, both proteins were shown to be neddylated in previous studies (Choo et al., 2012, Um et al., 2012). The methods that were used to identify neddylation targets in those studies are different than the one used in this thesis. To investigate whether our method can verify PINK1 and Parkin as neddylation targets, both proteins were analysed as well. The light microscopic images illustrate that both proteins were successfully expressed in HEK293T cells (see Figure 22C, D). Both proteins are cytosolic or associated with mitochondria, which is reflected in the evenly distribution of GFP signal. The GFP signal in cells transfectd with GFP-tagged PINK1 was observed to be faint. This suggests that the expression of PINK1-GFP was not as effective as intended. The blots of the lysate samples are consistent with this assumption.The GFP bands corresponding to PINK1-GFP are barely visible whereas the Parkin samples exhibit prominent and robust bands. The blot probing eluates from the pulldown assay demonstrated the presence of bands for both Parkin and PINK1 samples. The bands corresponding to Parkin-GFP are again more intense than the PINK1 bands (see Figure 22A). The carboxylase bands indicated that the observed difference is not attributable to the pulldown procedure, as the bands of all four samples exhibited similar intensities. This implies that the primary cause for the faint band intensity was the weak expression of PINK1-GFP. A comparison of the DMSO and MLN-4924 samples did not reveal any MLN-4924 sensitivity (see Figure 22B). Once again, MLN-4924 led to an increase in band intensity, contrary to expectations. Therefore, the present results could not verify PINK1 and Parkin as neddylation targets.

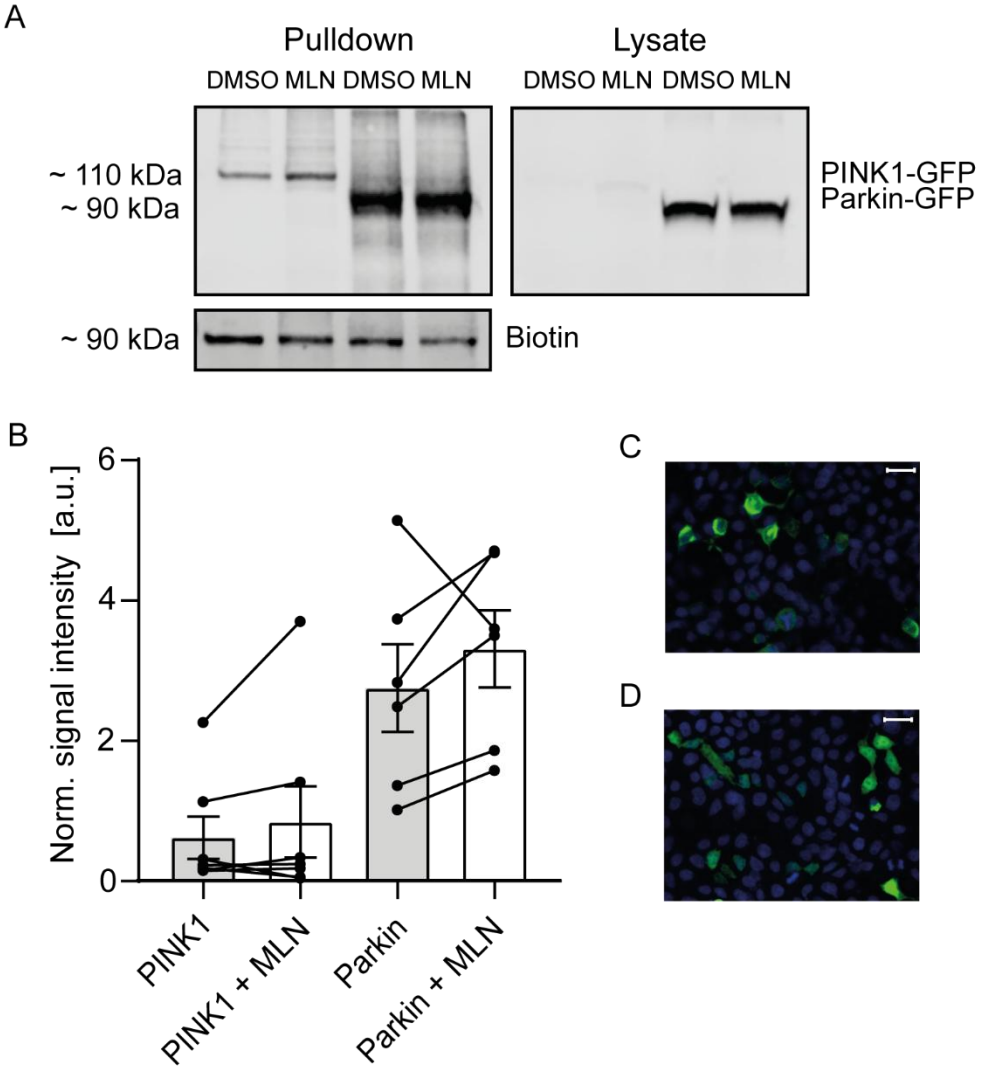

Figure 22: Neddylation of PINK1 and Parkin

(A) The representative western blot demonstrates that Parkin-GFP and PINK1-GFP could be isolated with magnetic streptavidin beads. A primary anti-GFP antibody was used for the Parkin-GFP and PINK1-GFP detection and fluorescently labelled streptavidin for biotinylated carboxylases. The samples on the left side of the blot were treated with vehicle (DMSO) and the samples on the right with 1 µM MLN-4924. The expected size of Parkin-GFP is approximately 80 kDa; PINK1-GFP has a molecular weight of 92 kDa; binding of Avi-Nedd8 increases the size by 14 kDa. Experiments were conducted using HEK293T cells. (B) The GFP signal was normalised with the carboxylase bands. Treatment with MLN-4924 resulted in an increase in Parkin-GFP and PINK1-GFP neddylation. The data is presented as mean ± SEM (Parkin: 20 % increase, paired t-test: p-value=0.2852, N=6; PINK1: 35 % increase, paired t-test: p-value=0.3387, N=7). The microscopic image shows HEK293T cells transfected with Parkin-GFP (C) and PINK1-GFP (D) and stained with DAPI. Scale bar, 20 µm

3.4.4 Neddylation of E-Syt1 and E-Syt2

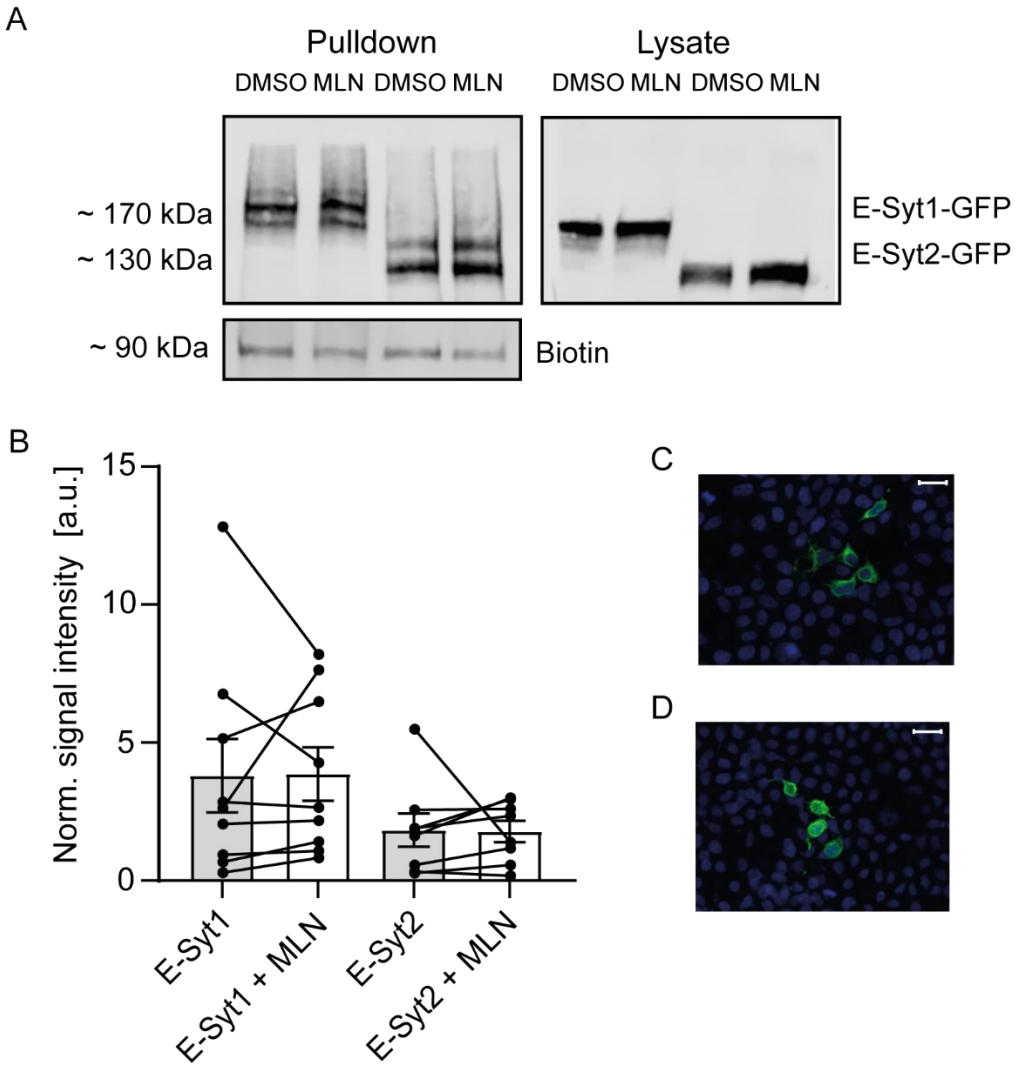

Figure 23: Neddylation of E-Syt1 and E-Syt2

(A) The representative western blot demonstrates that E-Syt1-GFP and E-Syt2-GFP could be isolated with magnetic streptavidin beads. A primary anti-GFP antibody was used for the E-Syt1-GFP and E-Syt2-GFP detection and fluorescently labelled streptavidin for biotinylated carboxylases. The samples on the left side of the blot were treated with vehicle (DMSO) and the samples on the right with 1 µM MLN-4924. The expected size of E-Syt1-GFP is approximately 151 kDa; E-Syt2-GFP has a molecular weight of 123 kDa binding of Avi-Nedd8 increases the size by 14 kDa. Experiments were conducted using HEK293T cells. (B) The GFP signal was normalised with the carboxylase bands. Treatment with MLN-4924 resulted in an increase in E-Syt1-GFP and E-Syt2-GFP neddylation. The data is presented as mean ± SEM (E-Syt1-GFP: 2 % increase, paired t-test: p-value=0.9431, N=9; E-Syt2-GFP: 3 % increase, paired t-test: p-value=0.9328, N=8). The microscopic image shows HEK293T cells transfected with E-Syt1-GFP (C) and E-Syt2-GFP (D) and stained with DAPI. Scale bar, 20 µm

Two further proteins have been identified to influence calcium homeostasis: E-Syt1 and E-Syt2. E-Syt2 is anchored to the cellular membrane, while E-Syt1 is translocated to the membrane of the endoplasmatic reticulum (Min et al., 2007, Perez-Lara and Jahn, 2015). Accordingly, the light microscopic images of E-Syt1 samples showed a more pronounced GFP signal in the membrane (see Figure 23C). The blot of the lysate samples exhibited prominent bands at 151 kDa and 123 kDa, which were detected by an anti-GFP antibody, thus indicates that the expression of E-Syt1-GFP and E-Syt2-GFP in HEK293T cells was successful. Following the pulldown procedure, an anti-GFP antibody identified bands corresponding to E-Syt1-GFP-Avi-Nedd8 complexes at 170 kDa and to E-Syt2-GFP-Avi-Nedd8 complexes at 150 kDa. The GFP bands exhibited a strong intensity, the carboxylase bands of the same blots appeared weaker (see Figure 23A). Once again, the MLN-4924 treatment did not reduce the band intensity, neither for GFP-tagged E-Syt1 nor for E-Syt2 (see Figure 23B). Instead, both the DMSO and MLN-4924 treated samples exhibited similar band intensity. Consequently, it remains inconclusive whether or not E-Syt1 and E-Syt2 are subject to neddylation.

In conclusion, the isolation of all proteins except SNAP-25b was successfully achieved through Avi-Nedd8 and magnetic streptavidin beads. Nevertheless, the requisite that MLN-4924 decreases the band intensity was not fulfilled for any of the proteins. Given that other studies have demonstrated that PINK1 and Parkin are neddylation targets, it is worth discussing whether the lack of MLN-4924 sensitivity is a clear sign that the protein in question is not neddylated.

3.5 Neddylation of carboxylases

Carboxylases are known to be endogenously biotinylated, which allows for their isolation using magnetic streptavidin beads. As part of the analysis, the signal from anti-GFP antibodies was normalised with streptavidin bands at 90 kDa that were suggested to be carboxylases. This was done to exclude any potential influence of the total protein amount and the efficiency of the pulldown assay. During the analysis of other proteins, it became apparent that the signal intensity of bands corresponding to carboxylases was decreased after MLN-4924 treatment. A comparison of the signal intensity of the carboxylases bands

revealed that MLN-4924 significantly reduced the signal (see Figure 24A) suggesting that neddylation might influence carboxylases. However, this influence is not necessarily a direct neddylation but may be the result of neddylation of upstream proteins that regulate carboxylases. To address the question whether Nedd8 is directly attached to carboxylases, the anti-GFP antibody was replaced by an anti-Nedd8 antibody. Western-blots demonstrated that the signal corresponding to the anti-Nedd8 antibody overlapped with the streptavidin signal indicating that Nedd8 was attached to biotinylated carboxylases (see Figure 24B). In order to exclude the possibility that Nedd8 was attached to another protein of similar size, the pulldown experiments were repeated with flag-tagged Ned8. Without the Avi-tag, Nedd8 itself cannot be isolated via streptavidin beads. The missing cullin band in blots with flag-Nedd8 confirmed this (see Figure 24B). However, anti-Nedd8 antibodies detected a signal overlapping the streptavidin band. This means that Nedd8 itself was isolated via streptavidin beads, despite the missing Avi-tag. Comparing the Avi-Nedd8 and the flag-Nedd8 pulldown, it stood out that the signal of the Avi-Nedd8 sample exhibited a broad smear around the definable band. This smear was

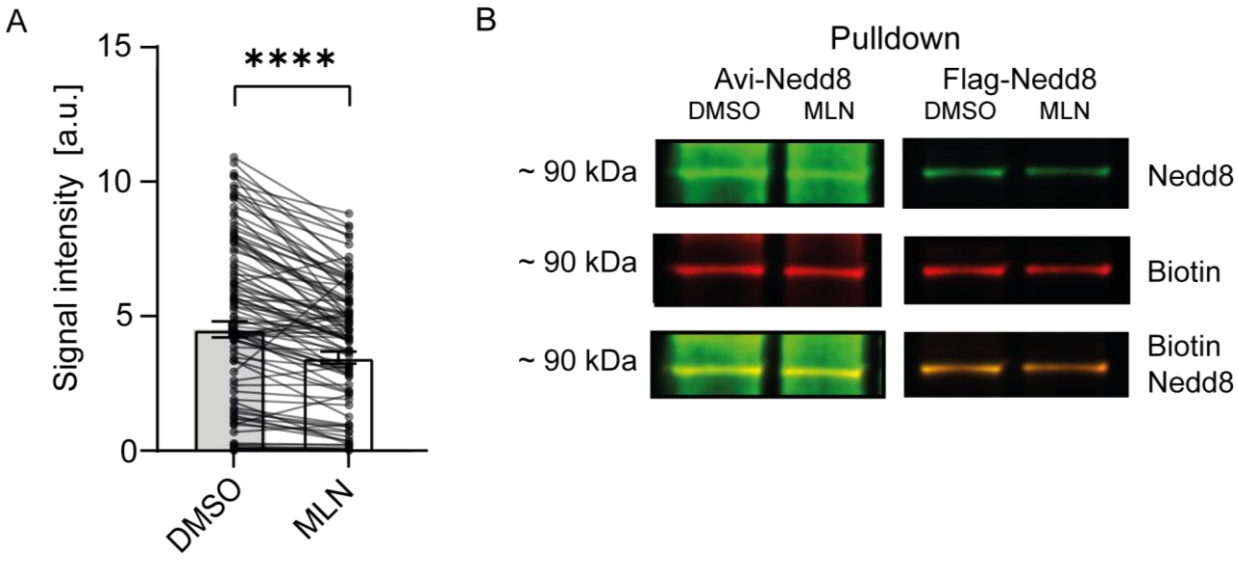

Figure 24: Neddylation of carboxylases

(A) MLN-4924 significantly reduced the signal intensity of the carboxylase bands, indicating that carboxylases undergo neddylation. The data is presented as mean ± SEM (23 % decrease, paired t-test: p-value=<0.0001, N=104). (B) To test if Nedd8 is attached to carboxylases, the anti-GFP antibody was replaced with an anti-Nedd8 antibody. Western blots showed that Nedd8 co-localised with streptavidin, suggesting that Nedd8 was attached to carboxylases. Although Nedd8 cannot be isolated without an Avi-tag, an anti-Nedd8 antibody detected a signal overlapping the streptavidin bands, indicating that carboxylases were neddylated.

missing in flag-Nedd8 samples. Given that Avi-Nedd8 was isolated through the beads, the smear may consist of different neddylated proteins of similar size. Flag-Nedd8 can only be isolated when it´s attached to endogenously biotinylated proteins. The missing smear in western blots of flag-Nedd8 suggests that flag-Nedd8 was only isolated due to its attachment to the carboxylases. These results indicated that carboxylases are neddylated.

4 Discussion

Previous studies indicated that neddylation has an influence on synaptic transmission and plasticity (Brockmann et al., 2019). For this reason, the identification of presynaptic neddylation target proteins its of great interest and importance. In the present thesis, I successfully identified four new neddylation target proteins: Stx1a, Stx3, Stx4 and RIM1α. Of these, Stx1a and RIM1α play a major role in the presynapse and may provide further insight into how neddylation influences synaptic transmission. To ensure the effective examination of the function, it is necessary to find a variant that cannot be neddylated. In this regard, this work also offers important findings. Several lysine residues of Stx4 were found to be neddylated, while two neddylated lysines were identified in Stx1a. In addition, I was able to demonstrate that the neddylated lysine in RIM1α that is located in the N-terminal region. Other tested proteins need further investigation to verify a connection to neddylation.

4.1 Identification of neddylation targets

In order to identify proteins as neddylation targets, specific prerequisites need to be fulfilled. The criteria as outlined by Rabut and Peter (2008), can function as a guideline for the characterisation of neddylated proteins. The minimum requirements for the study include the covalent binding of Nedd8 to the substrate, which must take place under endogenous conditions, and the involvement of specific components of the neddylation machinery. In order to further characterise a Nedd8 target, it is necessary to determine the phenotype of a non-neddylatable mutant and to identify the specific Nedd8 ligase and isopeptidase (Rabut and Peter, 2008).

The primary research focus is on the covalent attachment of Nedd8 to a lysine residue of the target protein. In my study the protein-protein-interaction between Nedd8 and potential target proteins was investigated through a pulldown assay. For this purpose, an Avi-tagged Nedd8 was isolated using magnetic streptavidin beads. If the GFP-tagged protein that was tested for neddylation was attached to Nedd8, it was isolated in conjunction with Nedd8 and could be detected in western blots probing the pulldown sample. A band detected by the anti-GFP antibody after the pulldown procedure is

therefore a sure sign that Nedd8 was covalently bound to the target protein, especially as urea washing steps had previously removed non-covalent bonds (Zangi et al., 2009). Similar pulldown assays already demonstrated the efficiency of the method to detect neddylation. Numerous studies using immunoprecipitation have been able to identify a significant number of new neddylation targets (Noh et al., 2012, Takashima et al., 2013, Xirodimas et al., 2004).

Another criterion that should be considered is the attachment of Nedd8 through specific components of the neddylation machinery. Because overexpressed Nedd8 can also be attached to a target protein through the ubiquitination machinery, it is imperative to ensure that the protein is genuinely neddylated (Hjerpe et al., 2012, Kim et al., 2011, Leidecker et al., 2012, Whitby et al., 1998). An established approach to identify the involved machinery is the treatment with MLN-4924. MLN-4924 has been shown to block NAE1, thereby specifically preventing neddylation by the E1 activating enzyme (Brownell et al., 2010, Soucy et al., 2009). MLN-4924 treatment should, therefore, result in a reduction of neddylation and consequently in a decreased level of signal detected by anti-GFP antibodies in blots that are used to analyse pulldwon samples. It is noteworthy that the reduction of neddylation depends on endogenous deneddylation via SENP8 (Wu et al., 2003, Yamoah et al., 2005), as the function of MLN-4924 is limited to the prevention of the de-novo neddylation. The enzymes required for deneddylation must be provided by the cell. All experiments were carried out in HEK293T cells. The investigated proteins, however, are synaptic proteins that are not always expressed in non-neuronal tissues. Unfortunately, the use of a heterologous system may potentially limit the accessibility of neurone-specific proteins contributing to neddylation and deneddylation. Thus, it is crucial to consider the possibility that a lack of neddylation or deneddylation may also be attributed to the limited conditions of the heterologous system. A less prominent reduction upon MLN-4924 treatment could be the result of a decreased deneddylase activity or an increased half-life of the target-Nedd8-complex in comparison to other targets.

To minimise the effect of cellular conditions and the eficancy of the pulldown assay, signal intensities were normalised with endogenously biotinylated carboxylases. As the carboxylases are the only endogenously biotinylated proteins observed in the blots probing pulldown eluates, with no requirement for further overexpression, the carboxylases were initially considered to be the optimal selection. However, a closer look

at the band intensity of the carboxylases revealed a slight decrease after MLN-4924 treatment, which was reliably visible in almost every blot. Moreover, experiments with flag-Nedd8 confirmed that Nedd8 is attached to carboxylases. It is therefore assumed that carboxylases are at least partly targets for neddylation. This complicates the normalisation with carboxylase bands. In general, the signal intensity was normalised by dividing the GFP signal through the streptavidin signal of carboxylases. The reduced band intensity of MLN-4924 treated carboxylases may lead to an erroneous normalisation, whereby the normalised signal is higher than it would be if the treatment had no impact on the carboxylases. As the comparison of the DMSO and MLN treated normalisation values is of significant interest, this implies that a clear reduction due to MLN-4924 is correctly indicating the neddylation of the protein in question. However, normalised values that exhibit a sligthly visible or even absent reduction after MLN-4924 treatment do not prove the absence of MLN-4924 sensitivity. Consequently, the normalisation is solely applicable for the identification of neddylated proteins but not necessarily for the discovery of proteins that are unable to undergo neddylation.

The subsequent step in characterising a neddylated protein is the identification of the lysine to which Nedd8 binds. It is standard practice to mutate individual lysines to arginine (Noh et al., 2012, Takashima et al., 2013, Xirodimas et al., 2004). Thereafter, western blots can be performed to analyse whether the protein is neddylated despite the mutation. Since Nedd8 can only bind to lysine residues and not to arginine, the mutation of the correct lysine prevents or reduces neddylation. Previous studies on ubiquitin showed that mutation of the targeted lysine results in a reduced ubiquitination level of 25 % (Lin et al., 2011). In addition, the same pulldown assay that was described in this thesis demonstrated that mutation of K112 in Cof1 led to a decreased signal intensity of 40-50 % (Einsfelder, 2022), whereby mass spectrometry previously confirmed lysine 112 to be a neddylation target (Vogl et al., 2020). In consideration of these results, it is hypothesised that a decrease of at least 50 % provides definitive evidence that the mutated lysine is neddylated. A reduction of 25 % on the other hand, indicates that a lysine is neddylated but is considered less reliable. The influence of more than one lysine could be a sign of promiscuity as observed for ubiquitin (Li et al., 2020a). However, the presence of multiple lysine residues that function as Nedd8 targets does not imply that all lysines are concurrently neddylated. Mass spectrometry studies have demonstrated that multiple

lysines of PSD-95 are neddylated, but not all lysines were consistently detected in every experimental run (Brockmann, 2014). Consequently, it can be suggested that some lysines that are essentially Nedd8 targets are not consistently neddylated. Unfortunately, the results of this thesis do not allow to answer the question whether these lysines are directly neddylated or whether they contribute to the neddylation process by interacting with E2 or E3 enzymes.

At present, cullins represent the only proteins that meet all the criteria for neddylated proteins. This is partly due to the difficulty of meeting the minimum requirements, let alone the additional ones. The detection of endogenous neddylation is often challenging as neddylation is a reversible modification, resulting in a comparatively small quantity of a particular protein. To facilitate the investigation of endogenously neddylated proteins, it is advantageous to enrich neddylated proteins, for example using deconjugatable Nedd8, and to isolate the neddylated proteins through a tagged Nedd8 (Coleman et al., 2017, Jeram et al., 2010, Zhang et al., 2024). In order to investigate the phenotype, it is first necessary to find a non-neddylable mutant. Previous results indicate that non-cullin targets are often neddylated at several lysines distributed over the entire surface (Enchev et al., 2015). This large number of Nedd8 target residues makes the search more difficult. In addition, the identification of the E2 and E3 proteins involved is rarely successful. As neddylation is a dynamic enzyme cascade involving transient and time-limited protein-protein interactions, the identification of individual enzymes can be challenging. At the present time, for example, no crystal structure of an E2/E3 complex with a non-cullin target has been identified (Zhang et al., 2024). In view of the difficulties encountered in the identification of NEDD8 targets, the findings of this study are of considerable importance for future research on neddylation.

All in all, the chosen method is a good and simple approach to test various proteins for neddylation. In accordance with the previously defined criteria, a thorough analysis of the results of this work was conducted, leading to the reliable identification of potential nedylation targets.

4.2 Neddylation of Syntaxin

Syntaxins belong to a family of proteins that participate in intracellular trafficking and membrane fusion. In humans, five syntaxins are expressed in the plasma membrane: Stx1a, Stx1b, Stx2, Stx3 and Stx4 (Teng et al., 2001). Given the results of this study Stx1a, Stx3 and Stx4 are neddylated.

4.2.1 Syntaxin4

Pulldown experiments with Stx4-mCitrine and Avi-Nedd8 demonstrated that Stx4 could be isolated in the presence of Avi-Nedd8 but not in samples missing Avi-Nedd8. This suggests that Avi-Nedd8 was covalently attached to Stx4 as Urea washing steps had previously removed non-covalent bonds (Zangi et al., 2009). Western blots of lysates supported this assumption showing two different bands corresponding to the size of Stx4 and Stx4 plus an attached Avi-Nedd8. The inhibition of NAE1 through MLN-4924 resulted in a 75 % reduction compared to WT values, indicating that the transfer of Avi-Nedd8 onto Stx4 can be attributed to the neddylation machinery. Removing the SNARE and the Hc domain hindered isolation of Stx4 through Avi-Nedd8. It can therefore be assumed that the neddylated lysine is located in the SNARE or Hc domain. To test individual lysine residues, K54, K102, K108, K123, K124, K140, K151 and K161 were mutated to arginine. Similar to MLN-4924 treatment, the mutation of lysines 102, 123, 140 and 161 caused a reduced signal intensity. Especially, the mutation of lysine 123 to arginine had a comparable effect on neddylation to that of MLN-4924 treatment, with a decrease in signal intensity of 67 %. In accordance with the previously defined criteria (see 4.1), the reduction that was observed for K123R, K140R and K161R indicates an involvement of these lysines in neddylation of Stx4. The influence of more than one lysine may be a sign of promiscuity as observed for ubiquitin (Li et al., 2020a). Unfortunately, the results do not allow to answer the question whether the lysines are directly neddylated or whether they contribute to the neddylation process by interacting with E2 or E3 enzymes. Based on the experiments examining ubiquitin targets, lysine 102 also appears to be a viable candidate, but since the mutation does not lead to a reduction of at least 50 %, as observed for the Cof1 K112R mutant, a definitive conclusion cannot yet be drawn. A comparison of the

signal intensity of individual western blots probing Stx4 K102R reveals that the values are distributed into two clusters. Three of the values are approximately equivalent to the mean value of the WT, while the remaining three samples exhibit significantly reduced intensity. The mean value of the low cluster reaches only 12.5 % of the mean value of the WT, which corresponds to a reduction of 87.5 %. This outcome clearly demonstrates neddylation of lysine 102 in at least half of the examined western blots. The results observed for lysine 102 are consistent with the MS results of PSD-95 (Brockmann, 2014). This suggests that the lysine is generally neddylated, although this does not appear to be as reliable as with other lysines. In contrast, lysine 54 demonstrated a prominent increase in signal intensity upon mutation. Given that Nedd8 covalently binds to a lysine and not to arginine, the increase excludes lysine 54 as target residue. Nevertheless, it might interact with the neddylation machinery, thereby influencing neddylation. The other investigated lysines 108, 124 and 151 did not change the level of neddylation and are therefore unlikely important for neddylation.

Table 12: Signal intensity of all Stx4 mutants compared to the WT

Mutation	Signal intensity compared to WT
K54R	145 %
K102R	66 %
K108R	113 %
K123R	33 %
K124R	116 %
K140R	37 %
K151R	87 %
K161R	41 %

4.2.2 Syntaxin1a

Isolation of Stx1a in the presence of Avi-Nedd8 indicated that Stx1a is also a neddylation target. However, MLN-4924 treatment did not result in a decreased neddylation level as observed for Stx4. As previously outlined, while MLN-4924 sensitivity is a crucial prerequisite, the extent of the reduction does not serve as a defence against neddylation. The provided results are therefore still sufficient to assume that Stx1a is neddylated.

For further characterisation of Stx1a as a Nedd8 substrate the homology to Stx4 was used to determine the neddylated lysine residues. Since lysine 123 was the residue that caused the most significant reduction in Stx4, the lysines in Stx1a located in the vicinity were initially analysed. Mutating lysines 117 and 126 to arginine reduced band intensity to 35 % of WT values. In accordance to the results of Stx4, this indicated that lysines 117 and 126 or at least one of the two is involved in neddylation of Stx1a. The provided results, unfortunately, cannot answer the question whether both lysin residues or just one is important for neddylation and whether this lysine is directly neddylated or influences neddylation in another way. This reduction of 65 % upon mutation was stronger than the reduction through MLN-4924. Given that MLN-4924 reduction depends on the deneddylation machinery of the heterologous system preventing neddylation by mutating the lysine gives even stronger evidence that Stx1a is neddylated.

4.2.3 Syntaxin3

The last member of the syntaxin family investigated was Stx3. In addition to Stx1a and Stx4, it was also possible to isolate Stx3 through magnetic streptavidin beads. MLN-4924 treatment caused a decrease of band intensity of about 70 %, indicating that Avi-Nedd8 was transferred to Stx3 via neddylation-specific machinery. Even if the neddylated lysine residue was not determined yet, the provided results still indicate that Stx3 is neddylated just like Stx1a and Stx4. In consideration of the homology of Stx1a and Stx3 and the existing data, lysines 117 and 126 are likely to be promising potential target residues.

In conclusion, the current findings demonstrate that Stx1a, Stx3 and Stx4 are Nedd8 target proteins. The results of the experiments conducted with Stx1a and Stx4 indicate that both the SNARE and Hc domains play a significant role in the process of neddylation. Moreover, in the context of Stx4, the lysine residues at positions 123, 140 and 161 are specifically involved in neddylation, while the lysines 117 and 126 are crucial for Stx1a neddylation. This conclusion gives rise to the question how neddylation might influence the function of the syntaxins.

4.2.4 Possible function of syntaxin neddylation

The syntaxin family is essential for intracellular membrane traffic, with Stx1a, as well as Stx3 and Stx4, forming the SNARE complex in conjunction with other t- and v-SNAREs (Morgans et al., 1996, Rehman et al., 2017, Rizo and Xu, 2015). Next to Stx1a, the neuronal SNARE complex consists of SNAP-25 (t-SNARE) and VAMP2 (v-SNARE) and mediates synaptic exocytosis. The interaction of all three SNARE proteins brings the membranes into close proximity and induces SV fusion (Rizo and Xu, 2015). The formation of the SNARE complex depends on the conformation of Stx. As mentioned before, Stx1a consists of different domains that adopt an open and closed conformation, whereby Munc18-1 and Munc13 influence the conformation of Stx1a (Dulubova et al., 1999, Richmond et al., 2001). Munc18-1 stabilises the closed conformation, which hinders formation of the SNARE complex, while Munc13 opens Stx1a and accelerates SNARE complex formation (Burkhardt et al., 2008, Chen et al., 2008, Deak et al., 2009, Ma et al., 2011). Nevertheless, it is not clear how Munc13 opens Stx1a and the involvement of other proteins is possible. A destabilizing mutation in the linker region of Stx1a (L165A, E166A; LE mutation) that favours the open conformation facilitates SNARE complex formation and increase release probability and speed of release (Dulubova et al., 1999, Gerber et al., 2008). Regulation of the different conformations of Stx1a, therefore mediates synaptic exocytosis. Previous studies on Nedd8 demonstrated that synaptic transmission is regulated by neddylation. Inhibition of neddylation in acute hippocampal brain slices reduced mEPSC amplitude and frequency significantly representing a change in postsynaptic response to the neurotransmitter release as well as a change in neurotransmitter release. In addition, paired-pulse facilitation (PPF) was increased in slices that were treated with MLN-4924. This demonstrates that inhibition of neddylation decreases the probability of vesicular release (Brockmann et al., 2019). Knowing that the conformational change of Stx1a and depending on this the formation of the SNARE complex influence release probability as well (Gerber et al., 2008), it can be suggested that neddylation of Stx1a may contribute to the opening of Stx1a and the formation of the SNARE complex.

Moreover, removal of the Habc domain of Stx1a only affects spontaneous release and vesicle priming but not evoked release, indicating that Habc is dispensable after

SNARE complex formation (Zhou et al., 2013). The importance of the Hc domain for neddylation observed in this thesis may favour the hypothesis that neddylation of Stx1a does not contribute to evoked release but rather to the conformational change and formation of the SNARE complex.

The reduction of mEPSC amplitude after MLN-4924 treatment in studies of Brockmann and collegues indicated that neddylation influences postsynaptic processes as well. Further experiments demonstrated that inhibition of neddylation decreased the number of AMPAR and NMDAR at postsynaptic sites and reduced post-synaptic AMPA and NMDA currents. In addition, neddylation is required to induce synaptic plasticity as inhibition of neddylation before and during induction reduced the expression of LTP (Brockmann et al., 2019, Scudder and Patrick, 2015). This influence could be explained through the interaction of AMPAR and NMDAR with PSD-95. PSD-95 is a known neddylation target, which anchors AMPARs at the synapse, while a non-neddylated PSD-95 variant is lacking this ability (Brockmann, 2014, Brockmann et al., 2019, Stein et al., 2003). Several studies on Stx3 and Stx4 revealed that both syntaxins are also involved in LTP induction. Both are known to insert AMPAR and NMDAR into postsynaptic membrane, and through this to influence LTP. In fact, Stx4 KO mice do not exhibit LTPs at all (Bin et al., 2018, Jurado et al., 2013, Kennedy et al., 2010, Mohanasundaram, 2010). The importance of Stx3 and Stx4 for AMPAR and NMDAR insertion and the subsequent influence on LTP could indicate that neddylation of Stx3 and Stx4 contribute to regulation of receptor density and LTP expression in combination with PSD-95. Given that Stx3 and Stx4 also change their conformation and form SNARE complexes (Christie et al., 2012, Giovannone et al., 2018), the role of neddylation in opening Stx and therefore facilitating SNARE complex formation may also be appropriate here. To make an accurate determination of the precise function in question, additional experimentation is essential, for which the non-neddylatable mutants could prove invaluable.

4.3 Neddylation of RIM1α

The active zone of synapses is composed of many different proteins interacting to organise docking and priming of synaptic vesicles (Mochida, 2020, Südhof, 2012, Südhof, 2014, Wu et al., 2023). RIM1α is a central component of this network mediating vesicle

priming, calcium-triggered vesicle exocytosis and synaptic plasticity (Calakos et al., 2004, Castillo et al., 2002, Kaeser and Südhof, 2005, Kaeser et al., 2012, Kintscher et al., 2013, Mittelstaedt et al., 2010, Schoch et al., 2002, Südhof, 2012, Südhof, 2013a, b, Wu et al., 2023, Yang and Calakos, 2011). The results of this thesis provide evidence that RIM1α is a neddylation target as well. The pulldown assays conducted with RIM1α-GFP and Avi-Nedd8 demonstrated that isolation of RIM1α via magnetic streptavidin beads was possible. The inhibition of neddylation by MLN-4924 decreased the amount of isolated RIM1α indicating that neddylation occurred via neddylation-specific enzymes. Similar to Stx1a, the comparatively low reduction after MLN-4924 treatment could be due to a longer half-life of RIM1α-Avi-Nedd8 complexes or due to an incomplete neddylation machinery. The abundance of RIM1α is focused on neuronal cells, which makes it likely that specialised enzymes are partially missing in heterologous systems. It can therefore be reasonably assumed that RIM1α undergoes neddylation.

Experiments with truncated variations of RIM1α revealed that the N-terminus including the zinc-finger domain is especially important for neddylation. Removal of only the N-terminus (RIM1α PRM 1-3, RIM1α PRM 3-B) resulted in a signal reduction of more than 50 %. RIM1α PRM 1-PA, which lacks both N-terminal and C-terminal regions, did not show an altered signal intensity and if only the C-terminal part was missing as in RIM1α Z-PRM 1-PA, the signal intensity was even higher compared to the WT. Nevertheless, the outcomes of the variants RIM1α PRM 1-PA and RIM1α Z-PRM 1-PA do not automatically disprove the significance of the N-terminus for neddylation. It is possible that the removal of the C-terminal domains PRM 2 and PRM 3 revealed an additional neddylation site in the PRM1, the PDZ or the C2A domain that is typically concealed within the protein structure, and therefore inaccessible to Nedd8 (see Figure 25; Jumper et al., 2021, Varadi et al., 2024, Varadi et al., 2022). This would give RIM1α Z-PRM 1-PA an additional Nedd8 binding site, which explains the signal increase, and RIM1α PRM1-PA could be neddylated despite the absence of the original neddylation site. Other truncated RIM1α that were investigated exhibited signal intensities comparable to WT values, which makes the involvement of the PRM 1-3 domains, the PDZ domain and the C2A and C2B domains in neddylation implausible. Therefore, the neddylated lysine residues are probably located in the N-terminal region including the zinc finger domain.

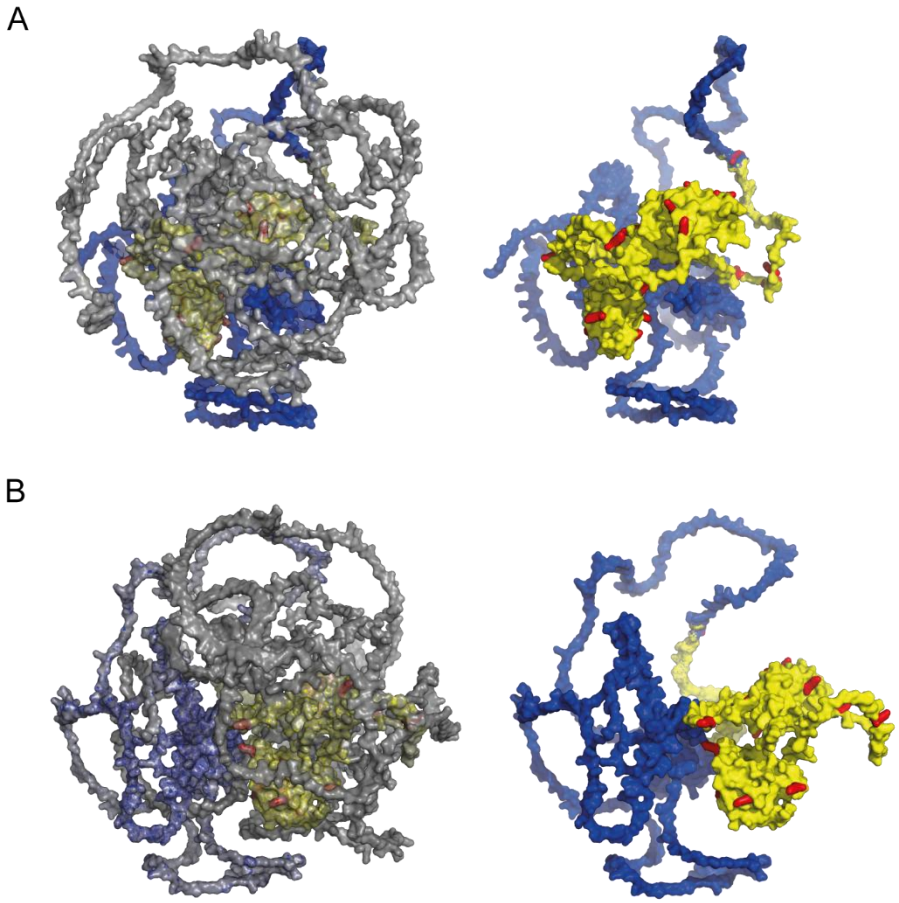

Figure 25: Hidden neddylation site of RIM1α

Removal of the C-terminal domains PRM 2, PRM 3 and C2B (grey) may reveal a hidden neddylation site in the PRM1, PDZ or C2A domain, providing RIM1α Z-PRM 1-PA (blue and yellow) and RIM1α PRM 1-PA (yellow) with an additional Nedd8 binding site. The structure used (AF-Q86UR5-F1-model_v4) was predicted by Alphafold (Jumper et al., 2021, Varadi et al., 2024, Varadi et al., 2022), colour coding was done with PyMOL.

RIM1α has several functions as it interacts with multiple presynaptic proteins like Bassoon, ELKS and Munc (Mittelstaedt et al., 2010). In connection with different protein interactions, different studies demonstrated the role of RIM1α in the anchoring of synaptic vesicles and their exocytosis and synaptic plasticity (Calakos et al., 2004, Kaeser et al., 2012, Mittelstaedt et al., 2010, Südhof, 2012, Wu et al., 2023, Yang and Calakos, 2011). The N-terminal region of RIM1α that might be a neddylation site is known for the interaction with two proteins: Rab3A and Munc13-1. Rab3A is a synaptic vesicle protein that regulates synaptic vesicle exocytosis via recruitment of vesicles (Geppert et al., 1994) and binds to α1-helix and a small sequence of α2-helix at the N-terminus of RIM1α

(Dulubova et al., 2005, Mittelstaedt et al., 2010). Knockout mice lacking Rab3A, RIM1α or both exhibited an increase in PPF. This suggests that the loss of RIM1α-Rab3A interaction is the reason for the PPF enhancement (Schoch et al., 2002). Thus, the increased PPF upon MLN-4924 treatment could be connected to RIM1αs interaction with Rab3A. The second protein that interacts with the N-terminal region of RIM1α is Munc13-1. The C2A domain of Munc13-1 binds to the zinc finger domain that was also shown to influence neddylation of RIM1α (Dulubova et al., 2005, Mittelstaedt et al., 2010). The interaction of RIM1α and Munc13-1 was demonstrated to stabilise Munc13-1 as the absence of RIM1α leads to a decrease in Munc13-1 expression (Schoch et al., 2002). Moreover, the formation of a RIM1α-Munc13-complex prevents homodimerisation of Munc13-1 (Dulubova et al., 2005). This is important because the heterodimer RIM1α-Munc13 regulates vesicle priming and maturation, while Munc mutants favouring the homodimerisation state show a 40 % reduction in docked synaptic vesicles (Camacho et al., 2017). Interestingly, in C. elegans a constitutively open form of Stx1a was able to rescue the effect of Unc-13 mutation and RIM1α KO (Koushika et al., 2001). This suggests that RIM1α-Munc13 interaction contributes to the opening of Stx1a and subsequently to the formation of the SNARE complex (Calakos et al., 2004, Koushika et al., 2001, Richmond et al., 2001). Nedd8 could therefore influence SNARE complex formation and through this vesicle release probability through the interaction of RIM1α and Stx1a with Munc13-1.

4.4 Interplay of SUMOylation and neddylation

Ribosomal protein L11 (PRL11) is a target for both neddylation and SUMOylation. It was demonstrated that the inhibition of neddylation upregulates SUMOylation of RPL11, while inhibition of SUMOylation promotes neddylation of RPL11. This interplay suggests that the two modifications are subject to some form of regulation. Neddylation and SUMOylation of RPL11 serve two distinct functions. Neddylation on the one side promotes the nuclear localisation of RPL11, whereas SUMOylation mediates the release of RPL11 from the nucleolus into cell nucleoplasm. Moreover, it was shown that nuclear stress induces SUMOylation resulting in activation of p53 (El Motiam et al., 2019). RPL11 is a good example of cooperation of different post-translational modifications in order to

regulate the function of a protein. Following the results of this thesis, the function of Stx1a and RIM1α is potentially regulated by the interplay of SUMOylation and neddylation as well. Studies on SUMOylation of Stx1a revealed that sumoylated Stx1a regulates synaptic vesicle enodcytosis, while significantly decreasing Stx1a binding to SNAP-25 and VAMP2. This suggests that SUMOylation may disturb the formation of the SNARE complex (Craig et al., 2015). Craig and collegues mention the possibility of two distinct pools of Stx1a, one with non-sumoylated Stx1a being involved in SNARE complex formation and membrane fusion, and a second pool of sumoylated Stx1a regulating synaptic vesicle endocytosis (Craig et al., 2015). If the hypothesis can be confirmed that neddylation is involved in the opening of Stx1a and the formation of the SNARE complex, the interplay of SUMOylation and neddylation could regulate the formation of the SNARE complex and the involvement of Stx1a in exo- and endocytosis.

SUMOylation of RIM1α is necessary for fast synaptic vesicle exocytosis via facilitation of $Ca_V2.1$ calcium channel clustering. In contrast to that, the abrogation of RIM1α SUMOylation did not defect docking and priming of synaptic vesicles. This leads to the assumption than un-sumoylated RIM1α is required for the maintenance of the active zone (Girach et al., 2013). Interestingly, my hypothesis regarding the function of RIM1α neddylation is consistent with the observed results. As previously stated, the interaction of RIM1α with Rab3A and Munc13-1 may influence processes such as the docking and priming of SV, which in turn affects the readily releasable pool (Dulubova et al., 2005, Luo et al., 2017, Rizo, 2018, Sakane et al., 2006, Südhof, 2012). Therefore, SUMOylation may promote the function of RIM1α in exocytosis, while neddylation could facilitate docking and priming of vesicles.

It is therefore plausible that SUMOylation and neddylation may alternate between various functions of a protein, thereby regulating synaptic transmission.

4.5 Neddylation of other proteins

The described method has also been used to analyse proteins apart from Stx and RIM1α for neddylation. Pulldown assays with E-Syt1, E-Syt2, SV2A, Rab3A and VAMP2 demonstrated that all four proteins could be isolated via magneitc streptavidin beads. Isolation of SNAP-25b was not as reliable but still possible. This suggests that Avi-Nedd8

was covalently attached to all proteins mentioned above. The first criterion to identify neddylation substrates is therefore fulfilled (Rabut and Peter, 2008). However, MLN-4924 sensitivity was not visible for any of the proteins. As already discussed, the validity of MLN-4924 as control needs to be critically examined. Nevertheless, overexpression of Nedd8 makes it necessary to exclude the influence of the ubiquitination machinery (Hjerpe et al., 2012, Kim et al., 2011, Leidecker et al., 2012, Whitby et al., 1998). Consequently, none of the proteins was shown to serve as nedylation targets.

PINK1 and Parkin are the only proteins that were previously described as neddylation targets (Choo et al., 2012, Um et al., 2012). Isolating the two proteins via magnetic streptavidin beads was successful, supporting the initial assumption. Unfortunately, MLN-4924 treatment did not result in reduced neddylation levels, which prevented fulfilment of the third criterion. Therefore, based on my data, neddylation of PINK and Parkin cannot be confirmed. Results of other studies on PINK and Parkin neddylation are partially based on methods similar to the one used in the present study. Um et al. overexpressed myc-tagged Parkin and T7-tagged Nedd8 in HEK293T cells and detected the anti-myc coimmunoprecipitates using anti-T7 and anti-myc antibodies (2012). In a second study, a similar immunoprecipitation assay was used to isolate VSVG- or flag-tagged Parkin and flag-tagged PINK, subsequently Nedd8 was visualised with an antibody (Choo et al., 2012). Neither of the two studies used MLN-4924 as control (Choo et al., 2012, Um et al., 2012). Choo and colleagues co-expressed Nedd8-specific deneddylation enzyme NEDP1 to verify the Nedd8 modification (2012), but this control provides no information pertaining to the machinery used for Nedd8 attachment. To avoid overexpression, Um and Shoo both investigated neddylation of endogenous Parkin and could confirm previous results (Choo et al., 2012, Um et al., 2012). This indicates that at least Parkin is a neddylation target despite my own data. In contrast, neddylation of endogenous PINK could not be analysed. It is therefore difficult to say whether Nedd8 was attached through neddylation or ubiquitination machinery. This means that further experiments addressing MLN-4924 sensitivity or endogenous neddylation of PINK1 should be performed to validate the protein as neddylation target.

All in all, my data does not provide sufficient evidence to confirm or deny neddylation of any of these proteins. Further experiments are required to achieve the fulfilment of more than one criterion (Rabut and Peter, 2008).

4.6 Conclusion and Outlook

The main purpose of this thesis was to find presynaptic proteins modified by neddylation. The present results indicate that Stx1a and RIM1α are neddylation targets as two criteria defined by Rabut and colleagues were fulfilled: Covalent attachment of Nedd8 and dependency on neddylation-specific machinery. In addition two homologs of Stx1a, Stx3 and Stx4, were identified as neddylation targets, resulting in a total of four Nedd8 targets being identified. In the case of Stx1a and Stx4, it was also demonstrated which lysines are involved in neddylation. The results of the experiments indicate that both the SNARE and Hc domains play a significant role in the process of Stx neddylation, especially the lysine residues at positions 102, 123, 140 and 161 (Stx4) and the lysines 117 and 126 (Stx1a). With regard to RIM1α, latest experiments could restrict the neddylation site to the N-terminal region and thus limit the number of possible lysines.

In a next step, the proof of endogenous nedylation will be addressed. For this, a protocol using Avi-Nedd8 KI mice has been established that allows endogenously neddylated proteins to be isolated from brain tissue and visualised in western blots. Unfortunately, the detection of individual proteins is not yet possible. Another approach to investigate endogenous neddylation is the usage of the SENP8 KO mouse, as preventing deneddylation enriches neddylated proteins and facilitate detection. The optimisation of western blots with brain tissue and establishing a protocol for SENP8 KO mice is essential to confirm endogenous neddylation of syntaxins and RIM1α.

In addition, further experiments should be performed to identify neddylated lysine residues of RIM1α. Non-neddylatable mutants can then be used to investigate the function of neddylation. For example, it nedds to be investigated whether neddylation has an influence on the formation of the SNARE complex or the interaction of Munc13-Rab3A-RIM1α. Pulldown experiments as described in this thesis, could be performed using Avi-Stx1a and Avi-RIM1α and non-neddylatable variants to compare their interaction with SNAP-25b and VAMP2 or with Rab3A and Munc13. Non-neddylatable mutants could also be used to investigate the contribution of neddylation to synaptic vesicle fusion. For instance, an electrophysiological approach using SynaptopHysin could lead to interesting results.

Another aspect that should be investigated further is neddylation of carboxylases. Preliminary results suggested that carboxylases are at least partly neddylated. Additional experiments could confirm this assumption and reveal possible new functions of neddylation.

Finally an important objective in this field of research is to identify additional proteins that undergo this process of neddylation. The present results were not able to confirm nor deny neddylation of several proteins. A particular issue encountered in the present research concerned the demonstration of MLN-4924 sensitivity. An approach to enhance the efficacy of MLN-4924 treatment could be to initiate the treatment at an earlier stage. The consequence of this would be a reduction in initial protein neddylation, thereby limiting the impact of deneddylation on the overall outcome, which might increase the effect of inhibiting de-novo neddylation. An alternative to verify neddylation, may be the prevention or acceleration of deneddylation. For instance, increased deneddylation could be used to enhance the effect of MLN-4924 treatment. In contrast, the inhibition of deneddylation results in an enrichment of neddylated proteins, thus facilitating detection. In the field of ubiquitin research, MG-132 has been shown to inhibit the proteasome and thus prevent the degradation of ubiquitinated proteins. This has been demonstrated to increase the amount of ubiquitinated proteins, which facilitates the identification of ubiquitin targets (Schimmel et al., 2008). However, to date, a comparable inhibitor for deneddylation is not known.

Moreover, checking other syntaxins or Rims for neddylation could be interesting as well. Especially Rim1β that lacks the N-terminal α-helix that is believed to be neddylated could be interesting to analyse.

All in all, my results confirm that research on neddylation is exciting as well as important. Although not all points could be elucidated, my thesis offers valuable insights and provides a solid foundation for further experimentation.

5 Abstract

Reversible post-translational modifications are essential for the regulation of cell functions. One such modification is the attachment of ubiquitin and ubiquitin-like proteins, including Nedd8 (neural-precursor-cell-expressed developmentally down-regulated 8) (Enchev et al., 2015). During neddylation, Nedd8 is linked to a specific lysine of the target protein through an isopeptide bond. It is well established, that neddylation is involved in the post-translational modification of synaptic proteins. Immunoblots of synaptosomes have revealed that both pre- and postsynaptic proteins undergo neddylation (Vogl et al 2015 Vogl et al., 2015). In addition, it was shown that neddylation has an influence on spine formation and maintenance, LTPs and AMPA- and NMDA-mediated neurotransmission (Brockmann et al., 2019, Vogl et al., 2015). As inhibition of neddylation has been demonstrated to decrease the probability of transmitter release (Brockmann, 2019 Brockmann et al., 2019), it can be hypothesised that proteins involved in synaptic transmission are neddylated. However, the target proteins of Nedd8 remain largely unexplored.

The main focus of my work was the identification of presynaptic proteins modified by neddylation. The investigation focused on three key criteria: the covalent binding of Nedd8 to the target protein, the contribution of the neddylation-specific machinery, and the identification of neddylated lysines. Here, I used an Avi-tagged NEDD8, which was co-expressed with the GFP-tagged candidate protein in HEK-293 cells. The Avi-tag was biotinylated by co-expressed BirA, thus facilitating the isolation of Avi-tagged Nedd8 and all covalently attached proteins through streptavidin-covered magnetic beads. Subsequently, neddylated proteins were detected by Western Blotting against the GFP-tag. The use of MLN-4924 as a control ensured that the attachment of Nedd8 occurred through the neddylation-specific machinery rather than through the ubiquitin pathway.

In my thesis, I identified Stx1a and the homologous proteins Stx3 and Stx4 as targets for neddylation. By mutating lysine residues to arginine, I revealed that lysine 117 or 126 play an essential role in the neddylation of Stx1a. In the case of Stx4, the lysines 123, 140 and 161 were identified as neddylated residues, while the lysines 102, 108, 124 and 151 are suggested to be irrelevant for neddylation.

Additionally, I also identified RIM1α as a target protein for Nedd8. Experiments using truncated proteins indicate that the neddylated lysine residue is located within the N-terminal region up to PRM 1. Therefore, I reduced the number of lysines that may serve as Nedd8 substrates.

I unexpectedly discovered that the carboxylases are prospective Nedd8 candidates as well. As my work does not provide any additional information, a precise conclusion cannot be drawn at present.

In conclusion, I identified four new neddylation targets: Stx1a, Stx3, Stx4 and RIM1α. The identification of Stx and RIM1α as Nedd8 targets will require further investigation of the function of Nedd8 in the synapse. In particular, the discovery of the neddylated lysines of Stx1a and Stx4, and the resulting availability of non-neddylatable variants, increases the potential for investigation of the influence of Nedd8 on the syntaxin family. Combining existing literature with the present study suggests that neddylation plays a role in vesicle priming, specifically in the assembly of the SNARE complex, and consequently in SV fusion and the probability of release. However, further experiments, for example using the non-neddylable variants of stx1a, will provide more precise insights into the function of neddylation.

6 List of figures

7 List of tables

8 References

Barazzuol L, Giamogante F, Brini M, Cali T. PINK1/Parkin Mediated Mitophagy, Ca(2+) Signalling, and ER-Mitochondria Contacts in Parkinson's Disease. International journal of molecular sciences 2020; 21(5):

Bawa-Khalfe T, Yeh ET. SUMO Losing Balance: SUMO Proteases Disrupt SUMO Homeostasis to Facilitate Cancer Development and Progression. Genes Cancer 2010; 1(7): 748-752

Bennett MK, Garcia-Arrarás J, Elferink LA, Peterson K, Fleming AM, Hazuka CD, Scheller RH. The Syntaxin Family of Vesicular Transport Receptors. Cell 1993; 74(5): 863-873

Betz A, Thakur P, Junge HJ, Ashery U, Rhee JS, Scheuss V, Rosenmund C, Rettig J, Brose N. Functional interaction of the active zone proteins Munc13-1 and RIM1 in synaptic vesicle priming. Neuron 2001; 30(1): 183-196

Bin NR, Ma K, Harada H, Tien CW, Bergin F, Sugita K, Luyben TT, Narimatsu M, Jia Z, Wrana JL, Monnier PP, Zhang L, Okamoto K, Sugita S. Crucial Role of Postsynaptic Syntaxin 4 in Mediating Basal Neurotransmission and Synaptic Plasticity in Hippocampal CA1 Neurons. Cell Reports 2018; 23(10): 2955-2966

Brockmann M. Nedd8 in the brain-Its impact on synaptic function and the role of PSD-95. Doctoral dissertation, Technische Universität München 2014;

Brockmann MM, Dongi M, Einsfelder U, Korber N, Refojo D, Stein V. Neddylation regulates excitatory synaptic transmission and plasticity. Scientific Reports 2019; 9(1): 17935

Brownell JE, Sintchak MD, Gavin JM, Liao H, Bruzzese FJ, Bump NJ, Soucy TA, Milhollen MA, Yang X, Burkhardt AL, Ma J, Loke HK, Lingaraj T, Wu D, Hamman KB, Spelman JJ, Cullis CA, Langston SP, Vyskocil S, Sells TB, Mallender WD, Visiers I, Li P, Claiborne CF, Rolfe M, Bolen JB, Dick LR. Substrate-assisted inhibition of ubiquitin-like protein-activating enzymes: the NEDD8 E1 inhibitor MLN4924 forms a NEDD8-AMP mimetic in situ. Molecular Cell 2010; 37(1): 102-111

Burkhardt P, Hattendorf DA, Weis WI, Fasshauer D. Munc18a controls SNARE assembly through its interaction with the syntaxin N-peptide. The EMBO Journal 2008; 27(7): 923-933

Calakos N, Schoch S, Südhof TC, Malenka RC. Multiple roles for the active zone protein RIM1α in late stages of neurotransmitter release. Neuron 2004; 42(6): 889-896

Camacho M, Basu J, Trimbuch T, Chang S, Pulido-Lozano C, Chang SS, Duluvova I, Abo-Rady M, Rizo J, Rosenmund C. Heterodimerization of Munc13 C(2)A domain with RIM regulates synaptic vesicle docking and priming. Nature communications 2017; 8(1): 15293

Castillo PE, Schoch S, Schmitz F, Südhof TC, Malenka RC. RIM1 α is required for presynaptic long-term potentiation. Nature 2002; 415(6869): 327-330

Chan Y, Yoon J, Wu JT, Kim HJ, Pan KT, Yim J, Chien CT. DEN1 deneddylates non-cullin proteins in vivo. Journal of cell science 2008; 121(19): 3218-3223

Chen W, Luo B, Gao N, Li H, Wang H, Li L, Cui W, Zhang L, Sun D, Liu F, Dong Z, Ren X, Zhang H, Su H, Xiong WC, Mei L. Neddylation stabilizes Nav1.1 to maintain interneuron excitability and prevent seizures in murine epilepsy models. J Clin Invest 2021; 131(8):

Chen X, Lu J, Dulubova I, Rizo J. NMR analysis of the closed conformation of syntaxin-1. Journal of biomolecular NMR 2008; 41(1): 43-54

Chen Y, Neve RL, Liu H. Neddylation dysfunction in Alzheimer's disease. Journal of Cellular and Molecular Medicine 2012; 16(11): 2583-2591

Chen Y, Liu W, McPhie DL, Hassinger L, Neve RL. APP-BP1 mediates APP-induced apoptosis and DNA synthesis and is increased in Alzheimer's disease brain. The Journal of cell biology 2003; 163(1): 27-33

Chen YA, Scheller RH. SNARE-mediated membrane fusion. Nature Reviews Molecular Cell Biology 2001; 2(2): 98-106

Chin LS, Vavalle JP, Li L. Staring, a novel E3 ubiquitin-protein ligase that targets syntaxin 1 for degradation. The Journal of Biological Chemistry 2002; 277(38): 35071-35079

Choo YS, Vogler G, Wang D, Kalvakuri S, Iliuk A, Tao WA, Bodmer R, Zhang Z. Regulation of parkin and PINK1 by neddylation. Human Molecular Genetics 2012; 21(11): 2514-2523
Christie MP, Whitten AE, King GJ, Hu SH, Jarrott RJ, Chen KE, Duff AP, Callow P, Collins BM, James DE, Martin JL. Low-resolution solution structures of Munc18:Syntaxin protein complexes indicate an open binding mode driven by the Syntaxin N-peptide. Proceedings of the National Academy of Sciences 2012; 109(25): 9816-9821
Coleman KE, Bekes M, Chapman JR, Crist SB, Jones MJ, Ueberheide BM, Huang TT. SENP8 limits aberrant neddylation of NEDD8 pathway components to promote cullin-RING ubiquitin ligase function. Elife 2017; 6(
Craig TJ, Anderson D, Evans AJ, Girach F, Henley JM. SUMOylation of Syntaxin1A regulates presynaptic endocytosis. Scientific Reports 2015; 5(17669
D'Andrea-Merrins M, Chang L, Lam AD, Ernst SA, Stuenkel EL. Munc18c interaction with syntaxin 4 monomers and SNARE complex intermediates in GLUT4 vesicle trafficking. The Journal of Biological Chemistry 2007; 282(22): 16553-16566
Deak F, Xu Y, Chang WP, Dulubova I, Khvotchev M, Liu X, Sudhof TC, Rizo J. Munc18-1 binding to the neuronal SNARE complex controls synaptic vesicle priming. Journal of Cell Biology 2009; 184(5): 751-764
Deas E, Wood NW, Plun-Favreau H. Mitophagy and Parkinson's disease: the PINK1-parkin link. Biochimica et Biophysica Acta (BBA) 2011; 1813(4): 623-633
Deng L, Kaeser PS, Xu W, Südhof TC. RIM proteins activate vesicle priming by reversing autoinhibitory homodimerization of Munc13. Neuron 2011; 69(2): 317-331
Dil Kuazi A, Kito K, Abe Y, Shin RW, Kamitani T, Ueda N. NEDD8 protein is involved in ubiquitinated inclusion bodies. The Journal of Pathology: A Journal of the Pathological Society of Great Britain and Ireland 2003; 199(2): 259-266
Duda DM, Borg LA, Scott DC, Hunt HW, Hammel M, Schulman BA. Structural insights into NEDD8 activation of cullin-RING ligases: conformational control of conjugation. Cell 2008; 134(6): 995-1006
Dulubova I, Khvotchev M, Liu S, Huryeva I, Südhof TC, Rizo J. Munc18-1 binds directly to the neuronal SNARE complex. Proceedings of the National Academy of Sciences 2007; 104(8): 2697-2702
Dulubova I, Sugita S, Hill S, Hosaka M, Fernandez I, Südhof TC, Rizo J. A conformational switch in syntaxin during exocytosis: role of munc18. The EMBO Journal 1999; 18(16): 4372–4382
Dulubova I, Lou X, Lu J, Huryeva I, Alam A, Schneggenburger R, Südhof TC, Rizo J. A Munc13/RIM/Rab3 tripartite complex: from priming to plasticity? The EMBO Journal 2005; 24(16): 2839-2850
Dye BT, Schulman BA. Structural mechanisms underlying posttranslational modification by ubiquitin-like proteins. The Annual Review ofBiophysics and Biomolecular Structure 2007; 36(1): 131-150
Einsfelder U. Charakterisierung der Neddylierung von Cofilin1 - Einfluss auf die neuronale Entwicklung. 2022;
El Motiam A, Vidal S, de la Cruz-Herrera CF, Da Silva-Alvarez S, Baz-Martinez M, Seoane R, Vidal A, Rodriguez MS, Xirodimas DP, Carvalho AS, Beck HC, Matthiesen R, Collado M, Rivas C. Interplay between SUMOylation and NEDDylation regulates RPL11 localization and function. The FASEB Journal 2019; 33(1): 643-651
Emperador-Melero J, Kaeser PS. Assembly of the presynaptic active zone. Current Opinion in Neurobiology 2020; 63(95-103
Enchev RI, Schulman BA, Peter M. Protein neddylation: beyond cullin–RING ligases. Nature Reviews Molecular Cell Biology 2015; 16(1): 30-44
Feligioni M, Nishimune A, Henley JM. Protein SUMOylation modulates calcium influx and glutamate release from presynaptic terminals. European Journal of Neuroscience 2009; 29(7): 1348-1356

Fernandez I, Ubach J, Dulubova I, Zhang X, Südhof TC, Rizo J. Three-dimensional structure of an evolutionarily conserved N-terminal domain of syntaxin 1A. Cell 1998; 94(6): 841-849.
Gan-Erdene T, Nagamalleswari K, Yin L, Wu K, Pan ZQ, Wilkinson KD. Identification and characterization of DEN1, a deneddylase of the ULP family. Journal of Biological Chemistry 2003; 278(31): 28892-28900
Gareau JR, Lima CD. The SUMO pathway: emerging mechanisms that shape specificity, conjugation and recognition. Nature Reviews Molecular Cell Biology 2010; 11(12): 861-871
Geppert M, Bolshakov VY, Siegelbaum SA, Takei K, De Camilli P, Hammer RE, Südhof TC. The role of Rab3A in neurotransmitter release. Nature 1994; 369(6480): 493-497
Gerber SH, Rah JC, Min SW, Liu X, De Wit H, Dulubova I, Meyer AC, Rizo J, Arancillo M, Hammer RE, Verhage M, Rosenmund C, Südhof TC. Conformational switch of syntaxin-1 controls synaptic vesicle fusion. Science 2008; 321(5895): 1507-1510
Giovannone AJ, Winterstein C, Bhattaram P, Reales E, Low SH, Baggs JE, Xu M, Lalli MA, Hogenesch JB, Weimbs T. Soluble syntaxin 3 functions as a transcriptional regulator. Journal of Biological Chemistry 2018; 293(15): 5478-5491
Girach F, Craig TJ, Rocca DL, Henley JM. RIM1alpha SUMOylation is required for fast synaptic vesicle exocytosis. Cell Rep 2013; 5(5): 1294-1301
Giraudo CG, Eng WS, Melia TJ, Rothman JE. A clamping mechanism involved in SNARE-dependent exocytosis. Science 2006; 313(5787): 676-680
Goldenberg SJ, Cascio TC, Shumway SD, Garbutt KC, Liu J, Xiong Y, Zheng N. Structure of the Cand1-Cul1-Roc1 complex reveals regulatory mechanisms for the assembly of the multisubunit cullin-dependent ubiquitin ligases. Cell 2004; 119(4): 517-528
Gong L, Yeh ET. Identification of the activating and conjugating enzymes of the NEDD8 conjugation pathway. Journal of Biological Chemistry 1999; 274(17): 12036-12042
Gramlich MW, Klyachko VA. Nanoscale Organization of Vesicle Release at Central Synapses. Trends in Neuroscience 2019; 42(6): 425-437
Haas AL, Ahrens P, Bright PM, Ankel H. Interferon induces a 15-kilodalton protein exhibiting marked homology to ubiquitin. Journal of Biological Chemistry 1987; 262(23): 11315-11323
Haas KF, Broadie K. Roles of ubiquitination at the synapse. Biochimica et Biophysica Acta (BBA) 2008; 1779(8): 495-506
Han J, Pluhackova K, Bockmann RA. The Multifaceted Role of SNARE Proteins in Membrane Fusion. Frontiers in Physiology 2017; 8(5
Harris KP, Littleton JT, Stewart BA. Postsynaptic Syntaxin 4 negatively regulates the efficiency of neurotransmitter release. Journal of Neurogenetics 2018; 32(3): 221-229
He ZX, Yang WG, Zengyangzong D, Gao G, Zhang Q, Liu HM, Zhao W, Ma LY. Targeting cullin neddylation for cancer and fibrotic diseases. Theranostics 2023; 13(14): 5017-5056
Hjerpe R, Thomas Y, Chen J, Zemla A, Curran S, Shpiro N, Dick LR, Kurz T. Changes in the ratio of free NEDD8 to ubiquitin triggers NEDDylation by ubiquitin enzymes. Biochemical Journal 2012; 441(3): 927-936
Hori T, Osaka F, Chiba T, Miyamoto C, Okabayashi K, Shimbara N, Kato S, Tanaka K. Covalent modification of all members of human cullin family proteins by NEDD8. Oncogene 1999; 18(48): 6829-6834
Hu J, Han J, Li H, Zhang X, Liu LL, Chen F, Zeng B. Human Embryonic Kidney 293 Cells: A Vehicle for Biopharmaceutical Manufacturing, Structural Biology, and Electrophysiology. Cells Tissues Organs 2018; 205(1): 1-8
Huang DT, Walden H, Duda D, Schulman BA. Ubiquitin-like protein activation. Oncogene 2004; 23(11): 1958-1971
Huang DT, Zhuang M, Ayrault O, Schulman BA. Identification of conjugation specificity determinants unmasks vestigial preference for ubiquitin within the NEDD8 E2. Nature Structural and Molecular Biology 2008; 15(3): 280-287
Huang DT, Hunt HW, Zhuang M, Ohi MD, Holton JM, Schulman BA. Basis for a ubiquitin-like protein thioester switch toggling E1-E2 affinity. Nature 2007; 445(7126): 394-398

Huang DT, Ayrault O, Hunt HW, Taherbhoy AM, Duda DM, Scott DC, Borg LA, Neale G, Murray PJ, Roussel MF, Schulman BA. E2-RING expansion of the NEDD8 cascade confers specificity to cullin modification. Molecular Cell 2009; 33(4): 483-495
Hutagalung AH, Novick PJ. Role of Rab GTPases in membrane traffic and cell physiology. Physiological reviews 2011; 91(1): 119-149
Ichimura Y, Kirisako T, Takao T, Satomi Y, Shimonishi Y, Ishihara N, Mizushima N, Tanida I, Kominami E, Ohsumi M, Noda T, Ohsumi Y. A ubiquitin-like system mediates protein lipidation. Nature 2000; 408(6811): 488-492
Jahn R, Fasshauer D. Molecular machines governing exocytosis of synaptic vesicles. Nature 2012; 490(7419): 201-207
Jeram SM, Srikumar T, Zhang XD, Anne Eisenhauer H, Rogers R, Pedrioli PG, Matunis M, Raught B. An improved SUMmOn-based methodology for the identification of ubiquitin and ubiquitin-like protein conjugation sites identifies novel ubiquitin-like protein chain linkages. Proteomics 2010; 10(2): 254-265
Jumper J, Evans R, Pritzel A, Green T, Figurnov M, Ronneberger O, Tunyasuvunakool K, Bates R, Zidek A, Potapenko A, Bridgland A, Meyer C, Kohl SAA, Ballard AJ, Cowie A, Romera-Paredes B, Nikolov S, Jain R, Adler J, Back T, Petersen S, Reiman D, Clancy E, Zielinski M, Steinegger M, Pacholska M, Berghammer T, Bodenstein S, Silver D, Vinyals O, Senior AW, Kavukcuoglu K, Kohli P, Hassabis D. Highly accurate protein structure prediction with AlphaFold. Nature 2021; 596(7873): 583-589
Jurado S, Goswami D, Zhang Y, Molina AJ, Sudhof TC, Malenka RC. LTP requires a unique postsynaptic SNARE fusion machinery. Neuron 2013; 77(3): 542-558
Kaeser PS. Pushing synaptic vesicles over the RIM. Cellular logistics 2011; 1(3): 106-110
Kaeser PS, Südhof TC. RIM function in short-and long-term synaptic plasticity. Biochemical Society Transactions 2005; 33(6)): 1345-1349
Kaeser PS, Deng L, Fan M, Südhof TC. RIM genes differentially contribute to organizing presynaptic release sites. Proceedings of the National Academy of Sciences 2012; 109(29): 11830-11835
Kaeser PS, Kwon HB, Chiu CQ, Deng L, Castillo PE, Südhof TC. RIM1alpha and RIM1beta are synthesized from distinct promoters of the RIM1 gene to mediate differential but overlapping synaptic functions. Journal of Neuroscience 2008; 28(50): 13435-13447
Kaeser PS, Deng L, Wang Y, Dulubova I, Liu X, Rizo J, Südhof TC. RIM proteins tether Ca2+ channels to presynaptic active zones via a direct PDZ-domain interaction. Cell 2011; 144(2): 282-295
Kamitani T, Kito K, Nguyen HP, Yeh ET. Characterization of NEDD8, a developmentally down-regulated ubiquitin-like protein. Journal of Biological Chemistry 1997; 272(45): 28557-28562
Kamura T, Conrad MN, Yan Q, Conaway RC, Conaway JW. The Rbx1 subunit of SCF and VHL E3 ubiquitin ligase activates Rub1 modification of cullins Cdc53 and Cul2. Genes & development 1999; 13(22): 2928-2933
Kawabe H, Brose N. The role of ubiquitylation in nerve cell development. Nature Reviews Neuroscience 2011; 12(5): 251-268
Kennedy MJ, Davison IG, Robinson CG, Ehlers MD. Syntaxin-4 defines a domain for activity-dependent exocytosis in dendritic spines. Cell 2010; 141(3): 524-535
Kerscher O, Felberbaum R, Hochstrasser M. Modification of proteins by ubiquitin and ubiquitin-like proteins. The Annual Review of Cell and Developmental Biology 2006; 22(1): 159-180
Kim W, Bennett EJ, Huttlin EL, Guo A, Li J, Possemato A, Sowa ME, Rad R, Rush J, Comb MJ, Harper JW, Gygi SP. Systematic and quantitative assessment of the ubiquitin-modified proteome. Molecular Cell 2011; 44(2): 325-340
Kintscher M, Wozny C, Johenning FW, Schmitz D, Breustedt J. Role of RIM1alpha in short- and long-term synaptic plasticity at cerebellar parallel fibres. Nature communications 2013; 4(2392

Kitada T, Asakawa S, Hattori N, Matsumine H, Yamamura Y, Minoshima S, Yokochi M, Mizuno Y, Shimizu N. Mutations in the parkin gene cause autosomal recessive juvenile parkinsonism. Nature 1998; 392(6676): 605-608
Kiyonaka S, Wakamori M, Miki T, Uriu Y, Nonaka M, Bito H, Beedle AM, Mori E, Hara Y, De Waard M, Kanagawa M, Itakura M, Takahashi M, Campbell KP, Mori Y. RIM1 confers sustained activity and neurotransmitter vesicle anchoring to presynaptic Ca2+ channels. Nature neuroscience 2007; 10(6): 691-701
Koushika SP, Richmond JE, Hadwiger G, Weimer RM, Jorgensen EM, Nonet ML. A post-docking role for active zone protein Rim. Nature neuroscience 2001; 4(10): 997-1005
Kumar S, Tomooka Y, Noda M. Identification of a set of genes with developmentally down-regulated expression in the mouse brain. Biochemical and biophysical research communications 1992; 185(3): 1155-1161
Kumar S, Yoshida Y, Noda M. Cloning of a cDNA which encodes a novel ubiquitin-like protein. Biochemical and biophysical research communications 1993; 195(1): 393-399
Kurihara LJ, Semenova E, Levorse JM, Tilghman SM. Expression and functional analysis of Uch-L3 during mouse development. Molecular and Cellular Biology 2000; 20(7): 2498-2504
Laemmli UK. Cleavage of structural proteins during the assembly of the head of bacteriophage T4. Nature 1970; 227(5259): 680-685
Lam PP, Leung YM, Sheu L, Ellis J, Tsushima RG, Osborne LR, Gaisano HY. Transgenic mouse overexpressing syntaxin-1A as a diabetes model. Diabetes 2005; 54(9): 2744-2754
Leidecker O, Matic I, Mahata B, Pion E, Xirodimas DP. The ubiquitin E1 enzyme Ube1 mediates NEDD8 activation under diverse stress conditions. Cell Cycle 2012; 11(6): 1142-1150
Li C, Zhang L, Qian D, Cheng M, Hu H, Hong Z, Cui Y, Yu H, Wang Q, Zhu J, Meng W, Xu JF, Sun Y, Zhang P, Wang C. RNF111-facilitated neddylation potentiates cGAS-mediated antiviral innate immune response. PLoS Pathog 2021; 17(3): e1009401
Li J, Zou J, Littlejohn R, Liu J, Su H. Neddylation, an Emerging Mechanism Regulating Cardiac Development and Function. Frontiers in Physiology 2020a; 11(612927
Li M, Oh TJ, Fan H, Diao J, Zhang K. Syntaxin Clustering and Optogenetic Control for Synaptic Membrane Fusion. Journal of molecular biology 2020b; 432(17): 4773-4782
Liakopoulos D, Doenges G, Matuschewski K, Jentsch S. A novel protein modification pathway related to the ubiquitin system. The EMBO Journal 1998; 17(8): 2208-2214
Lin A, Hou Q, Jarzylo L, Amato S, Gilbert J, Shang F, Man HY. Nedd4-mediated AMPA receptor ubiquitination regulates receptor turnover and trafficking. Journal of neurochemistry 2011; 119(1): 27-39
Liu H, Li L, Nedelcu D, Hall Q, Zhou L, Wang W, Yu Y, Kaplan JM, Hu Z. Heterodimerization of UNC-13/RIM regulates synaptic vesicle release probability but not priming in C. elegans. Elife 2019; 8(
Liu YC, Pan J, Zhang C, Fan W, Collinge M, Bender JR, Weissman SM. A MHC-encoded ubiquitin-like protein (FAT10) binds noncovalently to the spindle assembly checkpoint protein MAD2. Proceedings of the National Academy of Sciences 1999; 96(8): 4313-4318
Loeb KR, Haas AL. The interferon-inducible 15-kDa ubiquitin homolog conjugates to intracellular proteins. Journal of Biological Chemistry 1992; 267(11): 7806-7813
Luo F, Liu X, Südhof TC, Acuna C. Efficient stimulus-secretion coupling at ribbon synapses requires RIM-binding protein tethering of L-type Ca(2+) channels. Proceedings of the National Academy of Sciences 2017; 114(38): E8081-E8090
Ma C, Li W, Xu Y, Rizo J. Munc13 mediates the transition from the closed syntaxin-Munc18 complex to the SNARE complex. Nature Structural and Molecular Biology 2011; 18(5): 542-549
Mandon B, Chou CL, Nielsen S, Knepper MA. Syntaxin-4 is localized to the apical plasma membrane of rat renal collecting duct cells: possible role in aquaporin-2 trafficking. The Journal of clinical investigation 1996; 98(4): 906-913
Mao H, Lin X, Sun Y. Neddylation Regulation of Immune Responses. Research (Wash D C) 2023; 6(0283

Min SW, Chang WP, Südhof TC. E-Syts, a family of membranous Ca2+-sensor proteins with multiple C2 domains. Proceedings of the National Academy of Sciences 2007; 104(10): 3823-3828
Mistry AC, Mallick R, Klein JD, Weimbs T, Sands JM, Fröhlich O. Syntaxin specificity of aquaporins in the inner medullary collecting duct. American Journal of Physiology-Renal Physiology 2009; 297(2): F292-300
Misura KM, Scheller RH, Weis WI. Three-dimensional structure of the neuronal-Sec1–syntaxin 1a complex. Nature 2000; 404(6776): 355-362
Mittelstaedt T, Alvaréz-Baron E, Schoch S. RIM proteins and their role in synapse function. Biological Chemistry 2010; 391(6): 599-606
Mizushima N, Noda T, Yoshimori T, Tanaka Y, Ishii T, George MD, Klionsky DJ, Ohsumi M, Ohsumi Y. A protein conjugation system essential for autophagy. Nature 1998; 395(6700): 395-398
Mochida S. Neurotransmitter Release Site Replenishment and Presynaptic Plasticity. International journal of molecular sciences 2020; 22(1):
Mohanasundaram P, & Shanmugam, M. M. Role of syntaxin 4 in activity-dependent exocytosis and synaptic plasticity in hippocampal neurons. Science Signaling 2010; 3(144): jc7-jc7
Morgans CW, Brandstätter JH, Kellerman J, Betz H, Wässle H. A SNARE complex containing syntaxin 3 is present in ribbon synapses of the retina. Journal of Neuroscience 1996; 16(21): 6713-6721
Mori F, Nishie M, Piao YS, Kito K, Kamitani T, Takahashi H, Wakabayashi K. Accumulation of NEDD8 in neuronal and glial inclusions of neurodegenerative disorders. Neuropathology and applied neurobiology 2005; 31(1): 53-61
Noh EH, Hwang HS, Hwang HS, Min B, Im E, Chung KC. Covalent NEDD8 conjugation increases RCAN1 protein stability and potentiates its inhibitory action on calcineurin. PLoS ONE 2012; 7(10): e48315
Ogawa H, Harada S, Sassa T, Yamamoto H, Hosono R. Functional properties of the unc-64 gene encoding a Caenorhabditis elegans syntaxin. Journal of Biological Chemistry 1998; 273(4): 2192-2198
Osaka F, Kawasaki H, Aida N, Saeki M, Chiba T, Kawashima S, Tanaka K, Kato S. A new NEDD8-ligating system for cullin-4A. Genes & development 1998; 12(15): 2263-2268
Oved S, Mosesson Y, Zwang Y, Santonico E, Shtiegman K, Marmor MD, Kochupurakkal BS, Katz M, Lavi S, Cesareni G, Yarden Y. Conjugation to Nedd8 instigates ubiquitylation and down-regulation of activated receptor tyrosine kinases. Journal of Biological Chemistry 2006; 281(31): 21640-21651
Pan ZQ, Kentsis A, Dias DC, Yamoah K, Wu K. Nedd8 on cullin: building an expressway to protein destruction. Oncogene 2004; 23(11): 1985-1997
Perez-Lara A, Jahn R. Extended synaptotagmins (E-Syts): Architecture and dynamics of membrane contact sites revealed. Proceedings of the National Academy of Sciences 2015; 112(16): 4837-4838
Poirier MA, Xiao W, Macosko JC, Chan C, Shin YK, Bennett MK. The synaptic SNARE complex is a parallel four-stranded helical bundle. Nature structural biology 1998; 5(9): 765-769
Rabut G, Peter M. Function and regulation of protein neddylation. 'Protein modifications: beyond the usual suspects' review series. EMBO reports 2008; 9(10): 969-976
Ramazi S, Zahiri J. Posttranslational modifications in proteins: resources, tools and prediction methods. Database (Oxford) 2021; 2021(
Rauh R, Frost F, Korbmacher C. Effects of syntaxins 2, 3, and 4 on rat and human epithelial sodium channel (ENaC) in Xenopus laevis oocytes. Pflügers Archiv-European Journal of Physiology 2020; 472(4): 461-471
Ravid T, Hochstrasser M. Diversity of degradation signals in the ubiquitin-proteasome system. Nature Reviews Molecular Cell Biology 2008; 9(9): 679-690

Rehman A, Hu SH, Tnimov Z, Whitten AE, King GJ, Jarrott RJ, Norwood SJ, Alexandrov K, Collins BM, Christie MP, Martin JL. The nature of the Syntaxin4 C-terminus affects Munc18c-supported SNARE assembly. PLoS ONE 2017; 12(8): e0183366
Ribrault C, Reingruber J, Petkovic M, Galli T, Ziv NE, Holcman D, Triller A. Syntaxin1A lateral diffusion reveals transient and local SNARE interactions. Journal of Neuroscience 2011; 31(48): 17590-17602
Richmond JE, Weimer RM, Jorgensen EM. An open form of syntaxin bypasses the requirement for UNC-13 in vesicle priming. Nature 2001; 412(6844): 338-341
Rizo J. Mechanism of neurotransmitter release coming into focus. Protein Science 2018; 27(8): 1364-1391
Rizo J, Xu J. The synaptic vesicle release machinery. Annual review of biophysics 2015; 44(1): 339-367
Rizo J, Chen X, Arac D. Unraveling the mechanisms of synaptotagmin and SNARE function in neurotransmitter release. Trends in cellular biology 2006; 16(7): 339-350
Rossi R, Arjmand S, Baerentzen SL, Gjedde A, Landau AM. Synaptic Vesicle Glycoprotein 2A: Features and Functions. Frontiers in Neuroscience 2022; 16(864514
Russell RC, Ohh M. NEDD8 acts as a 'molecular switch' defining the functional selectivity of VHL. EMBO reports 2008; 9(5): 486-491
Saha A, Deshaies RJ. Multimodal activation of the ubiquitin ligase SCF by Nedd8 conjugation. Molecular Cell 2008; 32(1): 21-31
Sakane A, Manabe S, Ishizaki H, Tanaka-Okamoto M, Kiyokage E, Toida K, Yoshida T, Miyoshi J, Kamiya H, Takai Y, Sasaki T. Rab3 GTPase-activating protein regulates synaptic transmission and plasticity through the inactivation of Rab3. Proceedings of the National Academy of Sciences 2006; 103(26): 10029-10034
Sarikas A, Hartmann T, Pan ZQ. The cullin protein family. Genome Biology 2011; 12(1-12
Schaub JR, Lu X, Doneske B, Shin YK, McNew JA. Hemifusion arrest by complexin is relieved by Ca2+-synaptotagmin I. Nature Structural & Molecular Biology 2006; 13(8): 748-750
Schimmel J, Larsen KM, Matic I, van Hagen M, Cox J, Mann M, Andersen JS, Vertegaal AC. The ubiquitin-proteasome system is a key component of the SUMO-2/3 cycle. Mol Cell Proteomics 2008; 7(11): 2107-2122
Schlüter OM, Schmitz F, Jahn R, Rosenmund C, Südhof TC. A complete genetic analysis of neuronal Rab3 function. The Journal of Neuroscience 2004; 24(29): 6629-6637
Schneider R, Hosy E, Kohl J, Klueva J, Choquet D, Thomas U, Voigt A, Heine M. Mobility of calcium channels in the presynaptic membrane. Neuron 2015; 86(3): 672-679
Schoch S, Gundelfinger ED. Molecular organization of the presynaptic active zone. Cell and tissue research 2006; 326(2): 379-391
Schoch S, Castillo PE, Jo T, Mukherjee K, Geppert M, Wang Y, Schmitz F, R.C. M, Südhof TC. RIM1a forms a protein scaffold for regulating neurotransmitter release at theactivezone. Nature 2002; 415(6869): 321-326
Schreiber A, Peter M. Substrate recognition in selective autophagy and the ubiquitin-proteasome system. Biochimica et Biophysica Acta (BBA) 2014; 1843(1): 163-181
Schwartz AL, Ciechanover A. Targeting proteins for destruction by the ubiquitin system: implications for human pathobiology. Annual review of pharmacology and toxicology 2009; 49(1): 73-96
Scudder SL, Patrick GN. Synaptic structure and function are altered by the neddylation inhibitor MLN4924. Molecular and Cellular Neuroscience 2015; 65(52-57
Sehar U, Rawat P, Reddy AP, Kopel J, Reddy PH. Amyloid Beta in Aging and Alzheimer's Disease. International journal of molecular sciences 2022; 23(21):
Shen LN, Liu H, Dong C, Xirodimas D, Naismith JH, Hay RT. Structural basis of NEDD8 ubiquitin discrimination by the deNEDDylating enzyme NEDP1. The EMBO Journal 2005; 24(7): 1341-1351
Smyth AM, Rickman C, Duncan RR. Vesicle fusion probability is determined by the specific interactions of munc18. The Journal of Biological Chemistry 2010; 285(49): 38141-38148

Sokalingam S, Raghunathan G, Soundrarajan N, Lee SG. A study on the effect of surface lysine to arginine mutagenesis on protein stability and structure using green fluorescent protein. PLoS ONE 2012; 7(7): e40410
Söllner T, Bennett MK, Whiteheart SW, Scheller RH, Rothman JE. A protein assembly-disassembly pathway in vitro that may correspond to sequential steps of synaptic vesicle docking, activation, and fusion. Cell 1993; 74(3): 409-418
Soo Hoo L, Banna CD, Radeke CM, Sharma N, Albertolle ME, Low SH, Weimbs T, Vandenberg CA. The SNARE Protein Syntaxin 3 Confers Specificity for Polarized Axonal Trafficking in Neurons. PLoS ONE 2016; 11(9): e0163671
Soucy TA, Smith PG, Milhollen MA, Berger AJ, Gavin JM, Adhikari S, Brownell JE, Burke KE, Cardin DP, Critchley S, Cullis CA, Doucette A, Garnsey JJ, Gaulin JL, Gershman RE, Lublinsky AR, McDonald A, Mizutani H, Narayanan U, Olhava EJ, Peluso S, Rezaei M, Sintchak MD, Talreja T, Thomas MP, Traore T, Vyskocil S, Weatherhead GS, Yu J, Zhang J, Dick LR, Claiborne CF, Rolfe M, Bolen JB, Langston SP. An inhibitor of NEDD8-activating enzyme as a new approach to treat cancer. Nature 2009; 458(7239): 732-736
Stein V, House DR, Bredt DS, Nicoll RA. Postsynaptic density-95 mimics and occludes hippocampal long-term potentiation and enhances long-term depression. Journal of Neuroscience 2003; 23(13): 5503-5506
Stepanenko AA, Dmitrenko VV. HEK293 in cell biology and cancer research: phenotype, karyotype, tumorigenicity, and stress-induced genome-phenotype evolution. Gene 2015; 569(2): 182-190
Südhof TC. The presynaptic active zone. Neuron 2012; 75(1): 11-25
Südhof TC. A molecular machine for neurotransmitter release: synaptotagmin and beyond. Nature medicine 2013a; 19(10): 1227-1231
Südhof TC. Neurotransmitter release: the last millisecond in the life of a synaptic vesicle. Neuron 2013b; 80(3): 675-690
Südhof TC. The molecular machinery of neurotransmitter release (Nobel lecture). Angewandte Chemie International Edition 2014; 53(47): 12696-12717
Südhof TC, Rizo J. Synaptic vesicle exocytosis. Cold Spring Harbor perspectives in biology 2011; 3(12):
Sutton RB, Fasshauer D, Jahn R, Brunger AT. Crystal structure of a SNARE complex involved in synaptic exocytosis at 2.4 Å resolution. Nature 1998; 395(6700): 347-353
Takashima O, Tsuruta F, Kigoshi Y, Nakamura S, Kim J, Katoh MC, Fukuda T, Irie K, Chiba T. Brap2 regulates temporal control of NF-kappaB localization mediated by inflammatory response. PLoS ONE 2013; 8(3): e58911
Tan C, Wang SSH, de Nola G, Kaeser PS. Rebuilding essential active zone functions within a synapse. Neuron 2022; 110(9): 1498-1515 e1498
Teng FYH, Wang Y, Tang BL. The syntaxins. Genome Biology 2001; 2(11): 3012.3011–3012.3017
Trempe JF, Sauvé V, Grenier K, Seirafi M, Tang MY, Ménade M, Al-Abdul-Wahid S, Krett J, Wong K, Kozlov G, Nagar B, Fo EA, Gehring K. Structure of parkin reveals mechanisms for ubiquitin ligase activation. Science 2013; 340(6139): 1451-1455
Um JW, Han KA, Im E, Oh Y, Lee K, Chung KC. Neddylation positively regulates the ubiquitin E3 ligase activity of parkin. Journal of Neuroscience Research 2012; 90(5): 1030-1042
van den Bogaart G, Meyenberg K, Risselada HJ, Amin H, Willig KI, Hubrich BE, Dier M, Hell SW, Grubmuller H, Diederichsen U, Jahn R. Membrane protein sequestering by ionic protein-lipid interactions. Nature 2011; 479(7374): 552-555
van der Veen AG, Ploegh HL. Ubiquitin-like proteins. Annual review of biochemistry 2012; 81(1): 323-357
Varadi M, Bertoni D, Magana P, Paramval U, Pidruchna I, Radhakrishnan M, Tsenkov M, Nair S, Mirdita M, Yeo J, Kovalevskiy O, Tunyasuvunakool K, Laydon A, Zidek A, Tomlinson H, Hariharan D, Abrahamson J, Green T, Jumper J, Birney E, Steinegger M, Hassabis D, Velankar S. AlphaFold

Protein Structure Database in 2024: providing structure coverage for over 214 million protein sequences. Nucleic Acids Res 2024; 52(D1): D368-D375
Varadi M, Anyango S, Deshpande M, Nair S, Natassia C, Yordanova G, Yuan D, Stroe O, Wood G, Laydon A, Zidek A, Green T, Tunyasuvunakool K, Petersen S, Jumper J, Clancy E, Green R, Vora A, Lutfi M, Figurnov M, Cowie A, Hobbs N, Kohli P, Kleywegt G, Birney E, Hassabis D, Velankar S. AlphaFold Protein Structure Database: massively expanding the structural coverage of protein-sequence space with high-accuracy models. Nucleic Acids Res 2022; 50(D1): D439-D444
Vardar G, Salazar-Lazaro A, Zobel S, Trimbuch T, Rosenmund C. Syntaxin-1A modulates vesicle fusion in mammalian neurons via juxtamembrane domain dependent palmitoylation of its transmembrane domain. Elife 2022; 11(
Vogl AM, Phu L, Becerra R, Giusti SA, Verschueren E, Hinkle TB, Bordenave MD, Adrian M, Heidersbach A, Yankilevich P, Stefani FD, Wurst W, Hoogenraad CC, Kirkpatrick DS, Refojo D, Sheng M. Global site-specific neddylation profiling reveals that NEDDylated cofilin regulates actin dynamics. Nature Structural & Molecular Biology 2020; 27(2): 210-220
Vogl AM, Brockmann MM, Giusti SA, Maccarrone G, Vercelli CA, Bauder CA, Richter JS, Roselli F, Hafner AS, Dedic N, Wotjak CT, Vogt-Weisenhorn DM, Choquet D, Turck CW, Stein V, Deussing JM, Refojo D. Neddylation inhibition impairs spine development, destabilizes synapses and deteriorates cognition. Nature neuroscience 2015; 18(2): 239-251
Wada H, Kito K, Caskey LS, Yeh ET, Kamitani T. Cleavage of the C-terminus of NEDD8 by UCH-L3. Biochemical and biophysical research communications 1998; 251(3): 688-692
Walden H, Podgorski MS, Huang DT, Miller DW, Howard RJ, Minor DL, Holton JM, Schulman BA. The structure of the APPBP1-UBA3-NEDD8-ATP complex reveals the basis for selective ubiquitin-like protein activation by an E1. Molecular Cell 2003; 12(6): 1427-1437
Wang S, Choi UB, Gong J, Yang X, Li Y, Wang AL, Yang X, Brunger AT, Ma C. Conformational change of syntaxin linker region induced by Munc13s initiates SNARE complex formation in synaptic exocytosis. The EMBO Journal 2017; 36(6): 816-829
Wang X, Hu B, Zimmermann B, Kilimann MW. Rim1 and rabphilin-3 bind Rab3-GTP by composite determinants partially related through N-terminal alpha -helix motifs. The Journal of Biological Chemistry 2001; 276(35): 32480-32488
Wang Y, Okamoto M, Schmitz F, Hofmann K, Südhof TC. Rim is a putative Rab3 effector in regulating synaptic-vesicle fusion. Nature 1997; 388(6642): 593-598
Watson IR, Li BK, Roche O, Blanch A, Ohh M, Irwin MS. Chemotherapy induces NEDP1-mediated destabilization of MDM2. Oncogene 2010; 29(2): 297-304
Welchman RL, Gordon C, Mayer RJ. Ubiquitin and ubiquitin-like proteins as multifunctional signals. Nature Reviews Molecular Cell Biology 2005; 6(8): 599-609
Wheeler TC, Chin LS, Li Y, Roudabush FL, Li L. Regulation of synaptophysin degradation by mammalian homologues of seven in absentia. Journal of Biological Chemistry 2002; 277(12): 10273-10282
Whitby FG, Xia G, Pickart CM, Hill CP. Crystal structure of the human ubiquitin-like protein NEDD8 and interactions with ubiquitin pathway enzymes. Journal of Biological Chemistry 1998; 273(52): 34983-34991
Wilkinson KA, Nishimune A, Henley JM. Analysis of SUMO-1 modification of neuronal proteins containing consensus SUMOylation motifs. Neuroscience letters 2008; 436(2): 239-244
Wu K, Yamoah K, Dolios G, Gan-Erdene T, Tan P, Chen A, Lee CG, Wei N, Wilkinson KD, Wang R, Pan ZQ. DEN1 is a dual function protease capable of processing the C terminus of Nedd8 and deconjugating hyper-neddylated CUL1. Journal of Biological Chemistry 2003; 278(31): 28882-28891
Wu S, Fan J, Tang F, Chen L, Zhang X, Xiao D, Li X. The role of RIM in neurotransmitter release: promotion of synaptic vesicle docking, priming, and fusion. Frontiers in Neuroscience 2023; 17(1123561

Wu X, Cai Q, Shen Z, Chen X, Zeng M, Du S, Zhang M. RIM and RIM-BP Form Presynaptic Active-Zone-like Condensates via Phase Separation. Molecular Cell 2019; 73(5): 971-984 e975
Xiong H, Wang D, Chen L, Choo YS, Ma H, Tang C, Xia K, Jiang W, Ronai Z, Zhuang X, Zhang Z. Parkin, PINK1, and DJ-1 form a ubiquitin E3 ligase complex promoting unfolded protein degradation. The Journal of clinical investigation 2009; 119(3): 650-660
Xirodimas DP, Saville MK, Bourdon JC, Hay RT, Lane DP. Mdm2-mediated NEDD8 conjugation of p53 inhibits its transcriptional activity. Cell 2004; 118(1): 83-97
Yamoah K, Wu K, Pan ZQ. In vitro cleavage of Nedd8 from cullin 1 by COP9 signalosome and deneddylase 1. Methods in enzymology 2005; 398(509-522
Yang C, Coker KJ, Kim JK, Mora S, Thurmond DC, Davis AC, Yang B, Williamson RA, Shulman GI, Pessin JE. Syntaxin 4 heterozygous knockout mice develop muscle insulin resistance. The Journal of clinical investigation 2001; 107(10): 1311-1318
Yang X, Tu W, Gao X, Zhang Q, Guan J, Zhang J. Functional regulation of syntaxin-1: An underlying mechanism mediating exocytosis in neuroendocrine cells. Front Endocrinol (Lausanne) 2023; 14(1096365
Yang X, Wang S, Sheng Y, Zhang M, Zou W, Wu L, Kang L, Rizo J, Zhang R, Xu T, Ma C. Syntaxin opening by the MUN domain underlies the function of Munc13 in synaptic-vesicle priming. Nature Structural & Molecular Biology 2015; 22(7): 547-554
Yang Y, Calakos N. Munc13-1 is required for presynaptic long-term potentiation. Journal of Neuroscience 2011; 31(33): 12053-12057
Yao I, Takagi H, Ageta H, Kahyo T, Sato S, Hatanaka K, Fukuda Y, Chiba T, Morone N, Yuasa S, Inokuchi K, Ohtsuka T, Macgregor GR, Tanaka K, Setou M. SCRAPPER-dependent ubiquitination of active zone protein RIM1 regulates synaptic vesicle release. Cell 2007; 130(5): 943-957
Yeh ET, Gong L, Kamitani T. Ubiquitin-like proteins: new wines in new bottles. Gene 2000; 248(1-2): 1-14
Yi JJ, Ehlers MD. Emerging roles for ubiquitin and protein degradation in neuronal function. Pharmacological reviews 2007; 59(1): 14-39
Yu H, Rathore SS, Lopez JA, Davis EM, James DE, Martin JL, Shen J. Comparative studies of Munc18c and Munc18-1 reveal conserved and divergent mechanisms of Sec1/Munc18 proteins. Proceedings of the National Academy of Sciences 2013; 110(35): E3271-3280
Yuan J, W. Xu W, Jiang S, Yu H, Fai Poon H. The Scattered Twelve Tribes of HEK293. Biomedical and Pharmacology Journal 2018; 11(2): 621-623
Zangi R, Zhou R, Berne BJ. Urea's Action on Hydrophobic Interactions. Journal of the American Chemical Society 2009; 131(4): 1535–1541
Zhang S, Yu Q, Li Z, Zhao Y, Sun Y. Protein neddylation and its role in health and diseases. Signal Transduction and Targeted Therapy 2024; 9(1): 85
Zhang X, Ye Z, Pei Y, Qiu G, Wang Q, Xu Y, Shen B, Zhang J. Neddylation is required for herpes simplex virus type I (HSV-1)-induced early phase interferon-beta production. Cellular & Molecular Immunology 2016; 13(5): 578-583
Zhang Y, Hughson FM. Chaperoning SNARE Folding and Assembly. Annual review of biochemistry 2021; 90(581-603
Zhou P, Pang ZP, Yang X, Zhang Y, Rosenmund C, Bacaj T, Südhof TC. Syntaxin-1 N-peptide and Habc-domain perform distinct essential functions in synaptic vesicle fusion. The EMBO Journal 2013; 32(1): 159-171
Ziv NE, Garner CC. Cellular and molecular mechanisms of presynaptic assembly. Nature Reviews Neuroscience 2004; 5(5): 385-399
Zou J, Ma W, Littlejohn R, Li J, Stansfield BK, Kim IM, Liu J, Zhou J, Weintraub NL, Su H. Transient inhibition of neddylation at neonatal stage evokes reversible cardiomyopathy and predisposes the heart to isoproterenol-induced heart failure. American Journal of Physiology-Heart and Circulatory Physiology 2019; 316(6): H1406-H1416

Zürner M, Schoch S. The mouse and human Liprin-alpha family of scaffolding proteins: genomic organization, expression profiling and regulation by alternative splicing. Genomics 2009; 93(3): 243-253

9 Acknowledgements

This thesis would not have been possible without support of important people. Therefore, I would like to take this opportunity to say thank you to all the people who encouraged, motivated, and supported me on my way.

First of all, I would like to thank Prof. Dr. Valentin Stein for the opportunity to write this thesis in his laboratory group and for the great and time-consuming support. Thank you for always having an open ear and great advice. Thank you also for the important discussions about my results and that I had the opportunity to plan my experiments together with you. I really appreciated every conversation and learned an incredible amount. I am very excited that my time in your working group does not end with this work, but that I can continue to learn a lot. Thank you for that too.

I would also like to express my gratitude to Prof. Dr. Martin Müller, Prof. Dr. Susanne Schoch and Prof. Dr. Dirk Dietrich for assuming the role of my dissertation committee. Thank you for the valuable discussions and suggestions pertaining to my work.

In particular, I want to thank Prof. Dr. Martin Müller for taking on the task of being the second reviewer for my thesis.

I would also like to thank Prof. Dr. Dirk Dietrich for sharing his knowledge with me and providing me with the opportunity to learn new methods.

Special thanks also go to Prof. Dr. Susanne Schoch, who supported me throughout my work with plasmids, cell lines and especially with her expertise and knowledge, in particular, about the complex subject of Stx and RIM1α.

I would also like to express my gratitude to all members of AG Stein for the great atmosphere, engaging in constructive dialogue, providing valuable guidance on scientific and personal matters, and offering substantial support during laboratory meetings and beyond.

I would like to extend my gratitude to Dr. Michael Döngi for always tirelessly answering all my questions and for sharing his knowledge and expertise so generously with everybody. A very special thank you, of course, for proofreading my thesis.

I would also like to express my gratitude to Dorit for the wonderful cooperation in the lab130 and her great support, particularly with cloning, mouse handling, order processing and whenever else I needed help.

Thanks also to Isa for her contributions to cell culture and mouse handling, as well as for the many conversations and for making sure I had something to eat at lunchtime.
I would also like to thank Inés for always spreading good humour and her words of encouragement during challenging periods.
I would also like to thank the former members of the lab, Dr. Michael Rabenstein for his support and for everything he taught me, and Dr. Ulf Einsfelder for his extensive training and for sharing his knowledge and skills with me, especially regarding the method used.
I would also like to extend my appreciation to my family and friends for their unwavering support and encouragement, even in moments of doubt. I especially want to mention Michi, Nick and Jassi, who kindly proofread my thesis.
A very special thank you to my husband, who has always supported me and ensured that I have been able to focus on my work, especially in the last few weeks. Thank you for putting up with me and being there for me.
Finally, I would like to thank my parents, without whom I would not have come this far. Thank you for your unconditional support and love and for always making me feel like I could achieve anything.